

Zero-bin subtraction and the q_T spectrum beyond leading power

Giancarlo Ferrera ^{a,b} Wan-Li Ju ^b and Marek Schönherr ^c

^a*Dipartimento di Fisica, Università di Milano,
Via Celoria 16, 20133 Milan, Italy*

^b*INFN, Sezione di Milano,
Via Celoria 16, 20133 Milan, Italy*

^c*Institute for Particle Physics Phenomenology, Durham University,
Durham DH1 3LE, U.K.*

E-mail: giancarlo.ferrera@mi.infn.it, wanli.ju@mi.infn.it,
marek.schoenherr@durham.ac.uk

ABSTRACT: In this paper, we present an algorithm to construct the q_T distribution at NLO accuracy to arbitrary power precision, including the assembly of suitable zero-bin subtrahends, in a mathematically well-defined way for a generic choice of rapidity-divergence regularisation prescription. In its derivation, we divide the phase space into two sectors, the interior of the integration domain as well as the integration boundary, which we include here for the first time. To demonstrate the applicability and usefulness of our algorithm, we calculate the N²LP corrections for Higgs hadroproduction for the first time. We observe that our approximate N²LP-accurate q_T spectra replicate the asymptotic behaviour of the full QCD calculation to a much better degree than the previously available results, both within the $q_T \rightarrow 0$ limit and in the large- q_T domain for all the involved partonic processes. While playing a minor role at larger transverse momenta, we show that the newly incorporated boundary contribution plays a vital role in the $q_T \rightarrow 0$ limit, where any subleading power accuracy would be lost without them. In particular, our N²LP-accurate q_T expansion can approximate the exact q_T distribution up to $q_T \approx 30$ GeV at the percent level for rapidities $|Y_H| \lesssim 3$.

KEYWORDS: Effective Field Theories of QCD, Factorization, Renormalization Group, Higgs Production, Resummation

ARXIV EPRINT: [2312.14911](https://arxiv.org/abs/2312.14911)

Contents

1	Introduction	1
2	Theoretical framework	4
2.1	Analysis of the NLO fixed order results	4
2.2	Prerequisites for the power expansion	7
2.3	Power corrections on the boundary	10
2.4	Power corrections over the interior domain	11
2.5	Discussion and extrapolation	28
3	Implementation up to N²LP	30
3.1	Power expansion with momentum cutoffs	30
3.2	Power expansion with the pure rapidity regulator	37
3.3	Power expansion with the exponential rapidity regulator	40
4	Numerical results	44
5	Conclusions	50
A	Application and adaptation of the dissipative regulators	53
A.1	The Δ -regulator	53
A.2	The η -regulator	54
B	Comparison of the NLP results with the previous literature	55
C	Small q_T expansion for multi-boson hadroproduction	56

1 Introduction

Differential observables of the Drell-Yan processes and Higgs hadroproduction play paramount roles in precisely determining the Standard Model (SM) input parameters and probing New Physics scenarios. They have therefore drawn extensive experimental and theoretical attention in the recent decades. The latest measurements of the Drell-Yan processes have been carried out by the ATLAS [1–4], CMS [5–9] and LHCb [10] collaborations at the LHC at colliding energies of $\sqrt{s} = 7, 8,$ and 13 TeV, as well as the CDF and DØ collaborations at $\sqrt{s} = 1.96$ TeV at the Tevatron [11–14]. Inclusive and differential fiducial cross section measurements for Higgs boson production, on the other hand, have been presented in [15–24]. Along with the progress in experimental precision, strides were also made in the fixed-order calculations. The QCD corrections are known up to third order for both the Drell-Yan processes [25–34] and Higgs production [35–53]. Electroweak corrections have mostly been studied for Drell-Yan production [54–60], but are known for Higgs production as well [61, 62].

Of the differential observables, the transverse momentum distribution of the colourless final state is of the particular concern in this work. Even though fixed order calculations are

able to produce reliable predictions in the majority of the phase space, substantial corrections can emerge from higher perturbative order within the low q_T regime, as a result of soft and collinear radiation, where the bulk of the cross section resides. Hence, in order to arrive at a sufficiently convergent result in perturbation theory, a variety of the resummation techniques that are capable of exponentiating *the most singular*, so-called leading power (LP), behaviour of the q_T distribution at every order have been developed in the past decades. Examples are the CSS formalism [63–68], the momentum space resummation [69–73], and the SCET-based analyses [74–80]. The subsequent resummation improved q_T distributions have been evaluated up to approximate $N^4\text{LL}$ accuracy [32, 72–74, 81–95] for the Drell-Yan process and $N^3\text{LL}'$ in the case of Higgs production [50, 53, 67, 71, 73, 89, 96–101] as to the Higgs production. Recently, to further improve the precision as well as the phase space coverage of the q_T resummation, the factorisation pattern of *the subleading power* contribution has been investigated within both the non-perturbative region $\Lambda_H \lesssim q_T \ll Q_H$ [102–112] and the perturbative zone $\Lambda_H \ll q_T \ll Q_H$ [113–115], where Λ_H and Q_H characterise the hadronic and hard scales in the process under consideration, respectively. At present, a resummation of those subleading power corrections has not been accomplished yet beyond LL.

Similarly, subleading power corrections also play a role in the limit $q_T \rightarrow 0$. Here, the LP approximation can only recover the most singular behaviour of the exact distribution at any given order in a fixed-order expansion, leaving behind integrable (but numerically problematic) singularities and constant terms. These non-vanishing remainders are of particular concern in q_T -based subtraction and slicing methods for higher-order calculations [73, 92, 99]. Related results on power suppressed contribution can be found from [90, 116–119] concerning the slicing subtraction method, the endpoint singularity in the Higgs production and decay [120–127], the event shapes in the leptonic and hadron colliders [128–136], and the threshold resummation [137–158].

To derive the factorisation formulae beyond the leading power approximation, one of the prerequisites is to consistently combine the contributions from the constituent dynamic regions, generally comprising the hard, collinear, and soft modes [102–115].¹ Although these dynamic regions are well defined in given segments of the phase space or the loop integrals, in practical calculations one often extrapolates their contributions from their respective intrinsic domains to the entire integration range, necessitating a robust systematic subtraction process to remove their overlap. This procedure is frequently referred to as the *zero-bin subtraction* [163–166], the soft subtraction [75, 164, 165, 167, 168], or the overlap reduction [114, 169, 170]. At leading power, zero-bin subtraction proceeds with deducting the soft contribution from the collinear sectors, and has been demonstrated to be valid up to $N^3\text{LO}$ [79, 80, 171–176]. Similar conclusions can also be found in the analysis of the subleading angular coefficients (suppressed by a factor of q_T/Q_H w.r.t. leading singular terms) in the Drell-Yan process and the semi-inclusive deep-inelastic scatterings [106–108, 110]. However, for the subleading inclusive observables of the Drell-Yan process the zero-bin subtraction

¹The irrelevance of the Glauber vertices is presumed in the subleading power factorisation of [102–115]. Up to now, a rigorous proof of the cancellation of the Glauber contributions beyond the leading power approximation is still absent, to our best knowledge. The leading power discussion on inclusive observables can be found in [159–162].

becomes more involved, as it comprises mixed contributions in the overlapping area from the lowest power accuracy up to NLP [114, 170].

Even though such recipes to construct zero-bin subtractions can establish a factorisation at the NLP level, a robust algorithm that is capable of generating zero-bin subtrahends at an arbitrary power and choice of a rapidity-divergence regularisation prescription is still missing. Investigations towards this goal were pioneered by [177], in which a mathematically well-defined derivation was delivered for the power series of the one-loop integrals in a variety of kinematical limits. Therein, the analysis of the massive Sudakov form factor is intimately related to the asymptotic behaviour of the q_T distribution. Their power expansion begins with the introduction of a group of auxiliary cutoff scales along the integration path, from which the relevant scales of the process are well separated and the defining dynamic regions can be prescribed accordingly. Within these regions, the expansions are straightforward and always well-defined. This is then followed by a recombination procedure to lift all dependences on the auxiliary scales, thereby extrapolating the expanded integrands from their intrinsic domains to the entire integration range. During this procedure, however, a set of constituents emerge, consisting of doubly and triply expanded integrands in line with their respective distinct scaling laws which account for the overlapping contributions amongst different modes and turn out to be in part the zero-bin subtrahends. While integrals with a single definite scaling rule for every integration variable are subjected only to a single expansion, multiple expansions can induce ambiguous interpretations of the resulting integral as the integration variables in general observe distinct scaling rules for each dynamic mode. Subsequently, this ambiguity limits the applicability of the formalism in [177] to only a special range of rapidity regularisation schemes, such as the analytic regulator [74, 76] and the pure rapidity regulator [113, 178]. When using more generic regularisation schemes, e.g. the exponential regulator [79, 80], doubly and triply expanded integrals instead call for an unambiguous counting rule at each power accuracy to yield results that are independent of the scheme. As a matter of fact, any reliance on the choice of rapidity regulators in carrying out the power expansion will hinder the establishment of the rapidity renormalisation group [77], which, akin to the renormalisation group governing the virtuality divergence, requires the equivalence of the power series resulting from various rapidity-divergence regularisation approaches.

In the following, we will make use of the NLO q_T distribution of the process $pp \rightarrow H + X$ as a demonstrative example to accomplish this goal. Since our derivation mainly concerns the pattern of the denominators of the squared transition amplitudes, the conclusion here can also be generalised to the analysis of the Drell-Yan processes, $pp \rightarrow V + X$ with $V = W, Z$. We commence by following the strategy outlined in [177] to categorise the phase space so as to detach the emerging scales and thereby carry out the expansion in momentum space. Afterwards, instead of extrapolating the expanded integrands on the cumulative level, in this work we shift the auxiliary boundaries at a particular power accuracy only while maintaining the equality to the power series derived from the momentum space. As a result, a set of multiple expanded integrals emerge to balance the overextended collinear sectors power by power. We use these to construct the zero-bin subtrahends and thereby retrieve the scalings for the occurring integration variables. We will demonstrate that the zero-bin subtrahends proposed in this paper are straightforwardly applicable to all rapidity regulators

that preserve their expressions before and after asymptotic expansions, including the analytic regulator [74, 76], the exponential regulator [79, 80], and the pure rapidity regulator [113, 178]. In addition, with a few adaptations, our algorithm presented here can also be generalised to use the Δ -regulator [75, 166, 171, 172, 179] and the η -regulator [77, 78]. This accommodates the majority of the rapidity-divergence regularisation schemes in use at this time.

Our paper is organised as follows. In section 2 we develop our framework to compute, in a general way, all power corrections to NLO accuracy. To this end, we will use section 2.1 and 2.2, taking the example of Higgs hadroproduction at LHC, to review the fixed order calculation on the q_T spectrum and thereby categorise the phase space into two sectors according to the origins of the power corrections. The first sector, associated with the asymptotic expansion of the boundary condition, will be investigated in section 2.3. The other one takes in the bulk of phase space and thus forms the main concern of this paper. We will devote section 2.4 to elaborate on its expansion procedure, in particular highlighting the structural pattern of the emerging zero-bin subtrahends. At last, in section 2.5, we combine the relevant ingredients and present the power series of the q_T spectrum of our example process $pp \rightarrow H + X$. Section 3 then is dedicated to the application of the framework derived in section 2, where the power corrections will be appraised up to N²LP for the first time. We calculate it in three different approaches, including the momentum cutoff scales, the homogenous regularisation scheme, and the inhomogeneous regulator, to regulate the rapidity divergences. We will demonstrate that after appropriate combination, all three methods result in the same analytic expressions at least up to N²LP, echoing the rapidity renormalisation group [77]. Finally, we will scrutinise our N²LP results in section 4 by comparing to the full QCD calculation. Eventually, we summarise our findings in section 5.

2 Theoretical framework

In this section, we introduce the formalism to be utilised in the next-to-leading and next-to-next-to-leading power expansions, dubbed NLP and N²LP respectively. We will use the case of Higgs production at hadron colliders, $p + p \rightarrow H + X$, as an illustrative example. The results we derive, however, are similarly applicable to the production of any other colour-neutral final state.

2.1 Analysis of the NLO fixed order results

To introduce our notation, we start our analysis by recalling the general expression for the differential cross section of the process $p + p \rightarrow H + X$ in proton-proton collisions. According to the QCD factorization theorem [180], the differential q_T spectra at NLO can be calculated as follows,

$$\begin{aligned} \frac{d\sigma_H}{dY_H dq_T^2} &= \frac{1}{16\pi s^2} \sum_{i,j} \int_0^{k_+^{\max}} dk_+ \int_0^{k_-^{\max}} dk_- \delta(k_+ k_- - q_T^2) \frac{f_{i/n}(\xi_n)}{\xi_n} \frac{f_{j/\bar{n}}(\xi_{\bar{n}})}{\xi_{\bar{n}}} \overline{\sum_{\text{col,pol}} |\mathcal{M}(i+j \rightarrow H+k)|^2} \\ &= \frac{1}{16\pi s^2} \sum_{i,j} \int_{k_+^{\min}}^{k_+^{\max}} \frac{dk_+}{k_+} \frac{f_{i/n}(\xi_n)}{\xi_n} \frac{f_{j/\bar{n}}(\xi_{\bar{n}})}{\xi_{\bar{n}}} \overline{\sum_{\text{col,pol}} |\mathcal{M}(i+j \rightarrow H+k)|^2}, \end{aligned} \tag{2.1}$$

where \sqrt{s} denotes the collider centre-of-momentum energy of the incoming protons. Y_H and q_T stand for the rapidity and transverse momentum of the Higgs boson measured in

the laboratory reference frame, respectively. The boundaries of the phase space integral are given by the variables k_+^{\max} and k_+^{\min} , with

$$k_+^{\max} = \sqrt{s} - m_T e^{-Y_H}, \quad k_+^{\min} = \frac{q_T^2}{k_-^{\max}} = \frac{q_T^2}{\sqrt{s} - m_T e^{+Y_H}}. \quad (2.2)$$

Therein, $m_T^2 \equiv m_H^2 + q_T^2$ is the transverse mass of the Higgs boson, m_H being the mass of the Higgs boson.

In the integrand of eq. (2.1), $f_{i/n}$ and $f_{j/\bar{n}}$ represent the parton distribution functions (PDFs) for the partons i and j in the protons n and \bar{n} , respectively, with the argument $\xi_{n(\bar{n})}$ encoding the momentum fractions carried by the incident particle $i(j)$ with respect to its mother proton $n(\bar{n})$. In this paper, we will use the 5 flavour scheme, and correspondingly, the partons $\{i, j, k\} \in \{u, \bar{u}, d, \bar{d}, c, \bar{c}, s, \bar{s}, b, \bar{b}, g\}$ will be considered massless and taken fully into account in the following analysis.

$|\mathcal{M}|^2$ denotes the squared amplitudes for the contributing partonic channel $i + j \rightarrow H + k$. Since the main focus of this paper is on the region where q_T approaches, but is not equal to, zero, only tree level contributions will participate in eq. (2.1). In the large top mass limit, the amplitudes for the processes $i + j \rightarrow H + k$ can be calculated in the low energy Higgs effective field theory (HEFT) [181–187]. Therein, the creation and annihilation of the Higgs boson are governed by the effective Lagrangian,

$$\mathcal{L}_{\text{eff}} = \frac{\alpha_s(\mu)}{12\pi v} C_t(m_t, \mu) G^{\mu\nu, a} G_{\mu\nu}^a H, \quad (2.3)$$

where α_s stands for the strong coupling constant and v denotes the Higgs vacuum expectation value, while H and $G_{\mu\nu}^a$ represent the Higgs field operator and the gluon field strength tensor, respectively. The closed top quark loop, coupling the gluons to the Higgs, is encoded by the Wilson coefficient C_t , which, up to now, has been calculated up to the four-loop order [185, 187–192]. In this work, we only take into account its LO contribution in accordance with the perturbative accuracy of eq. (2.1). In writing eq. (2.3), we have omitted the operators inducing the Higgs-light-quark interaction, as the 5 active flavour scheme is adhered to throughout our investigation.

Combining eq. (2.3) with the QCD Lagrangian enables the generation of the squared amplitudes for the process $i + j \rightarrow H + k$. Having summed and averaged, as appropriate, over all the colour and polarisation configurations, the results read [193, 194],

$$\begin{aligned} \overline{\sum_{\text{col, pol}}} |\mathcal{M}(g + g \rightarrow H + g)|^2 &= \frac{3\lambda_t^2}{32} \frac{m_H^8 + s_{ij}^4 + s_{ik}^4 + s_{jk}^4}{s_{ij}s_{ik}s_{jk}}, \\ \overline{\sum_{\text{col, pol}}} |\mathcal{M}(g + q(\bar{q}) \rightarrow H + q(\bar{q}))|^2 &= -\frac{\lambda_t^2}{24} \frac{s_{ij}^2 + s_{ik}^2}{s_{jk}}, \\ \overline{\sum_{\text{col, pol}}} |\mathcal{M}(q + \bar{q} \rightarrow H + g)|^2 &= \frac{\lambda_t^2}{9} \frac{s_{ik}^2 + s_{jk}^2}{s_{ij}}, \end{aligned} \quad (2.4)$$

where the parameter λ_t is introduced to collect the coupling constants, i.e. $\lambda_t^2 \equiv 4\alpha_s^3 C_t^2 / (9\pi v^2)$. The missing expressions for $q(\bar{q})g$ and $\bar{q}q$ initial states can be derived from the above by swapping the roles of i and j .

The expressions in eq. (2.4) involve the scalar products of the momenta of the initial and final particles,

$$\begin{aligned}
 s_{ij} &= 2p_i \cdot p_j = \left(k_+ + m_{\text{T}}e^{-Y_H}\right) \left(k_- + m_{\text{T}}e^{+Y_H}\right), \\
 s_{ik} &= -2p_i \cdot p_k = -\left(k_+ + m_{\text{T}}e^{-Y_H}\right) k_-, \\
 s_{jk} &= -2p_j \cdot p_k = -\left(k_- + m_{\text{T}}e^{+Y_H}\right) k_+.
 \end{aligned}
 \tag{2.5}$$

Therein, k_{\pm} denotes the light cone component of the momentum of the emitted parton k . To be precise, with the help of the light-like reference vectors n^{μ} and \bar{n}^{μ} , aligned with incoming beams and satisfying $n \cdot \bar{n} = 2$, it is defined as

$$p_k^{\mu} = \frac{p_k \cdot n}{2} \bar{n}^{\mu} + \frac{p_k \cdot \bar{n}}{2} n^{\mu} + p_{k,\perp}^{\mu} \equiv \frac{k_-}{2} \bar{n}^{\mu} + \frac{k_+}{2} n^{\mu} + k_{\perp}^{\mu} \equiv [k_-, k_+, k_{\perp}].
 \tag{2.6}$$

In this notation, the momentum fractions ξ_n and $\xi_{\bar{n}}$ of eq. (2.1) can be written as

$$\xi_n = \frac{k_+ + m_{\text{T}}e^{-Y_H}}{\sqrt{s}} \quad \text{and} \quad \xi_{\bar{n}} = \frac{k_- + m_{\text{T}}e^{+Y_H}}{\sqrt{s}}.
 \tag{2.7}$$

In the following sections, we will investigate the asymptotic properties of eq. (2.1) in the vicinity of $q_{\text{T}} = 0$, adhering to the following definition of the expansion accuracy, counting powers of q_{T}^2 , throughout,

$$\frac{d\sigma_H}{dY_H dq_{\text{T}}^2} = \underbrace{\sum_m \frac{\Delta_{\text{LP}}^{(m)} (L_H)^m}{q_{\text{T}}^2}}_{\text{LP}} + \underbrace{\sum_m \Delta_{\text{NLP}}^{(m)} (L_H)^m}_{\text{NLP}} + \underbrace{\sum_m q_{\text{T}}^2 \Delta_{\text{N}^2\text{LP}}^{(m)} (L_H)^m}_{\text{N}^2\text{LP}} + \dots
 \tag{2.8}$$

Therein, the q_{T} differential distribution in eq. (2.1) is expanded in the low q_{T} domain. At a given power precision, e.g. $\text{N}^{\omega+1}\text{LP}$, all non-logarithmic q_{T} dependences have been collected in the pre-factor $q_{\text{T}}^{2\omega}$ with ($\omega \geq -1$). They leave behind the logarithmic terms $L_H \equiv \ln[q_{\text{T}}^2/m_H^2]$ and the coefficient functions $\Delta_{\text{N}^{\omega+1}\text{LP}}^{(m)} \equiv \Delta_{\text{N}^{\omega+1}\text{LP}}^{(m)}[m_H, s, Y_H; f_{i/n}, f_{j/\bar{n}}]$ which accounts for the convolution of the PDFs $f_{i/n}$ and $f_{j/\bar{n}}$ as well as the functions of the hard scales s and m_H . According to this definition, the LP contribution is expected to accommodate the most singular behaviour in the low q_{T} regime, while the higher power corrections experience progressively stronger suppression factor $q_{\text{T}}^{2(\omega-1)}$. Correspondingly, Δ_{LP} is known extremely precisely, up to approximate fourth order [100, 173–176, 179, 187, 189–191, 195–210], while the Δ_{NLP} has only been computed recently to NLO accuracy [113]. All further higher-power corrections are hitherto unknown, and we will use the remainder of this section to introduce a mathematically well-defined approach to develop a framework to compute the $\Delta_{\text{N}^{\omega+1}\text{LP}}$ for all $\omega \geq -1$ at NLO accuracy before deriving the respective NLO-correct expression for $\Delta_{\text{N}^2\text{LP}}$ explicitly.

In the following subsections we will be evaluating the coefficients $\Delta_{\text{N}^{\omega+1}\text{LP}}^{(m)}$. In section 2.2, we will derive additional power corrections originating from the kinematics of the process and thereby categorise the phase space integral of eq. (2.1) into two sectors. The first sector encompasses the domains in the vicinity of k_+^{max} and k_-^{max} , accounting for the power suppressed contributions induced by the boundary conditions of the phase space integral, see eq. (2.2). We will make use of section 2.3 to discuss the asymptotic properties from this

region. The second sector consists of the remaining regions, entailing a variety of scales along the integration path and is therefore the main concern of this paper. We will elaborate in section 2.4 on the power expansion of this contribution. Eventually, with the results of the two, we are capable of deriving the power series for the q_T spectrum in section 2.5.

2.2 Prerequisites for the power expansion

We start the discussion with the transformation of the squared amplitudes of eq. (2.4). As the power expansion in the low q_T domain primarily concerns the relation of the kinematic variables k_\pm and $m_T e^{\pm Y_H}$, it is beneficial for us to regroup the results in eq. (2.4) according to their k_\pm and $m_T e^{\pm Y_H}$ dependences. To this end, it merits reminding that the numerators of the $|\mathcal{M}|^2$ can be all recast in terms of the polynomials in the invariants s_{ij} , s_{ik} , and s_{jk} , on account of the on-shell condition $m_H^2 = s_{ij} + s_{ik} + s_{jk}$. Hence, with eq. (2.5) and carrying out the polynomial expansion, the numerators of the $|\mathcal{M}|^2$ are then cast into a finite series of the products of k_\pm and $m_T e^{\pm Y_H}$, more specifically,

$$\overline{\sum_{\text{col,pol}} |\mathcal{M}_{[\kappa]}|^2} \Big|_{\text{Numerator}} \rightarrow \sum_{m,n} (k_+)^m (k_-)^n c_{[\kappa]}^{m,n} (m_T, Y_H), \quad (2.9)$$

where the contributing partonic channels are denoted by the subscript $\kappa = \{gg, gq(\bar{q}), q(\bar{q})g, q\bar{q}, \bar{q}q\}$. The coefficients $c_{[\kappa]}^{m,n}$ are a function of the hard scales $m_T e^{\pm Y_H}$, with the superscripts $\{m, n\} \geq 0$ corresponding to the powers of k_\pm . Combining eq. (2.9) with the denominators of the $|\mathcal{M}|^2$ in eq. (2.4) and factoring out common prefactors consisting of the coupling parameter λ_t and the colliding energy \sqrt{s} , it yields that,

$$\overline{\sum_{\text{col,pol}} |\mathcal{M}_{[\kappa]}|^2} \equiv 16\pi \lambda_t^2 s \sum_{\{\beta\}} \sum_{\rho, \sigma} \frac{(k_+)^{\rho}}{(k_+ + m_T e^{-Y_H})^{\beta_n - 1}} \frac{(k_-)^{\sigma}}{(k_- + m_T e^{Y_H})^{\beta_{\bar{n}} - 1}} \mathcal{H}_{[\kappa], \{\beta\}}^{\rho, \sigma} (m_T, Y_H, s), \quad (2.10)$$

where a novel hard sector $\mathcal{H}_{[\kappa], \{\beta\}}^{\rho, \sigma}$ is introduced to assimilate the $c_{[\kappa], \{\beta\}}^{\rho, \sigma}$ of eq. (2.9) as well as the colliding energy \sqrt{s} . Based on eq. (2.4), the indices ρ and σ as well as β_n and $\beta_{\bar{n}}$ in $\mathcal{H}_{[\kappa], \{\beta\}}^{\rho, \sigma}$ are always integers for the process $pp \rightarrow H + X$ at NLO. At variance with m and n in eq. (2.9), the superscripts ρ and σ in eq. (2.10) can be of negative value, as the squared amplitudes in the $g + g \rightarrow H + g$ and $g + q(\bar{q}) \rightarrow H + q(\bar{q})$ channels are both able to contribute additional light-cone components k_\pm from the denominators, thereby lowering the powers of eq. (2.9). β_n and $\beta_{\bar{n}}$, however, also following eq. (2.4), are always taken greater than or equal to one. At last, it should be emphasised that the parameterisation in eq. (2.10) is not unique, since one can always reweight the numerator and denominator of the results in eq. (2.4) by a common factor, e.g. $(k_- + m_T e^{+Y_H})^2$, and then expand the numerator without modifying the fraction. Although this arbitrariness may impact the expressions of individual $\mathcal{H}_{[\kappa], \{\beta\}}^{\rho, \sigma}$ in eq. (2.10), but will not impact the squared amplitudes $|\mathcal{M}|^2$.

Substituting eq. (2.10) together with eq. (2.7) into eq. (2.1), we recast the q_T spectrum as,

$$\begin{aligned} \frac{d\sigma_H}{dY_H dq_T^2} &= \lambda_t^2 \sum_{\kappa} \sum_{\{\beta\}} \sum_{\rho, \sigma} \mathcal{H}_{[\kappa], \{\beta\}}^{\rho, \sigma} (m_T, Y_H, s) \\ &\quad \times \int_{k_+^{\min}}^{k_+^{\max}} \frac{dk_+}{k_+} (k_-)^{\rho} (k_+)^{\sigma} F_{i/n, \beta_n}^{(0)} \left(k_+ + m_T e^{-Y_H} \right) F_{j/\bar{n}, \beta_{\bar{n}}}^{(0)} \left(k_- + m_T e^{+Y_H} \right). \end{aligned} \quad (2.11)$$

Herein, the integrand contains the derivatives of the scaled PDFs of the light-cone components ($k_{\pm} + m_{\text{T}} e^{\mp Y_H}$), generically defined as

$$F_{i/n, \beta_n}^{(\alpha_n)}(Q_n) \equiv \frac{\partial^{\alpha_n}}{\partial Q_n^{\alpha_n}} \left[\frac{f_{i/n}(Q_n/\sqrt{s})}{Q_n^{\beta_n}} \right], \quad F_{j/\bar{n}, \beta_{\bar{n}}}^{(\alpha_{\bar{n}})}(Q_{\bar{n}}) \equiv \frac{\partial^{\alpha_{\bar{n}}}}{\partial Q_{\bar{n}}^{\alpha_{\bar{n}}}} \left[\frac{f_{j/\bar{n}}(Q_{\bar{n}}/\sqrt{s})}{Q_{\bar{n}}^{\beta_{\bar{n}}}} \right], \quad (2.12)$$

where Q_n and $Q_{\bar{n}}$ represent the two kinematic variables, α_n and $\alpha_{\bar{n}}$ determine the rank of the derivative, and β_n and $\beta_{\bar{n}}$ are the powers to which they scale their respective PDFs. Collectively, we denote the latter $\{\alpha\}$ and $\{\beta\}$.

For the results derived in full QCD, see eq. (2.1), only the zero-rank scaled PDFs are involved. Hence, only the $\alpha_n = \alpha_{\bar{n}} = 0$ case is present in eq. (2.11). The $\alpha_n, \alpha_{\bar{n}} > 0$ expressions, however, will enter in the higher-power q_{T} expansion.

In the following, we will concern ourselves with the analytic properties of the functions $F_{i/n, \beta_n}^{(\alpha_n)}(Q_n)$ and $F_{j/\bar{n}, \beta_{\bar{n}}}^{(\alpha_{\bar{n}})}(Q_{\bar{n}})$. However, due to the fact that the PDFs $f_{i/n}$ and $f_{j/\bar{n}}$ have their origin in the non-perturbative regime of QCD and, thus, their analytic expressions are not fully established, we make the following assumptions:

- (a) For a given $\alpha_n, \alpha_{\bar{n}} > 0$ the $F_{i/n, \beta_n}^{(\alpha_n)}(Q_n)$ and $F_{j/\bar{n}, \beta_{\bar{n}}}^{(\alpha_{\bar{n}})}(Q_{\bar{n}})$, as well as their arbitrary order derivatives, exist and are bounded over the domain $\Lambda_{\text{H}} \leq Q_{n(\bar{n})} \leq \sqrt{s}$ for all β_n and $\beta_{\bar{n}}$, where Λ_{H} represents a hadronisation scale.
- (b) $F_{i/n, \beta_n}^{(\alpha_n)}(Q_n + \delta Q_n)$ and $F_{j/\bar{n}, \beta_{\bar{n}}}^{(\alpha_{\bar{n}})}(Q_{\bar{n}} + \delta Q_{\bar{n}})$ have convergence radii $|\delta Q_{n(\bar{n})}| < Q_{n(\bar{n})}$ as long as $(Q_{n(\bar{n})} + \delta Q_{n(\bar{n})})$ and $Q_{n(\bar{n})}$ are both well within the interval $[\Lambda_{\text{H}}, \sqrt{s}]$.

Please note, if the PDFs are fitted in a basis of Chebyshev polynomials, as proposed in [211–213], and thereby $f_{i/n}$ and $f_{j/\bar{n}}$ can be then expressed in terms of $\ln^k(\xi_n)/\xi_n^h$ and $\ln^k(\xi_{\bar{n}})/\xi_{\bar{n}}^h$, respectively, the second assumption is immediately fulfilled.

Equipped with the above ansatz, we are able to expand eq. (2.11) in the vicinity of $q_{\text{T}} = 0$. To this end, we start with the expansion of the kinematic variable m_{T} in the hard coefficient function $\mathcal{H}_{[\kappa], \{\beta\}}^{\rho, \sigma}$. In the small q_{T} domain where $q_{\text{T}} \ll m_{\text{H}}$, we can perform an expansion of the transverse mass m_{T} of the Higgs boson around its invariant mass m_{H} ,

$$m_{\text{T}} = m_{\text{H}} \cdot \sum_{h=0}^{\infty} \frac{1}{h!} \frac{\Gamma[\frac{3}{2}]}{\Gamma[\frac{3}{2} - h]} \left(\frac{q_{\text{T}}^2}{m_{\text{H}}^2} \right)^h. \quad (2.13)$$

We can use this result to expand the hard coefficient $\mathcal{H}_{[\kappa], \{\beta\}}^{\rho, \sigma}$ around $q_{\text{T}} = 0$, giving

$$\begin{aligned} & \mathcal{H}_{[\kappa], \{\beta\}}^{\rho, \sigma}(m_{\text{T}}, Y_H, s) \\ &= \sum_{h=0}^{\infty} \frac{(m_{\text{T}} - m_{\text{H}})^h}{h!} \left\{ \frac{\partial^h}{\partial m_{\text{T}}^h} \mathcal{H}_{[\kappa], \{\beta\}}^{\rho, \sigma}(m_{\text{T}}, Y_H, s) \Big|_{m_{\text{T}} \rightarrow m_{\text{H}}} \right\} \\ &= \sum_{h,l=0}^{\infty} \sum_{g=0}^h \frac{(-1)^{h-g}}{g! l! (h-g)!} \frac{\Gamma[\frac{g}{2} + 1]}{\Gamma[\frac{g}{2} - l + 1]} \left(\frac{q_{\text{T}}^2}{m_{\text{H}}^2} \right)^l m_{\text{H}}^h \mathcal{H}_{[\kappa], \{\beta\}}^{(h), \rho, \sigma}(m_{\text{H}}, Y_H, s), \end{aligned} \quad (2.14)$$

where we have introduced $\mathcal{H}_{[\kappa], \{\beta\}}^{(h), \rho, \sigma}(m_{\text{H}}, Y_H, s) \equiv \frac{\partial^h}{\partial m_{\text{T}}^h} \mathcal{H}_{[\kappa], \{\beta\}}^{\rho, \sigma}(m_{\text{T}}, Y_H, s) \Big|_{m_{\text{T}} \rightarrow m_{\text{H}}}$. An analogous expansion can also be applied to the derivatives of the scaled PDFs $F_{i/n, \beta_n}^{(\alpha_n)}$ and $F_{j/\bar{n}, \beta_{\bar{n}}}^{(\alpha_{\bar{n}})}$.

To this end, we re-express their arguments below in order to isolate all q_T dependences,

$$k_{\pm} + m_T e^{\mp Y_H} \rightarrow \left[k_{\pm} + m_H e^{\mp Y_H} \right] + (m_T - m_H) e^{\mp Y_H}. \quad (2.15)$$

In proximity to $q_T = 0$, the second term on the right handed side (r.h.s) is always smaller in magnitude with respect to the first one. Therefore, we can expand $F_{i/n, \beta_n}^{(\alpha_n)}(k_+ + m_T e^{-Y_H})$ and $F_{j/\bar{n}, \beta_{\bar{n}}}^{(\alpha_{\bar{n}})}(k_- + m_T e^{+Y_H})$ around $(k_+ + m_H e^{-Y_H})$ and $(k_- + m_H e^{+Y_H})$, respectively,

$$\begin{aligned} & F_{i/n, \beta_n}^{(0)}(k_+ + m_T e^{-Y_H}) \\ &= \sum_{h=0}^{\infty} \frac{(m_T - m_H)^h}{h!} (e^{-Y_H})^h F_{i/n, \beta_n}^{(h)}(k_+ + m_H e^{-Y_H}) \\ &= \sum_{h,l=0}^{\infty} \sum_{g=0}^h \frac{(-1)^{h-g}}{g! l! (h-g)!} \frac{\Gamma[\frac{g}{2} + 1]}{\Gamma[\frac{g}{2} - l + 1]} \left(\frac{q_T^2}{m_H^2} \right)^l (m_H e^{-Y_H})^h F_{i/n, \beta_n}^{(h)}(k_+ + m_H e^{-Y_H}), \\ & F_{j/\bar{n}, \beta_{\bar{n}}}^{(0)}(k_- + m_T e^{+Y_H}) \\ &= \sum_{h=0}^{\infty} \frac{(m_T - m_H)^h}{h!} (e^{+Y_H})^h F_{j/\bar{n}, \beta_{\bar{n}}}^{(h)}(k_- + m_H e^{+Y_H}) \\ &= \sum_{h,l=0}^{\infty} \sum_{g=0}^h \frac{(-1)^{h-g}}{g! l! (h-g)!} \frac{\Gamma[\frac{g}{2} + 1]}{\Gamma[\frac{g}{2} - l + 1]} \left(\frac{q_T^2}{m_H^2} \right)^l (m_H e^{+Y_H})^h F_{j/\bar{n}, \beta_{\bar{n}}}^{(h)}(k_- + m_H e^{+Y_H}). \end{aligned} \quad (2.16)$$

Inserting the expressions of eqs. (2.14)–(2.16) into eq. (2.11), the q_T spectrum now takes the following form,

$$\frac{d\sigma_H}{dY_H dq_T^2} = \lambda_t^2 \sum_{\omega} (q_T^2)^{\omega} \sum_{[\kappa]} \sum_{\{\alpha, \beta\}} \sum_{\rho, \sigma} \tilde{\mathcal{H}}_{[\kappa], \{\alpha, \beta\}}^{(\omega), \rho, \sigma}(m_H, Y_H, s) \left\{ \tilde{\mathcal{I}}_{[\kappa], \{\alpha, \beta\}}^{\rho, \sigma} + \Delta \tilde{\mathcal{I}}_{[\kappa], \{\alpha, \beta\}}^{\rho, \sigma} \right\}. \quad (2.17)$$

Therein, $\tilde{\mathcal{H}}_{[\kappa], \{\alpha, \beta\}}^{(\omega), \rho, \sigma}$ is introduced to absorb the factorials, gamma functions, as well as powers of the hard scales m_H and \sqrt{s} emerging from eqs. (2.14)–(2.16),

$$\begin{aligned} \tilde{\mathcal{H}}_{[\kappa], \{\alpha, \beta\}}^{(\omega), \rho, \sigma} &= \left(\frac{1}{m_H^2} \right)^{\omega} \sum_{l_n=0}^{\omega} \sum_{l_{\bar{n}}=0}^{\omega-l_n} \sum_{\alpha_h=0}^{\infty} \prod_{x=\{h, n, \bar{n}\}} \left\{ \sum_{g_x=0}^{\alpha_x} \frac{(-1)^{\alpha_x - g_x}}{g_x! l_x! (\alpha_x - g_x)!} \frac{\Gamma[\frac{g_x}{2} + 1]}{\Gamma[\frac{g_x}{2} - l_x + 1]} \right\} \\ &\times (m_H e^{-Y_H})^{\alpha_n} (m_H e^{+Y_H})^{\alpha_{\bar{n}}} (m_H)^{\alpha_h} \mathcal{H}_{[\kappa], \{\alpha, \beta\}}^{(\alpha_h), \rho, \sigma}, \end{aligned} \quad (2.18)$$

where $l_h = \omega - l_n - l_{\bar{n}} \geq 0$. The q_T dependences have been factored out from $\tilde{\mathcal{H}}_{[\kappa], \{\alpha, \beta\}}^{(\omega), \rho, \sigma}$ and the arguments of $F_{i/n, \beta_n}^{(\alpha_n)}$ and $F_{j/\bar{n}, \beta_{\bar{n}}}^{(\alpha_{\bar{n}})}$. The remaining ones participate through boundary conditions as defined in eq. (2.2). To address them as well, we divide the phase space integral of eq. (2.17) into two sectors, $\tilde{\mathcal{I}}_{[\kappa], \{\alpha, \beta\}}^{\rho, \sigma}$ and $\Delta \tilde{\mathcal{I}}_{[\kappa], \{\alpha, \beta\}}^{\rho, \sigma}$, with

$$\tilde{\mathcal{I}}_{[\kappa], \{\alpha, \beta\}}^{\rho, \sigma} = \int_{\tilde{k}_+^{\min}}^{\tilde{k}_+^{\max}} \frac{dk_+}{k_+} (k_-)^{\rho} (k_+)^{\sigma} F_{i/n, \beta_n}^{(\alpha_n)}(k_+ + m_H e^{-Y_H}) F_{j/\bar{n}, \beta_{\bar{n}}}^{(\alpha_{\bar{n}})}(k_- + m_H e^{+Y_H}), \quad (2.19)$$

$$\Delta \tilde{\mathcal{I}}_{[\kappa], \{\alpha, \beta\}}^{\rho, \sigma} = \left(\int_{\tilde{k}_+^{\max}}^{\tilde{k}_+^{\min}} + \int_{\tilde{k}_+^{\min}}^{\tilde{k}_+^{\max}} \right) \frac{dk_+}{k_+} (k_-)^{\rho} (k_+)^{\sigma} F_{i/n, \beta_n}^{(\alpha_n)}(k_+ + m_H e^{-Y_H}) F_{j/\bar{n}, \beta_{\bar{n}}}^{(\alpha_{\bar{n}})}(k_- + m_H e^{+Y_H}), \quad (2.20)$$

by means of the following boundaries,

$$\tilde{k}_+^{\max} = \sqrt{s} - m_H e^{-Y_H}, \quad \tilde{k}_+^{\min} = q_T^2 / (\sqrt{s} - m_H e^{+Y_H}). \quad (2.21)$$

Consequently, $\Delta \tilde{\mathcal{I}}_{[\kappa],\{\alpha,\beta\}}^{\rho,\sigma}$ contains all m_T dependences. In analysing the scaling behaviour, we find that within the central region $e^{\pm Y_H} \sim \mathcal{O}(1)$, the integration variables k_{\pm} exhibit unambiguous scaling in each integration region. Therefore, as will be illustrated in section 2.3, the power expansion of $\Delta \tilde{\mathcal{I}}_{[\kappa],\{\alpha,\beta\}}^{\rho,\sigma}$ follows an analogous pattern to those in eqs. (2.14)–(2.16). Nevertheless, $\tilde{\mathcal{I}}_{[\kappa],\{\alpha,\beta\}}^{\rho,\sigma}$ behaves differently. From its expression in eq. (2.19), a number of different scales have been enclosed in the integration range of $\tilde{\mathcal{I}}_{[\kappa],\{\alpha,\beta\}}^{\rho,\sigma}$, starting from the ultrasoft scale $k_+^{\min} \sim \mathcal{O}(q_T^2/m_H)$, through the soft one $k_{\pm} \sim \mathcal{O}(q_T)$, and ending up with the hard scale $k_+^{\max} \sim \mathcal{O}(m_H)$. They all correspond to a distinct way of expanding the integrands. To this end, in section 2.4, we will make use of a set of momentum cutoffs to unambiguously treat them.

2.3 Power corrections on the boundary

We have mentioned above that besides the integrand itself, the integration boundaries are other sources for power corrections. In the following, we will thus expand the integral $\Delta \tilde{\mathcal{I}}_{[\kappa],\{\alpha,\beta\}}^{\rho,\sigma}$ within the central region $e^{\pm Y_H} \sim \mathcal{O}(1)$. As illustrated in eq. (2.20), $\Delta \tilde{\mathcal{I}}_{[\kappa],\{\alpha,\beta\}}^{\rho,\sigma}$ consists of the integral of k_+ over two intervals, $k_+ \in [\tilde{k}_+^{\max}, k_+^{\max}]$ and $k_+ \in [k_+^{\min}, \tilde{k}_+^{\min}]$. In each of them, the momentum k^{μ} of the emitted particle is subject to an unambiguous scaling,

$$k_+ \in [\tilde{k}_+^{\max}, k_+^{\max}] : \quad k_+ \sim \mathcal{O}(m_H), \quad k_- \sim \mathcal{O}(q_T^2/m_H), \quad \vec{k}_T = -\vec{q}_T, \quad (2.22)$$

$$k_+ \in [k_+^{\min}, \tilde{k}_+^{\min}] : \quad k_+ \sim \mathcal{O}(q_T^2/m_H), \quad k_- \sim \mathcal{O}(m_H), \quad \vec{k}_T = -\vec{q}_T, \quad (2.23)$$

where the transverse recoil \vec{k}_T is determined by the momentum conservation. Considering that the momenta k_{\pm} in eqs. (2.22)–(2.23) are nearly corresponding to the hardest emission along the beam direction that are kinematically allowed (in a logarithmic sense), henceforth, we dub them the n -ultra-collinear and \bar{n} -ultra-collinear modes, respectively. In the following, we will make use of those two scaling laws to expand $\Delta \tilde{\mathcal{I}}_{[\kappa],\{\alpha,\beta\}}^{\rho,\sigma}$ within the low q_T regime.

We first consider the n -ultra-collinear contribution, applying eq. (2.22) to eq. (2.20) yields

$$\begin{aligned} \Delta \tilde{\mathcal{I}}_{[\kappa],\{\alpha,\beta\}}^{\rho,\sigma} \Big|_{uc} &= \int_{\tilde{k}_+^{\max}}^{k_+^{\max}} \frac{dk_+}{k_+} (k_-)^{\rho} (k_+)^{\sigma} F_{i/n,\beta_n}^{(\alpha_n)} \left(k_+ + m_H e^{-Y_H} \right) F_{j/\bar{n},\beta_{\bar{n}}}^{(\alpha_{\bar{n}})} \left(k_- + m_H e^{+Y_H} \right) \\ &= (q_T^2)^{\rho} \int_0^{(m_H - m_T) e^{-Y_H}} d\hat{k}_+ (\hat{k}_+ + \tilde{k}_+^{\max})^{\sigma - \rho - 1} \\ &\quad \times F_{i/n,\beta_n}^{(\alpha_n)} \left(\hat{k}_+ + \sqrt{s} \right) F_{j/\bar{n},\beta_{\bar{n}}}^{(\alpha_{\bar{n}})} \left(\frac{q_T^2}{\hat{k}_+ + \tilde{k}_+^{\max}} + m_H e^{+Y_H} \right) \\ &= \sum_{\tilde{\alpha}_n, \tilde{\alpha}_{\bar{n}}=0}^{\infty} \frac{(q_T^2)^{\rho + \tilde{\alpha}_{\bar{n}}}}{\tilde{\alpha}_n! \tilde{\alpha}_{\bar{n}}!} F_{i/n,\beta_n}^{(\alpha_n + \tilde{\alpha}_n)} (\sqrt{s}) F_{j/\bar{n},\beta_{\bar{n}}}^{(\alpha_{\bar{n}} + \tilde{\alpha}_{\bar{n}})} (m_H e^{+Y_H}) \mathcal{B}_{+,\{\alpha,\beta\}}^{\rho,\sigma}, \end{aligned} \quad (2.24)$$

where in the second step the integration variable is transformed such that the power suppressed residual terms can be extracted, i.e.

$$k_+ \rightarrow \underbrace{\hat{k}_+}_{\sim \mathcal{O}(q_T^2/m_H)} + \underbrace{\tilde{k}_+^{\max}}_{\sim \mathcal{O}(m_H)}. \quad (2.25)$$

Based on this scaling behaviour, the functions $F_{i/n,\beta_n}^{(\alpha_n)}$ and $F_{j/\bar{n},\beta_{\bar{n}}}^{(\alpha_{\bar{n}})}$ can be expanded around \sqrt{s} and $m_H e^{+Y_H}$, respectively, in the last step of eq. (2.24), thereby removed from the \hat{k}_+ -integral. The remaining \hat{k}_+ dependences are collected in the function $\mathcal{B}_{+,\{\alpha,\beta\}}^{\rho,\sigma}$, defined through

$$\begin{aligned} \mathcal{B}_{+,\{\alpha,\beta\}}^{\rho,\sigma} &\equiv \int_0^{(m_H - m_T)e^{-Y_H}} d\hat{k}_+ (\hat{k}_+ + \tilde{k}_+^{\max})^{\sigma - \rho - \tilde{\alpha}_{\bar{n}} - 1} (\hat{k}_+)^{\tilde{\alpha}_n} \\ &= \int_0^{(m_H - m_T)e^{-Y_H}} d\hat{k}_+ (\hat{k}_+)^{\tilde{\alpha}_n} (\tilde{k}_+^{\max})^{\sigma - \rho - \tilde{\alpha}_{\bar{n}} - 1} \\ &\quad \times \left\{ \theta(\sigma - \rho - \tilde{\alpha}_{\bar{n}} - 1) \sum_{\gamma=0}^{\sigma - \rho - \tilde{\alpha}_{\bar{n}} - 1} \frac{1}{\gamma!} \left(\frac{\hat{k}_+}{\tilde{k}_+^{\max}} \right)^\gamma \frac{\Gamma[\sigma - \rho - \tilde{\alpha}_{\bar{n}}]}{\Gamma[\sigma - \rho - \tilde{\alpha}_{\bar{n}} - \gamma]} \right. \\ &\quad \left. + \bar{\theta}(\sigma - \rho - \tilde{\alpha}_{\bar{n}} - 1) \sum_{\gamma=0}^{\infty} \frac{(-1)^\gamma}{\gamma!} \frac{\Gamma[\gamma - \sigma + \rho + \tilde{\alpha}_{\bar{n}} + 1]}{\Gamma[-\sigma + \rho + \tilde{\alpha}_{\bar{n}} + 1]} \left(\frac{\hat{k}_+}{\tilde{k}_+^{\max}} \right)^\gamma \right\}. \end{aligned} \quad (2.26)$$

Herein, we use the Heaviside theta function $\theta(x)$, with $\theta(x) = 1$ for $x \geq 0$ and 0 otherwise, and its counter part $\bar{\theta}(x) \equiv 1 - \theta(x)$ to account for the expansion of the integrand. Even though within the central rapidity region $e^{\pm Y_H} \sim \mathcal{O}(1)$ and thus $\tilde{k}_+^{\max} \sim \mathcal{O}(m_H e^{\pm Y_H})$, the integrand of eq. (2.26) has already admitted a formally asymptotic series in $(\hat{k}_+/\tilde{k}_+^{\max})$, the participation of m_T into the upper boundary condition can invoke inhomogeneous behaviour after completing the phase space integral. To this end, a further expansion is necessary with the aid of eq. (2.13). It follows that

$$\begin{aligned} \int_0^{(m_H - m_T)e^{-Y_H}} d\hat{k}_+ \hat{k}_+^{\tilde{\alpha}_n + \gamma} &= \sum_{\gamma_2=0}^{\infty} \sum_{\gamma_1=0}^{1 + \gamma + \tilde{\alpha}_n} \frac{(-1)^{\gamma_1}}{\gamma_1! \gamma_2!} \left(\frac{q_T^2}{m_H^2} \right)^{\gamma_2} (e^{-Y_H} m_H)^{1 + \tilde{\alpha}_n + \gamma} \\ &\quad \times \frac{\Gamma[1 + \frac{\gamma_1}{2}]}{\Gamma[1 - \gamma_2 + \frac{\gamma_1}{2}]} \frac{\Gamma[\tilde{\alpha}_n + \gamma + 1]}{\Gamma[\tilde{\alpha}_n + \gamma - \gamma_1 + 2]}. \end{aligned} \quad (2.27)$$

Combining eqs. (2.26)–(2.27) with eq. (2.24), we then accomplish the expansion of the n -ultra-collinear sector in the small parameter (q_T/m_H) . An analogous procedure can be similarly applied onto the \bar{n} -ultra-collinear case, with the exception of the conversion of the integration variable k_+ to k_- by means of the on-shell condition $k_+ k_- = q_T^2$ and the substitution of e^{+Y_H} for e^{-Y_H} in eq. (2.27), as appropriate.

From those results, we observe that the boundary corrections here are always associated with PDFs at the opposite end and therefore are a priori expected to play a negligible role in comparison to $\tilde{\mathcal{I}}_{[\kappa],\{\alpha,\beta\}}^{\rho,\sigma}$ in eq. (2.19). While this is expected to hold for the first few terms in the power expansion, it is possible that the higher power corrections from $\tilde{\mathcal{I}}_{[\kappa],\{\alpha,\beta\}}^{\rho,\sigma}$ become of a similar size as the boundary corrections from $\Delta\tilde{\mathcal{I}}_{[\kappa],\{\alpha,\beta\}}^{\rho,\sigma}$, such that both parts of contributions are essential to reproduce the desired asymptotic behaviour of the q_T spectrum. In section 4, we will deliver a quantitative assessment thereof.

2.4 Power corrections over the interior domain

2.4.1 Asymptotic expansion in momentum space

We can now perform the power expansion on the integral $\tilde{\mathcal{I}}_{[\kappa],\{\alpha,\beta\}}^{\rho,\sigma}$ in the low q_T area within the central rapidity region $e^{\pm Y_H} \sim \mathcal{O}(1)$. As exhibited in eq. (2.19), $\tilde{\mathcal{I}}_{[\kappa],\{\alpha,\beta\}}^{\rho,\sigma}$ encompasses a

variety of scales along the integration path, including the ultra-soft scale $k_+ \sim \mathcal{O}(q_T^2/m_H)$, the soft one $k_+ \sim \mathcal{O}(q_T)$, and the hard one $k_+ \sim \mathcal{O}(m_H)$. Every one of those momentum modes in practice prompts a distinct expansion of $\tilde{\mathcal{I}}_{[\kappa],\{\alpha,\beta\}}^{\rho,\sigma}$. Hence, in the spirit of the expansion by regions method [177, 214–217] and also according to the pattern of the resulting power series, we categorise the phase space as follows,²

$$\begin{aligned}
 n\text{-collinear mode} &: \nu_n < k_+ \leq \tilde{k}_+^{\max}; \\
 \text{transitional range} &: \frac{q_T^2}{\nu_{\bar{n}}} < k_+ \leq \nu_n; \\
 \bar{n}\text{-collinear mode} &: \tilde{k}_+^{\min} \leq k_+ \leq \frac{q_T^2}{\nu_{\bar{n}}}.
 \end{aligned}
 \tag{2.28}$$

Here, a pair of auxiliary scales $\{\nu_n, \nu_{\bar{n}}\}$ are introduced to separate the n - and \bar{n} -collinear regions from the moderate range in between. Throughout this paper, $\{\nu_n, \nu_{\bar{n}}\}$ are chosen to be of similar magnitudes to the hard scales $m_H e^{\pm Y_H}$ but always small enough that in the intermediate domain of eq. (2.28) the light-cone components k_+ and k_- are both well contained within the convergence radii of $F_{i/n, \beta_n}^{(\alpha_n)}$ and $F_{j/\bar{n}, \beta_{\bar{n}}}^{(\alpha_{\bar{n}})}$, as stipulated in section 2.2, more specifically,

$$m_H e^{-Y_H} \gtrsim \nu_n \sim \mathcal{O}(m_H) \gg q_T, \quad m_H e^{Y_H} \gtrsim \nu_{\bar{n}} \sim \mathcal{O}(m_H) \gg q_T.
 \tag{2.29}$$

Alternative choices of those two auxiliary boundaries can be used to examine the asymptotic behaviour of $\tilde{\mathcal{I}}_{[\kappa],\{\alpha,\beta\}}^{\rho,\sigma}$. For example, the scales proposed in [222] may impact the expressions of the individual sectors defined in eq. (2.28) but will leave the resulting power series unchanged upon summation of all ingredients. Having chosen $\{\nu_n, \nu_{\bar{n}}\}$ according to eq. (2.29), the momentum k^μ obeys the unambiguous scaling law $k_+ \sim \mathcal{O}(m_H) \gg k_- \sim \mathcal{O}(q_T^2/m_H)$ in the n -collinear mode, from which we can expand $F_{j/\bar{n}, \beta_{\bar{n}}}^{(\alpha_{\bar{n}})}$ around the intrinsic scale $m_H e^{+Y_H}$,

$$\tilde{\mathcal{I}}_{[\kappa],\{\alpha,\beta\}}^{\rho,\sigma} \Big|_c = \sum_{\omega=\rho}^{\infty} (q_T^2)^\omega \tilde{\mathcal{I}}_{[\kappa],\{\alpha,\beta\}}^{\rho,\sigma,(\omega)} \Big|_c,
 \tag{2.30}$$

where

$$\tilde{\mathcal{I}}_{[\kappa],\{\alpha,\beta\}}^{\rho,\sigma,(\omega)} \Big|_c \equiv \int_{\nu_n}^{\tilde{k}_+^{\max}} \frac{dk_+}{k_+} \frac{(k_+)^{\sigma-\omega}}{(\omega-\rho)!} F_{i/n, \beta_n}^{(\alpha_n)} \left(k_+ + m_H e^{-Y_H} \right) F_{j/\bar{n}, \beta_{\bar{n}}}^{(\alpha_{\bar{n}}+\omega-\rho)} \left(m_H e^{+Y_H} \right).
 \tag{2.31}$$

Here, all q_T dependences have been extracted into the prefactor of eq. (2.30) to express the manifest power accuracy of the contribution. $\tilde{\mathcal{I}}_{[\kappa],\{\alpha,\beta\}}^{\rho,\sigma,(\omega)}$ collects all hard scales and thus is always of $\mathcal{O}(1)$. It merits noting that in the central rapidity region $e^{\pm Y_H} \sim \mathcal{O}(1)$, the lower boundary ν_n in eq. (2.31) is well separated from the upper one and thus there is no need to utilise a further expansion here, in contrast to eq. (2.24).

²It is interesting to note that the analogous strategy in refining the dynamic regions has also been utilised previously in the literature [105, 218–222] in probing the k_T factorisation in the small- x area.

The same method can also be applied to the \bar{n} -collinear mode, after transforming the integration variable from k_+ to k_- through the on-shell condition $k_+k_- = q_T^2$. It evaluates to,

$$\tilde{\mathcal{I}}_{[\kappa],\{\alpha,\beta\}}^{\rho,\sigma} \Big|_{\bar{c}} = \sum_{\omega=\sigma}^{\infty} (q_T^2)^\omega \tilde{\mathcal{I}}_{[\kappa],\{\alpha,\beta\}}^{\rho,\sigma,(\omega)} \Big|_{\bar{c}}, \quad (2.32)$$

with

$$\tilde{\mathcal{I}}_{[\kappa],\{\alpha,\beta\}}^{\rho,\sigma,(\omega)} \Big|_{\bar{c}} \equiv \int_{\nu_{\bar{n}}}^{\frac{q_T^2}{k_+^{\min}}} \frac{dk_-}{k_-} \frac{(k_-)^{\rho-\omega}}{(\omega-\sigma)!} F_{i/n,\beta_n}^{(\alpha_n+\omega-\sigma)} \left(m_H e^{-Y_H} \right) F_{j/\bar{n},\beta_{\bar{n}}}^{(\alpha_{\bar{n}})} \left(k_- + m_H e^{+Y_H} \right). \quad (2.33)$$

This leaves the transitional domain, as defined in eq. (2.28), to be calculated. In light of the scaling rules of eq. (2.29), we can expand both $F_{i/n,\beta_n}^{(\alpha_n)}$ and $F_{j/\bar{n},\beta_{\bar{n}}}^{(\alpha_{\bar{n}})}$ around the scales $m_H e^{\pm Y_H}$, more specifically,

$$\begin{aligned} \tilde{\mathcal{I}}_{[\kappa],\{\alpha,\beta\}}^{\rho,\sigma} \Big|_t &= \sum_{\lambda,\eta=0}^{\infty} \int_{\frac{q_T^2}{\nu_n}}^{\nu_n} \frac{dk_+}{k_+} \frac{(k_-)^{\rho+\lambda} (k_+)^{\sigma+\eta}}{\lambda! \eta!} F_{i/n,\beta_n}^{(\alpha_n+\eta)} \left(m_H e^{-Y_H} \right) F_{j/\bar{n},\beta_{\bar{n}}}^{(\alpha_{\bar{n}}+\lambda)} \left(m_H e^{+Y_H} \right) \\ &= \sum_{\lambda,\eta=0}^{\infty} \frac{F_{i/n,\beta_n}^{(\alpha_n+\eta)} \left(m_H e^{-Y_H} \right) F_{j/\bar{n},\beta_{\bar{n}}}^{(\alpha_{\bar{n}}+\lambda)} \left(m_H e^{+Y_H} \right)}{\lambda! \eta!} \\ &\quad \times \left\{ \underbrace{\frac{(q_T^2)^{\rho+\lambda} \nu_n^{\sigma+\eta-\rho-\lambda}}{\sigma+\eta-\rho-\lambda} \bar{\delta}_{\rho+\lambda}^{\sigma+\eta}}_{n\text{-col}} + \underbrace{\frac{(q_T^2)^{\sigma+\eta} \nu_{\bar{n}}^{\rho+\lambda-\sigma-\eta}}{\rho+\lambda-\sigma-\eta} \bar{\delta}_{\rho+\lambda}^{\sigma+\eta}}_{\bar{n}\text{-col}} + \underbrace{(q_T^2)^{\sigma+\eta} \ln \left[\frac{\nu_n \nu_{\bar{n}}}{q_T^2} \right] \delta_{\rho+\lambda}^{\sigma+\eta}}_{n\text{-col}, \bar{n}\text{-col}, s} \right\}, \end{aligned} \quad (2.34)$$

where we have already grouped the expression according to their powers in ν_n and $\nu_{\bar{n}}$. δ_β^α is the Kronecker Delta, $\delta_\beta^\alpha = 1$ if $\alpha = \beta$ and zero otherwise, $\bar{\delta}_\beta^\alpha \equiv 1 - \delta_\beta^\alpha$ is its complement. We note that even for fixed values of λ and η , the phase space integral results in terms with a variety of power accuracies. For instance, in the first term on r.h.s. the power precision is determined by the exponent of q_T , which is identical to that of k_- in the integrand. Hence, the scaling of the emitted momentum k^μ here is determined by the n -collinear mode $k_- \sim \mathcal{O}(q_T^2/m_H)$ and $k_+ \sim \mathcal{O}(m_H)$. Similarly, applying this scaling analysis to the second term, its power precision is given by the exponent of k_+ and the \bar{n} -collinear mode with $k_- \sim \mathcal{O}(m_H)$ and $k_+ \sim \mathcal{O}(q_T^2/m_H)$. The interpretation of the scaling of the integration variable of the last term of eq. (2.34) is more flexible due to the presence of the constraint $\rho + \lambda = \sigma + \eta$. Hence, the emitted parton can be constituted of either the $n(\bar{n})$ -collinear particle or the soft one $k_- \sim k_+ \sim \mathcal{O}(q_T)$. This inhomogeneity stems from our choice of the momentum cutoffs ν_n and $\nu_{\bar{n}}$ in eq. (2.29), from which multiple dynamic modes are allowed to participate in the transitional area, such as the n -collinear one, \bar{n} -collinear one, or the soft one. In principle, reducing ν_n and $\nu_{\bar{n}}$ down to $\mathcal{O}(q_T)$ will filter out the collinear modes in the transitional domain rendering it homogeneous again, at the price of additional soft scales in both collinear sectors through the boundary condition, necessitating a second expansion in the small parameters ν_n/m_H and $\nu_{\bar{n}}/m_H$ within there. It remains to be noted, while alternative choices of ν_n and $\nu_{\bar{n}}$ may modify the dynamics in each sector, their combined power series is invariant under this choice. Hence, in this work we choose the prescription of eq. (2.29), i.e. homogenous collinear sectors, for simplicity.

By collecting and refactoring terms of a common power in q_T we can recast eq. (2.34) as

$$\tilde{\mathcal{I}}_{[\kappa],\{\alpha,\beta\}}^{\rho,\sigma} \Big|_t = \left(\sum_{\omega=\rho}^{\infty} (q_T^2)^\omega \tilde{\mathcal{I}}_{[\kappa],\{\alpha,\beta\}}^{\rho,\sigma,(\omega)} \Big|_{cs} \right) + \left(\sum_{\omega=\sigma}^{\infty} (q_T^2)^\omega \tilde{\mathcal{I}}_{[\kappa],\{\alpha,\beta\}}^{\rho,\sigma,(\omega)} \Big|_{\bar{cs}} \right), \quad (2.35)$$

where

$$\begin{aligned} \tilde{\mathcal{I}}_{[\kappa],\{\alpha,\beta\}}^{\rho,\sigma,(\omega)} \Big|_{cs} &= \sum_{\eta=0}^{\infty} \frac{F_{i/n,\beta_n}^{(\eta+\alpha_n)}(m_H e^{-Y_H}) F_{j/\bar{n},\beta_{\bar{n}}}^{(\alpha_{\bar{n}}+\omega-\rho)}(m_H e^{+Y_H})}{(\omega-\rho)! \eta!} \left\{ \frac{\nu_n^{\sigma+\eta-\omega}}{\sigma+\eta-\omega} \bar{\delta}_\omega^{\sigma+\eta+\ln\left[\frac{\nu_n}{q_T}\right]} \delta_\omega^{\sigma+\eta} \right\}, \\ \tilde{\mathcal{I}}_{[\kappa],\{\alpha,\beta\}}^{\rho,\sigma,(\omega)} \Big|_{\bar{cs}} &= \sum_{\lambda=0}^{\infty} \frac{F_{i/n,\beta_n}^{(\alpha_n+\omega-\sigma)}(m_H e^{-Y_H}) F_{j/\bar{n},\beta_{\bar{n}}}^{(\alpha_{\bar{n}}+\lambda)}(m_H e^{+Y_H})}{(\omega-\sigma)! \lambda!} \left\{ \frac{\nu_{\bar{n}}^{\rho+\lambda-\omega}}{\rho+\lambda-\omega} \bar{\delta}_\omega^{\rho+\lambda+\ln\left[\frac{\nu_{\bar{n}}}{q_T}\right]} \delta_\omega^{\rho+\lambda} \right\}. \end{aligned} \quad (2.36)$$

Here we have re-organized the logarithmic terms in eq. (2.34) into the n -collinear-soft (cs) and \bar{n} -collinear-soft (\bar{cs}) sectors based on their scale dependences. At variance from the results in eq. (2.31) and eq. (2.33) in the n - and \bar{n} -collinear sectors, where the coefficients at each power consist of only the hard scales k_\pm , respectively, eq. (2.36) here introduces an additional dependence on $\ln(\nu_{n(\bar{n})}/q_T)$. In order to facilitate numerical calculations of these coefficients, we rewrite the infinite series in eq. (2.36) in terms of the integrals over k_\pm , in analogy to eqs. (2.31) and (2.33). If $\omega < \sigma$ in eq. (2.36), this transformation is immediate,

$$\begin{aligned} \bar{\theta}(\omega-\sigma) \sum_{\eta=0}^{\infty} \frac{F_{i/n,\beta_n}^{(\eta+\alpha_n)}(m_H e^{-Y_H}) F_{j/\bar{n},\beta_{\bar{n}}}^{(\alpha_{\bar{n}}+\omega-\rho)}(m_H e^{+Y_H})}{(\omega-\rho)! \eta!} \frac{\nu_n^{\sigma+\eta-\omega}}{\sigma+\eta-\omega} \\ \implies \frac{\bar{\theta}(\omega-\sigma)}{(\omega-\rho)!} \int_0^{\nu_n} \frac{dk_+}{k_+} k_+^{\sigma-\omega} F_{i/n,\beta_n}^{(\alpha_n)}(k_+ + m_H e^{-Y_H}) F_{j/\bar{n},\beta_{\bar{n}}}^{(\alpha_{\bar{n}}+\omega-\rho)}(m_H e^{+Y_H}). \end{aligned} \quad (2.37)$$

Here we have removed $\bar{\delta}_\omega^{\sigma+\eta}$ from the expressions since it always equals unity while $\omega < \sigma$ and $\eta \geq 0$. The same reasoning can also be used to neglect the logarithmic contributions in eq. (2.36). However, it is not straightforward to apply eq. (2.37) in the remaining space with $\omega \geq \sigma$ as the integrand is singular in the limit $k_+ \rightarrow 0$. To this end, we make use of the higher-ranked star distribution,

$$\int_0^\Lambda dx \left[\frac{1}{x^m} \right]_*^\nu f(x) \equiv \int_\nu^\Lambda dx \frac{f(x)}{x^m} + \int_0^\nu dx \frac{1}{x^m} \left[f(x) - \sum_{n=0}^{m-1} \frac{x^n}{n!} f^{(n)}(0) \right], \quad (2.38)$$

to maintain the end point analyticity. Therein, $f(x)$ is assumed to be always differentiable at $x = 0$. With $m = 1$, eq. (2.38) reduces to the customary star distribution proposed in [223, 224]. Equipped with eq. (2.38), we are now able to convert the n -collinear-soft contribution in the case $\omega \geq \sigma$ and $\eta > \omega - \sigma$,

$$\begin{aligned} \theta(\omega-\sigma) \sum_{\eta=\omega-\sigma+1}^{\infty} \frac{F_{i/n,\beta_n}^{(\eta+\alpha_n)}(m_H e^{-Y_H}) F_{j/\bar{n},\beta_{\bar{n}}}^{(\alpha_{\bar{n}}+\omega-\rho)}(m_H e^{+Y_H})}{(\omega-\rho)! \eta!} \frac{\nu_n^{\sigma+\eta-\omega}}{\sigma+\eta-\omega} \\ \implies \frac{\theta(\omega-\sigma)}{(\omega-\rho)!} \int_0^{\nu_n} dk_+ \left[\frac{1}{k_+^{\omega-\sigma+1}} \right]_*^{\nu_n} F_{i/n,\beta_n}^{(\alpha_n)}(k_+ + m_H e^{-Y_H}) F_{j/\bar{n},\beta_{\bar{n}}}^{(\alpha_{\bar{n}}+\omega-\rho)}(m_H e^{+Y_H}). \end{aligned} \quad (2.39)$$

The remaining contributions in eq. (2.36) include the logarithms $\ln(\nu_n/q_T)$ as well as the first $(\omega - \sigma)$ terms of the Taylor series. We will refrain from transforming those contributions here since, at a given power precision, the number of remaining terms are always finite.

Combining above results we can recast the n -collinear-soft contribution of eq. (2.36) as follows

$$\begin{aligned}
 \tilde{\mathcal{I}}_{[\kappa],\{\alpha,\beta\}}^{\rho,\sigma,(\omega)} \Big|_{cs} &= \frac{\bar{\theta}(\omega - \sigma)}{(\omega - \rho)!} \int_0^{\nu_n} \frac{dk_+}{k_+} k_+^{\sigma - \omega} F_{i/n,\beta_n}^{(\alpha_n)}(k_+ + m_H e^{-Y_H}) F_{j/\bar{n},\beta_{\bar{n}}}^{(\alpha_{\bar{n}} + \omega - \rho)}(m_H e^{+Y_H}) \\
 &+ \frac{\theta(\omega - \sigma)}{(\omega - \rho)!} \int_0^{\nu_n} dk_+ \left[\frac{1}{k_+^{\omega - \sigma + 1}} \right]_*^{\nu_n} F_{i/n,\beta_n}^{(\alpha_n)}(k_+ + m_H e^{-Y_H}) F_{j/\bar{n},\beta_{\bar{n}}}^{(\alpha_{\bar{n}} + \omega - \rho)}(m_H e^{+Y_H}) \\
 &+ \frac{\theta(\omega - \sigma - 1)}{(\omega - \rho)!} \sum_{\eta=0}^{\omega - \sigma - 1} \frac{F_{i/n,\beta_n}^{(\alpha_n + \eta)}(m_H e^{-Y_H}) F_{j/\bar{n},\beta_{\bar{n}}}^{(\alpha_{\bar{n}} + \omega - \rho)}(m_H e^{+Y_H})}{\eta!} \frac{\nu_n^{\sigma + \eta - \omega}}{\sigma + \eta - \omega} \\
 &+ \frac{\theta(\omega - \sigma)}{(\omega - \rho)!} \ln \left[\frac{\nu_n}{q_T} \right] \frac{F_{i/n,\beta_n}^{(\alpha_n + \omega - \sigma)}(m_H e^{-Y_H}) F_{j/\bar{n},\beta_{\bar{n}}}^{(\alpha_{\bar{n}} + \omega - \rho)}(m_H e^{+Y_H})}{(\omega - \sigma)!}. \tag{2.40}
 \end{aligned}$$

By analogy, the contribution of the \bar{n} -collinear-soft sector in eq. (2.36) can be transformed to finite integrals following an analogous path, giving

$$\begin{aligned}
 \tilde{\mathcal{I}}_{[\kappa],\{\alpha,\beta\}}^{\rho,\sigma,(\omega)} \Big|_{\bar{cs}} &= \frac{\bar{\theta}(\omega - \rho)}{(\omega - \sigma)!} \int_0^{\nu_{\bar{n}}} \frac{dk_-}{k_-} k_-^{\rho - \omega} F_{i/n,\beta_n}^{(\alpha_n + \omega - \sigma)}(m_H e^{-Y_H}) F_{j/\bar{n},\beta_{\bar{n}}}^{(\alpha_{\bar{n}})}(k_- + m_H e^{+Y_H}) \\
 &+ \frac{\theta(\omega - \rho)}{(\omega - \sigma)!} \int_0^{\nu_{\bar{n}}} dk_- \left[\frac{1}{k_-^{\omega - \rho + 1}} \right]_*^{\nu_{\bar{n}}} F_{i/n,\beta_n}^{(\alpha_n + \omega - \sigma)}(m_H e^{-Y_H}) F_{j/\bar{n},\beta_{\bar{n}}}^{(\alpha_{\bar{n}})}(k_- + m_H e^{+Y_H}) \\
 &+ \frac{\theta(\omega - \rho - 1)}{(\omega - \sigma)!} \sum_{\lambda=0}^{\omega - \rho - 1} \frac{F_{i/n,\beta_n}^{(\alpha_n + \omega - \sigma)}(m_H e^{-Y_H}) F_{j/\bar{n},\beta_{\bar{n}}}^{(\alpha_{\bar{n}} + \lambda)}(m_H e^{+Y_H})}{\lambda!} \frac{\nu_{\bar{n}}^{\rho + \lambda - \omega}}{\rho + \lambda - \omega} \\
 &+ \frac{\theta(\omega - \rho)}{(\omega - \sigma)!} \ln \left[\frac{\nu_{\bar{n}}}{q_T} \right] \frac{F_{i/n,\beta_n}^{(\alpha_n + \omega - \sigma)}(m_H e^{-Y_H}) F_{j/\bar{n},\beta_{\bar{n}}}^{(\alpha_{\bar{n}} + \omega - \rho)}(m_H e^{+Y_H})}{(\omega - \rho)!}. \tag{2.41}
 \end{aligned}$$

Using the above result we can now combine the n -collinear sector of eq. (2.30), the \bar{n} -collinear sector of eq. (2.32), and the transitional sector of eqs. (2.40) and (2.41), arriving at the expansion of $\tilde{\mathcal{I}}_{[\kappa],\{\alpha,\beta\}}^{\rho,\sigma}$ of eq. (2.19) in powers of q_T^2 in the small q_T domain,

$$\tilde{\mathcal{I}}_{[\kappa],\{\alpha,\beta\}}^{\rho,\sigma} = \sum_{\omega} (q_T^2)^{\omega} \tilde{\mathcal{I}}_{[\kappa],\{\alpha,\beta\}}^{\rho,\sigma,(\omega)} \equiv \sum_{\omega} (q_T^2)^{\omega} \left\{ \tilde{\mathcal{I}}_{[\kappa],\{\alpha,\beta\}}^{\rho,\sigma,(\omega)} \Big|_c + \tilde{\mathcal{I}}_{[\kappa],\{\alpha,\beta\}}^{\rho,\sigma,(\omega)} \Big|_{\bar{c}} + \tilde{\mathcal{I}}_{[\kappa],\{\alpha,\beta\}}^{\rho,\sigma,(\omega)} \Big|_{cs} + \tilde{\mathcal{I}}_{[\kappa],\{\alpha,\beta\}}^{\rho,\sigma,(\omega)} \Big|_{\bar{cs}} \right\}. \tag{2.42}$$

At this point it merits reminding that the pair of auxiliary scales, ν_n and $\nu_{\bar{n}}$, that we have employed to define and separate the dynamic regions in eq. (2.28) appear explicitly in the expressions of all three individual domains. For consistency's sake, it is of the essence to examine whether the combination of all domains also exhibits such a dependence, or whether this dependence, in fact, vanishes after summing over all the ingredients. To this end, we take the derivatives of the r.h.s. of eq. (2.42) with respect to ν_n , and it evaluates to

$$\frac{\partial}{\partial \nu_n} \tilde{\mathcal{I}}_{[\kappa],\{\alpha,\beta\}}^{\rho,\sigma,(\omega)} \Big|_c = - \frac{\partial}{\partial \nu_n} \tilde{\mathcal{I}}_{[\kappa],\{\alpha,\beta\}}^{\rho,\sigma,(\omega)} \Big|_{cs} = - \frac{(\nu_n)^{\sigma - \omega - 1}}{(\omega - \rho)} F_{i/n,\beta_n}^{(\alpha_n)}(\nu_n + m_H e^{-Y_H}) F_{j/\bar{n},\beta_{\bar{n}}}^{(\alpha_{\bar{n}} + \omega - \rho)}(m_H e^{+Y_H}),$$

$$\left. \frac{\partial}{\partial \nu_n} \tilde{\mathcal{I}}_{[\kappa],\{\alpha,\beta\}}^{\rho,\sigma,(\omega)} \right|_{\bar{c}} = \left. \frac{\partial}{\partial \nu_n} \tilde{\mathcal{I}}_{[\kappa],\{\alpha,\beta\}}^{\rho,\sigma,(\omega)} \right|_{c\bar{s}} = 0, \quad (2.43)$$

where the results of eqs. (2.31) and (2.40) are utilised to derive the r.h.s. of eq. (2.43). In addition, the terms arising from the derivative of the star distribution, defined in eq. (2.38), have been cancelled against the ν_n dependences arising from the logarithmic term and the truncated Taylor polynomials in eq. (2.40). A similar result can also be found for the $\nu_{\bar{n}}$ dependence of eq. (2.42), giving

$$\begin{aligned} \left. \frac{\partial}{\partial \nu_{\bar{n}}} \tilde{\mathcal{I}}_{[\kappa],\{\alpha,\beta\}}^{\rho,\sigma,(\omega)} \right|_c &= \left. \frac{\partial}{\partial \nu_{\bar{n}}} \tilde{\mathcal{I}}_{[\kappa],\{\alpha,\beta\}}^{\rho,\sigma,(\omega)} \right|_{c\bar{s}} = 0, \\ \left. \frac{\partial}{\partial \nu_{\bar{n}}} \tilde{\mathcal{I}}_{[\kappa],\{\alpha,\beta\}}^{\rho,\sigma,(\omega)} \right|_{\bar{c}} &= - \left. \frac{\partial}{\partial \nu_{\bar{n}}} \tilde{\mathcal{I}}_{[\kappa],\{\alpha,\beta\}}^{\rho,\sigma,(\omega)} \right|_{c\bar{s}} = - \frac{(\nu_{\bar{n}})^{\rho-\omega-1}}{(\omega-\sigma)!} F_{i/n,\beta_n}^{(\alpha_n+\omega-\sigma)} \left(m_H e^{-Y_H} \right) F_{j/\bar{n},\beta_{\bar{n}}}^{(\alpha_{\bar{n}})} \left(\nu_{\bar{n}} + m_H e^{+Y_H} \right). \end{aligned} \quad (2.44)$$

Combining the results of eqs. (2.43) and (2.44), respectively, we can conclude that the coefficient $\tilde{\mathcal{I}}_{[\kappa],\{\alpha,\beta\}}^{\rho,\sigma,(\omega)}$ in eq. (2.42) is indeed independent of the choice of the separators ν_n and $\nu_{\bar{n}}$ at each power. This agrees with the expectation from a direct expansion of $\tilde{\mathcal{I}}_{[\kappa],\{\alpha,\beta\}}^{\rho,\sigma}$, currently beyond our capabilities as the PDFs are not rigorously known analytically, that it should be a function of q_T , s , and m_H only and independent of ν_n or $\nu_{\bar{n}}$.

2.4.2 Rapidity regularisation and zero-bin subtraction

In the previous section, with the help of the auxiliary scales ν_n and $\nu_{\bar{n}}$, we have derived the power series for $\tilde{\mathcal{I}}_{[\kappa],\{\alpha,\beta\}}^{\rho,\sigma}$ in eq. (2.42) in the vicinity $q_T = 0$ at central rapidities, $e^{\pm Y_H} \sim \mathcal{O}(1)$. Even though this strategy has accomplished an asymptotic expansion of $\tilde{\mathcal{I}}_{[\kappa],\{\alpha,\beta\}}^{\rho,\sigma}$, and in turn the q_T distribution, at NLO, it is not straightforward to generalise this method to higher perturbative orders. The presence of subdivisions of phase space through the auxiliary scales ν_n and $\nu_{\bar{n}}$, generally inducing additional scales to phase space and loop integrals, complicates the calculations substantially. Further, the absence of additional constraints on the integration paths is also one of prerequisites to establish the factorisation in a SCET-based analysis. To this end, we will discuss the rearrangement of the ingredients defined in eqs. (2.31) and (2.33) as well as eqs. (2.40) and (2.41) such that the dependence on the auxiliary scales to subdivide the phase space is removed. In particular, recalling our findings regarding the $\nu_{n(\bar{n})}$ -independence of $\tilde{\mathcal{I}}_{[\kappa],\{\alpha,\beta\}}^{\rho,\sigma}$, but not its components in eqs. (2.43) and (2.44), such a rearrangement is warranted. Although in the discussion below, we will still restrict ourselves to the NLO constituent $\tilde{\mathcal{I}}_{[\kappa],\{\alpha,\beta\}}^{\rho,\sigma}$ extracted from eq. (2.4) as an illustrative example, it is expected that the conclusion here can provide the theoretical baseline for an analysis in more general situations.

We start by examining the collinear sectors. Here, eliminating the dependences of the auxiliary scales ν_n and $\nu_{\bar{n}}$ amounts to reducing the lower boundaries in eq. (2.31) and eq. (2.33) from their intrinsic domains defined in eq. (2.29) to the origin. To be precise, we split

$$\tilde{\mathcal{I}}_{[\kappa],\{\alpha,\beta\}}^{\rho,\sigma,(\omega)} \Big|_c = \tilde{\mathcal{G}}_{[\kappa],\{\alpha,\beta\}}^{\rho,\sigma,(\omega)} \Big|_c - \tilde{\mathcal{I}}_{[\kappa],\{\alpha,\beta\}}^{\rho,\sigma,(\omega)} \Big|_{c0}, \quad \tilde{\mathcal{I}}_{[\kappa],\{\alpha,\beta\}}^{\rho,\sigma,(\omega)} \Big|_{\bar{c}} = \tilde{\mathcal{G}}_{[\kappa],\{\alpha,\beta\}}^{\rho,\sigma,(\omega)} \Big|_{\bar{c}} - \tilde{\mathcal{I}}_{[\kappa],\{\alpha,\beta\}}^{\rho,\sigma,(\omega)} \Big|_{\bar{c}0}, \quad (2.45)$$

where $\tilde{\mathcal{G}}_{[\kappa],\{\alpha,\beta\}}^{\rho,\sigma,\omega}|_c$ and $\tilde{\mathcal{G}}_{[\kappa],\{\alpha,\beta\}}^{\rho,\sigma,\omega}|_{\bar{c}}$ collect the collinear contributions, integrating the light-cone momentum over the entire range. Their expressions read

$$\begin{aligned} \tilde{\mathcal{G}}_{[\kappa],\{\alpha,\beta\}}^{\rho,\sigma,\omega}|_c &\equiv \lim_{\tau \rightarrow 0} \int_0^{\tilde{k}_+^{\max}} \frac{dk_+}{k_+} \mathcal{R}(k_-, k_+, \tau) \frac{(k_+)^{\sigma-\omega}}{(\omega-\rho)!} F_{i/n,\beta_n}^{(\alpha_n)} \left(k_+ + m_H e^{-Y_H} \right) F_{j/\bar{n},\beta_{\bar{n}}}^{(\alpha_{\bar{n}}+\omega-\rho)} \left(m_H e^{+Y_H} \right), \\ \tilde{\mathcal{G}}_{[\kappa],\{\alpha,\beta\}}^{\rho,\sigma,\omega}|_{\bar{c}} &\equiv \lim_{\tau \rightarrow 0} \int_0^{\frac{q_{\text{T}}^2}{\tilde{k}_+^{\min}}} \frac{dk_-}{k_-} \mathcal{R}(k_-, k_+, \tau) \frac{(k_-)^{\rho-\omega}}{(\omega-\sigma)!} F_{i/n,\beta_n}^{(\alpha_n+\omega-\sigma)} \left(m_H e^{-Y_H} \right) F_{j/\bar{n},\beta_{\bar{n}}}^{(\alpha_{\bar{n}})} \left(k_- + m_H e^{+Y_H} \right). \end{aligned} \quad (2.46)$$

Therein, in order to regularise the rapidity divergence in the limit $k_{\pm} \rightarrow 0$, we multiply the original integrand by $\mathcal{R}(k_-, k_+, \tau)$, which is a function of the light-cone momenta k_{\pm} and a real parameter τ , satisfying,

$$\lim_{\tau \rightarrow 0} \mathcal{R}(k_-, k_+, \tau) = \begin{cases} 1 & k_{\pm} \neq 0, \\ 0 & k_+ = 0 \text{ or } k_- = 0. \end{cases} \quad (2.47)$$

For the regions $k_{\pm} \neq 0$, the integrands in eq. (2.46) are uniformly convergent, which permits reducing the rapidity regulator $\mathcal{R}(k_-, k_+, \tau)$ in the limit $\tau \rightarrow 0$ and restoring the integrands to their original forms. Nevertheless, in the asymptotic area $k_+ = 0$ or $k_- = 0$, the role of the rapidity regulator becomes indispensable, ensuring that the phase space integrals in eq. (2.46) are always well defined. The discussion in this section will emphasise rapidity regulators that are able to preserve their expressions in both the n -collinear and \bar{n} -collinear sectors for all powers, such as the analytic regulator of [74, 76], the exponential regulator of [79, 80], and the pure rapidity regulator of [113, 178]. We will dub them the conservative rapidity regulator or conservative regularisation scheme (CRa) hereafter. Other than that, there are also alternative proposals, including the Δ -regulator [75, 166, 171, 172, 179] and the η -regulator [77, 78]. At this point, either the rapidity regulators themselves or the regulator-dressed propagators will participate in the power expansion such that in practice the rapidity divergences can be regularised in varying strategies in different ingredients from power to power. They will be called dissipative rapidity regulator (DRa) in this work. We will postpone their investigation for now but discuss the possible prescriptions in appendix A.

In eq. (2.45), we have also introduced $\tilde{\mathcal{I}}_{[\kappa],\{\alpha,\beta\}}^{\rho,\sigma,\omega}|_{c0}$ and $\tilde{\mathcal{I}}_{[\kappa],\{\alpha,\beta\}}^{\rho,\sigma,\omega}|_{\bar{c}0}$ in order to restore the equality after. Their expressions read,

$$\begin{aligned} \tilde{\mathcal{I}}_{[\kappa],\{\alpha,\beta\}}^{\rho,\sigma,\omega}|_{c0} &= \lim_{\tau \rightarrow 0} \int_0^{\nu_n} \frac{dk_+}{k_+} \mathcal{R}(k_-, k_+, \tau) \frac{(k_+)^{\sigma-\omega}}{(\omega-\rho)!} F_{i/n,\beta_n}^{(\alpha_n)} \left(k_+ + m_H e^{-Y_H} \right) F_{j/\bar{n},\beta_{\bar{n}}}^{(\alpha_{\bar{n}}+\omega-\rho)} \left(m_H e^{+Y_H} \right), \\ \tilde{\mathcal{I}}_{[\kappa],\{\alpha,\beta\}}^{\rho,\sigma,\omega}|_{\bar{c}0} &= \lim_{\tau \rightarrow 0} \int_0^{\nu_{\bar{n}}} \frac{dk_-}{k_-} \mathcal{R}(k_-, k_+, \tau) \frac{(k_-)^{\rho-\omega}}{(\omega-\sigma)!} F_{i/n,\beta_n}^{(\alpha_n+\omega-\sigma)} \left(m_H e^{-Y_H} \right) F_{j/\bar{n},\beta_{\bar{n}}}^{(\alpha_{\bar{n}})} \left(k_- + m_H e^{+Y_H} \right). \end{aligned} \quad (2.48)$$

Since these functions are always associated with the k_{\pm} integrals from the origin point up to the cutoffs $\nu_{n(\bar{n})}$, we will make use of the subscripts “c0” (“ $\bar{c}0$ ”) to represent them hereafter. From eq. (2.48), noting that the integration variables k_{\pm} are both well situated within the

convergence radii of $F_{i/n, \beta_n}$ and $F_{j/\bar{n}, \beta_{\bar{n}}}$, according to section 2.2, we can now perform the power expansion in k_{\pm} . We then have,

$$\begin{aligned} \tilde{\mathcal{I}}_{[\kappa], \{\alpha, \beta\}}^{\rho, \sigma, (\omega)} \Big|_{c0} &= \frac{F_{j/\bar{n}, \beta_{\bar{n}}}^{(\alpha_{\bar{n}} + \omega - \rho)} (m_H e^{+Y_H})}{(\omega - \rho)!} \left\{ \tilde{\mathcal{I}}_{[\kappa], \{\alpha, \beta\}}^{\rho, \sigma, (\omega)} \Big|_{c0r} + \theta(\omega - \sigma) \tilde{\mathcal{I}}_{[\kappa], \{\alpha, \beta\}}^{\rho, \sigma, (\omega)} \Big|_{c0d} \right\}, \\ \tilde{\mathcal{I}}_{[\kappa], \{\alpha, \beta\}}^{\rho, \sigma, (\omega)} \Big|_{\bar{c}0} &= \frac{F_{i/n, \beta_n}^{(\alpha_n + \omega - \sigma)} (m_H e^{-Y_H})}{(\omega - \sigma)!} \left\{ \tilde{\mathcal{I}}_{[\kappa], \{\alpha, \beta\}}^{\rho, \sigma, (\omega)} \Big|_{\bar{c}0r} + \theta(\omega - \rho) \tilde{\mathcal{I}}_{[\kappa], \{\alpha, \beta\}}^{\rho, \sigma, (\omega)} \Big|_{\bar{c}0d} \right\}, \end{aligned} \quad (2.49)$$

where

$$\begin{aligned} \tilde{\mathcal{I}}_{[\kappa], \{\alpha, \beta\}}^{\rho, \sigma, (\omega)} \Big|_{c0r} &= \sum_{\eta = \max\{0, (\omega - \sigma + 1)\}}^{\infty} \frac{\nu_n^{\sigma - \omega + \eta} F_{i/n, \beta_n}^{(\alpha_n + \eta)} (m_H e^{-Y_H})}{\sigma - \omega + \eta \eta!}, \\ \tilde{\mathcal{I}}_{[\kappa], \{\alpha, \beta\}}^{\rho, \sigma, (\omega)} \Big|_{\bar{c}0r} &= \sum_{\lambda = \max\{0, (\omega - \rho + 1)\}}^{\infty} \frac{\nu_{\bar{n}}^{\rho - \omega + \lambda} F_{j/\bar{n}, \beta_{\bar{n}}}^{(\alpha_{\bar{n}} + \lambda)} (m_H e^{+Y_H})}{\rho - \omega + \lambda \lambda!}, \end{aligned} \quad (2.50)$$

are the regular components, in which the regulator could be safely removed by the means of eq. (2.47), and

$$\begin{aligned} \tilde{\mathcal{I}}_{[\kappa], \{\alpha, \beta\}}^{\rho, \sigma, (\omega)} \Big|_{c0d} &= \sum_{\eta=0}^{\omega - \sigma} \frac{F_{i/n, \beta_n}^{(\alpha_n + \eta)} (m_H e^{-Y_H})}{\eta!} \left\{ \lim_{\tau \rightarrow 0} \int_0^{\nu_n} \frac{dk_+}{k_+} \mathcal{R}(k_-, k_+, \tau) (k_+)^{\sigma - \omega + \eta} \right\}, \\ \tilde{\mathcal{I}}_{[\kappa], \{\alpha, \beta\}}^{\rho, \sigma, (\omega)} \Big|_{\bar{c}0d} &= \sum_{\lambda=0}^{\omega - \rho} \frac{F_{j/\bar{n}, \beta_{\bar{n}}}^{(\alpha_{\bar{n}} + \lambda)} (m_H e^{+Y_H})}{\lambda!} \left\{ \lim_{\tau \rightarrow 0} \int_0^{\nu_{\bar{n}}} \frac{dk_-}{k_-} \mathcal{R}(k_-, k_+, \tau) (k_-)^{\rho - \omega + \lambda} \right\}, \end{aligned} \quad (2.51)$$

contain the (regulated) rapidity divergences at $k_{\pm} \rightarrow 0$. Here, the regulator $\mathcal{R}(k_-, k_+, \tau)$ is essential and the respective integrals are therefore dependent on the choice of the regularisation scheme. Substituting eq. (2.50) into eq. (2.49), we observe that the results for $\tilde{\mathcal{I}}_{[\kappa], \{\alpha, \beta\}}^{\rho, \sigma, (\omega)} \Big|_{c0}$ and $\tilde{\mathcal{I}}_{[\kappa], \{\alpha, \beta\}}^{\rho, \sigma, (\omega)} \Big|_{\bar{c}0}$ still explicitly depend on the auxiliary scales $\nu_{n(\bar{n})}$. However, according to eq. (2.43), all those dependences will drop out upon combining them with the contributions from the transitional region of eq. (2.36), and it follows that

$$\tilde{\mathcal{I}}_{[\kappa], \{\alpha, \beta\}}^{\rho, \sigma, (\omega)} \Big|_{cs} + \tilde{\mathcal{I}}_{[\kappa], \{\alpha, \beta\}}^{\rho, \sigma, (\omega)} \Big|_{\bar{c}s} - \tilde{\mathcal{I}}_{[\kappa], \{\alpha, \beta\}}^{\rho, \sigma, (\omega)} \Big|_{c0} - \tilde{\mathcal{I}}_{[\kappa], \{\alpha, \beta\}}^{\rho, \sigma, (\omega)} \Big|_{\bar{c}0} = \tilde{\mathcal{G}}_{[\kappa], \{\alpha, \beta\}}^{\rho, \sigma, (\omega)} \Big|_{comb}, \quad (2.52)$$

where on the r.h.s., $\tilde{\mathcal{G}}_{[\kappa], \{\alpha, \beta\}}^{\rho, \sigma, (\omega)} \Big|_{comb}$, comprises a set of one-fold integrals of k_+ or k_- over the range $[0, +\infty]$. Its precise form will be specified below.

In the literature, there are two preferences for expressing this combined result. The first one, used extensively when using the method of expansion by regions [177, 214–217] and SCET [225–234], comprises the soft interaction $k_{\pm} \sim \mathcal{O}(q_T)$ in full as well as the subtraction terms to remove the overlap with the collinear regions. Hereafter, we will refer to the results from this formulation as the full soft (FS) prescription. It yields that

$$\tilde{\mathcal{G}}_{[\kappa], \{\alpha, \beta\}}^{\rho, \sigma, (\omega)} \Big|_{comb} = \tilde{\mathcal{G}}_{[\kappa], \{\alpha, \beta\}}^{\rho, \sigma, (\omega)} \Big|_s^{(FS)} - \tilde{\mathcal{G}}_{[\kappa], \{\alpha, \beta\}}^{\rho, \sigma, (\omega)} \Big|_{\bar{c}cs}^{(FS)}. \quad (2.53)$$

Here $\tilde{\mathcal{G}}_{[\kappa],\{\alpha,\beta\}}^{\rho,\sigma,(\omega)}|_s^{(\text{FS})}$ stands for the soft contribution, derived by expanding the integrand in eq. (2.19) in accordance with the soft scaling $k_{\pm} \sim \mathcal{O}(q_T)$. At the ω th-power, the result reads,

$$\begin{aligned} \tilde{\mathcal{G}}_{[\kappa],\{\alpha,\beta\}}^{\rho,\sigma,(\omega)} \Big|_s^{(\text{FS})} &= \theta(\omega - \rho - \sigma) \sum_{\eta=0}^{(\omega - \rho - \sigma)} F_{i/n, \beta_n}^{(\alpha_n + \omega - \rho - \sigma - \eta)} \left(m_H e^{-Y_H} \right) F_{j/\bar{n}, \beta_{\bar{n}}}^{(\alpha_{\bar{n}} + \eta)} \left(m_H e^{+Y_H} \right) \lim_{\tau \rightarrow 0} \int_0^{\infty} \frac{dk_+}{k_+} \\ &\times \mathcal{R}(k_-, k_+, \tau) \frac{(k_-)^{\rho + \eta - \omega}}{\eta!} \frac{(k_+)^{-\rho - \eta}}{(\omega - \rho - \sigma - \eta)!}, \end{aligned} \quad (2.54)$$

where we have extracted the factor of $(q_T^2)^\omega$ from the integrals in eq. (2.54), in line with the definition of the power series in eq. (2.42). Given the expression in eq. (2.54), we can obtain an expression for $\tilde{\mathcal{G}}_{[\kappa],\{\alpha,\beta\}}^{\rho,\sigma,(\omega)}|_{c\bar{c}s}^{(\text{FS})}$ by comparing eq. (2.53) with eq. (2.52). As this subtrahend at LP is intimately associated with the soft limit of the collinear functions and thus the zeroth-bin of the label momentum within the position-momentum space hybrid representation, $\tilde{\mathcal{G}}_{[\kappa],\{\alpha,\beta\}}^{\rho,\sigma,(\omega)}|_{c\bar{c}s}^{(\text{FS})}$ is frequently dubbed the zero-bin contribution [163–166] or the soft subtraction term [75, 164, 165, 167, 168].

On the other hand, there are also alternative proposals in the literature [106, 111, 114, 169, 170]. There, a decomposition of eq. (2.52) without an explicit soft sector is chosen. The virtue of such a scheme is that in absence of the soft contribution the soft-collinear interaction vertices do not need to be expanded using multiple scaling regimes, and the factorisation of the distinct dynamic modes is thus considerably simplified. In this work, we will dub this approach the one in the non-soft $\langle \text{NS} \rangle$ prescription. It follows that,

$$\tilde{\mathcal{G}}_{[\kappa],\{\alpha,\beta\}}^{\rho,\sigma,(\omega)} \Big|_{comb} = -\tilde{\mathcal{G}}_{[\kappa],\{\alpha,\beta\}}^{\rho,\sigma,(\omega)} \Big|_{c\bar{c}}^{\langle \text{NS} \rangle}. \quad (2.55)$$

Hence, the interior contribution $\tilde{\mathcal{I}}_{[\kappa],\{\alpha,\beta\}}^{\rho,\sigma,(\omega)}$ in eq. (2.19) consists of only the collinear sectors in eq. (2.46) as well as $\tilde{\mathcal{G}}_{[\kappa],\{\alpha,\beta\}}^{\rho,\sigma,(\omega)}|_{c\bar{c}}^{\langle \text{NS} \rangle}$. Since $\tilde{\mathcal{G}}_{[\kappa],\{\alpha,\beta\}}^{\rho,\sigma,(\omega)}|_{c\bar{c}}^{\langle \text{NS} \rangle}$ here effectively removes the overlap between the n -collinear and \bar{n} -collinear contributions, it is also named the overlap subtraction term in [114, 169, 170]. Notwithstanding, in view of the functional similarity of $\tilde{\mathcal{G}}_{[\kappa],\{\alpha,\beta\}}^{\rho,\sigma,(\omega)}|_{c\bar{c}}^{\langle \text{NS} \rangle}$ and $\tilde{\mathcal{G}}_{[\kappa],\{\alpha,\beta\}}^{\rho,\sigma,(\omega)}|_{c\bar{c}s}^{(\text{FS})}$, we will not further distinguish the terminologies in this paper, such as the overlapping subtraction, the zero-bin contribution, or the soft remover. Instead, they will be all regarded to be conceptually equivalent but evaluated within different prescriptions.

Comparing eq. (2.55) with eq. (2.53), we note that the subtraction terms in those two schemes possess the following relation,

$$\tilde{\mathcal{G}}_{[\kappa],\{\alpha,\beta\}}^{\rho,\sigma,(\omega)} \Big|_{c\bar{c}}^{\langle \text{NS} \rangle} = \tilde{\mathcal{G}}_{[\kappa],\{\alpha,\beta\}}^{\rho,\sigma,(\omega)} \Big|_{c\bar{c}s}^{(\text{FS})} - \tilde{\mathcal{G}}_{[\kappa],\{\alpha,\beta\}}^{\rho,\sigma,(\omega)} \Big|_s^{(\text{FS})}. \quad (2.56)$$

In the following, we will be focused on the derivation of $\tilde{\mathcal{G}}_{[\kappa],\{\alpha,\beta\}}^{\rho,\sigma,(\omega)}|_{c\bar{c}}^{\langle \text{NS} \rangle}$. The expressions within the $\langle \text{FS} \rangle$ prescription can be obtained by means of the relationship above.

We begin with the transformation of $\tilde{\mathcal{I}}_{[\kappa],\{\alpha,\beta\}}^{\rho,\sigma,(\omega)}|_{cs}$ and $\tilde{\mathcal{I}}_{[\kappa],\{\alpha,\beta\}}^{\rho,\sigma,(\omega)}|_{c\bar{s}}$. As illustrated in eq. (2.36), $\tilde{\mathcal{I}}_{[\kappa],\{\alpha,\beta\}}^{\rho,\sigma,(\omega)}|_{cs}$ comprises the logarithmic terms in the case of $\omega = (\sigma + \eta)$ and powers of the auxiliary scales $\nu_{n(\bar{n})}$ otherwise. The latter contribution can be further categorised

based on the relation between ω and $(\sigma + \eta)$, more specifically,

$$\begin{aligned}
 & \sum_{\eta=0}^{\infty} \frac{F_{i/n, \beta_n}^{(\eta+\alpha_n)} (m_H e^{-Y_H}) F_{j/\bar{n}, \beta_{\bar{n}}}^{(\alpha_{\bar{n}}+\omega-\rho)} (m_H e^{+Y_H})}{(\omega - \rho)! \eta!} \frac{\nu_n^{\sigma+\eta-\omega}}{\sigma + \eta - \omega} \bar{\delta}_{\omega}^{\sigma+\eta} \\
 &= \frac{F_{j/\bar{n}, \beta_{\bar{n}}}^{(\alpha_{\bar{n}}+\omega-\rho)} (m_H e^{+Y_H})}{(\omega - \rho)!} \left\{ \sum_{\eta=\max\{0, (\omega-\sigma+1)\}}^{\infty} \frac{F_{i/n, \beta_n}^{(\alpha_n+\eta)} (m_H e^{-Y_H})}{\eta!} \frac{\nu_n^{\sigma+\eta-\omega}}{\sigma + \eta - \omega} \right. \\
 & \quad \left. - \theta(\omega - \sigma - 1) \sum_{\eta=0}^{\omega-\sigma-1} \frac{F_{i/n, \beta_n}^{(\alpha_n+\eta)} (m_H e^{-Y_H})}{\eta!} \lim_{\tau \rightarrow 0} \int_{\nu_n}^{\infty} \frac{dk_+}{k_+} \mathcal{R}(k_-, k_+, \tau) (k_+)^{\sigma-\omega+\eta} \right\}. \tag{2.57}
 \end{aligned}$$

Therein, within the curly brackets, the first term collects all the contributions with $\omega < (\sigma + \eta)$, whilst the second term collects all contributions with $\omega > (\sigma + \eta)$ and has been transformed into its integral form. Aiming at a representation for $\tilde{\mathcal{I}}_{[\kappa], \{\alpha, \beta\}}^{\rho, \sigma, (\omega)}|_{cs}$ that can manifestly cancel against the ν_n dependences in eq. (2.50) and eq. (2.51), the rapidity regulator $\mathcal{R}(k_-, k_+, \tau)$ is introduced here for bookkeeping purposes. Once the relationship $\omega < (\sigma + \eta)$ is satisfied, $\mathcal{R}(k_-, k_+, \tau)$ always stays inactive in the limit $\tau \rightarrow 0$.

An analogous rearrangement is also applicable to $\tilde{\mathcal{I}}_{[\kappa], \{\alpha, \beta\}}^{\rho, \sigma, (\omega)}|_{\bar{cs}}$ in eq. (2.36). It yields that

$$\begin{aligned}
 & \sum_{\lambda=0}^{\infty} \frac{F_{i/n, \beta_n}^{(\alpha_n+\omega-\sigma)} (m_H e^{-Y_H}) F_{j/\bar{n}, \beta_{\bar{n}}}^{(\alpha_{\bar{n}}+\lambda)} (m_H e^{+Y_H})}{(\omega - \sigma)! \lambda!} \frac{\nu_{\bar{n}}^{\rho+\lambda-\omega}}{\rho + \lambda - \omega} \bar{\delta}_{\omega}^{\rho+\lambda} \\
 &= \frac{F_{i/n, \beta_n}^{(\alpha_n+\omega-\sigma)} (m_H e^{-Y_H})}{(\omega - \sigma)!} \left\{ \sum_{\lambda=\max\{0, (\omega-\rho+1)\}}^{\infty} \frac{F_{j/\bar{n}, \beta_{\bar{n}}}^{(\alpha_{\bar{n}}+\lambda)} (m_H e^{+Y_H})}{\lambda!} \frac{\nu_{\bar{n}}^{\rho+\lambda-\omega}}{\rho + \lambda - \omega} \right. \\
 & \quad \left. - \theta(\omega - \rho - 1) \sum_{\lambda=0}^{\omega-\rho-1} \frac{F_{j/\bar{n}, \beta_{\bar{n}}}^{(\alpha_{\bar{n}}+\lambda)} (m_H e^{+Y_H})}{\lambda!} \lim_{\tau \rightarrow 0} \int_{\nu_{\bar{n}}}^{\infty} \frac{dk_-}{k_-} \mathcal{R}(k_-, k_+, \tau) (k_-)^{\rho+\lambda-\omega} \right\}. \tag{2.58}
 \end{aligned}$$

We can now recast the logarithmic contributions of $\tilde{\mathcal{I}}_{[\kappa], \{\alpha, \beta\}}^{\rho, \sigma, (\omega)}|_{cs}$ and $\tilde{\mathcal{I}}_{[\kappa], \{\alpha, \beta\}}^{\rho, \sigma, (\omega)}|_{\bar{cs}}$ in integral form, as presented in eqs. (2.35) and (2.36). It is worth noting at this point that the logarithmic terms from both sectors always and only appear together once $\omega \geq \rho$ and $\omega \geq \sigma$ simultaneously. Therefore, in the following, we cope with them simultaneously, i.e.,

$$\begin{aligned}
 & \frac{F_{i/n, \beta_n}^{(\alpha_n+\omega-\sigma)} (m_H e^{-Y_H}) F_{j/\bar{n}, \beta_{\bar{n}}}^{(\alpha_{\bar{n}}+\omega-\rho)} (m_H e^{+Y_H})}{(\omega - \rho)! (\omega - \sigma)!} \left\{ \ln \left[\frac{\nu_n}{q_T} \right] + \ln \left[\frac{\nu_{\bar{n}}}{q_T} \right] \right\} \\
 &= \frac{F_{i/n, \beta_n}^{(\alpha_n+\omega-\sigma)} (m_H e^{-Y_H}) F_{j/\bar{n}, \beta_{\bar{n}}}^{(\alpha_{\bar{n}}+\omega-\rho)} (m_H e^{+Y_H})}{(\omega - \rho)! (\omega - \sigma)!} \\
 & \quad \times \left\{ - \lim_{\tau \rightarrow 0} \int_{\nu_n}^{\infty} \frac{dk_+}{k_+} \mathcal{R}(k_-, k_+, \tau) + \lim_{\tau \rightarrow 0} \int_0^{\infty} \frac{dk_+}{k_+} \mathcal{R}(k_-, k_+, \tau) - \lim_{\tau \rightarrow 0} \int_{\nu_{\bar{n}}}^{\infty} \frac{dk_-}{k_-} \mathcal{R}(k_-, k_+, \tau) \right\}, \tag{2.59}
 \end{aligned}$$

where in the last step we revert the logarithms into their integral form and employ $\mathcal{R}(k_-, k_+, \tau)$ to regulate their possibly singular behaviour in the limit $k_{\pm} \rightarrow 0$.

Comparing the above expressions with eq. (2.50), we observe that terms containing powers of the auxiliary scale $\nu_{n(\bar{n})}$ take the same form in eqs. (2.57) and (2.58) and eq. (2.50), and hence cancel upon combination. Similarly, the dependences of the integral on the auxiliary scales through their boundaries in eqs. (2.57)–(2.59) can be assimilated in their entirety by combining them with the corresponding integrals in eq. (2.51). Therefore, we arrive at,

$$\tilde{\mathcal{G}}_{[\kappa],\{\alpha,\beta\}}^{\rho,\sigma,(\omega)} \Big|_{c\bar{c}}^{\langle\text{NS}\rangle} = \tilde{\mathcal{G}}_{[\kappa],\{\alpha,\beta\}}^{\rho,\sigma,(\omega)} \Big|_{c0}^{\langle\text{NS}\rangle} + \tilde{\mathcal{G}}_{[\kappa],\{\alpha,\beta\}}^{\rho,\sigma,(\omega)} \Big|_{c\bar{0}}^{\langle\text{NS}\rangle}, \quad (2.60)$$

where

$$\begin{aligned} \tilde{\mathcal{G}}_{[\kappa],\{\alpha,\beta\}}^{\rho,\sigma,(\omega)} \Big|_{c0}^{\langle\text{NS}\rangle} &= \theta(\omega - \sigma) \sum_{\eta=0}^{\omega-\sigma} \sum_{\lambda=0}^{\omega-\rho} \frac{F_{i/n,\beta_n}^{(\alpha_n+\eta)}(m_H e^{-Y_H}) F_{j/\bar{n},\beta_{\bar{n}}}^{(\alpha_{\bar{n}}+\lambda)}(m_H e^{+Y_H})}{\eta! \lambda!} \\ &\quad \times \lim_{\tau \rightarrow 0} \int_0^\infty \frac{dk_+}{k_+} \left(1 - \frac{\delta_\omega^{\sigma+\eta}}{2}\right) \mathcal{R}(k_-, k_+, \tau) (k_+)^{\sigma-\omega+\eta} \delta_{\lambda+\rho}^\omega, \\ \tilde{\mathcal{G}}_{[\kappa],\{\alpha,\beta\}}^{\rho,\sigma,(\omega)} \Big|_{c\bar{0}}^{\langle\text{NS}\rangle} &= \theta(\omega - \rho) \sum_{\eta=0}^{\omega-\sigma} \sum_{\lambda=0}^{\omega-\rho} \frac{F_{i/n,\beta_n}^{(\alpha_n+\eta)}(m_H e^{-Y_H}) F_{j/\bar{n},\beta_{\bar{n}}}^{(\alpha_{\bar{n}}+\lambda)}(m_H e^{+Y_H})}{\eta! \lambda!} \\ &\quad \times \lim_{\tau \rightarrow 0} \int_0^\infty \frac{dk_-}{k_-} \left(1 - \frac{\delta_\omega^{\rho+\lambda}}{2}\right) \mathcal{R}(k_-, k_+, \tau) (k_-)^{\rho-\omega+\lambda} \delta_{\eta+\sigma}^\omega. \end{aligned} \quad (2.61)$$

Here, we have divided $\tilde{\mathcal{G}}_{[\kappa],\{\alpha,\beta\}}^{\rho,\sigma,(\omega)} \Big|_{c\bar{c}}^{\langle\text{NS}\rangle}$ into two pieces, $\tilde{\mathcal{G}}_{[\kappa],\{\alpha,\beta\}}^{\rho,\sigma,(\omega)} \Big|_{c0}^{\langle\text{NS}\rangle}$ and $\tilde{\mathcal{G}}_{[\kappa],\{\alpha,\beta\}}^{\rho,\sigma,(\omega)} \Big|_{c\bar{0}}^{\langle\text{NS}\rangle}$, inheriting the structure from eq. (2.51). At variance with eq. (2.51), however, additional factors $\delta_\omega^{\sigma+\eta}$ and $\delta_\omega^{\rho+\lambda}$ are present in the integrands now, induced by the unbounded integrals of eq. (2.59). During the derivation, we have evenly distributed these terms into the n -collinear and \bar{n} -collinear sectors symmetrically, incurring a factor $\frac{1}{2}$ in eq. (2.61). Alternative assignments are in principle possible, which may impact the expressions in the individual sectors but will leave the sum in eq. (2.60) invariant.

Equipped with the collinear functions of eq. (2.46) and the subtrahends of eq. (2.61), we are now able to re-express the interior contribution $\tilde{\mathcal{I}}_{[\kappa],\{\alpha,\beta\}}^{\rho,\sigma}$ as follows,

$$\tilde{\mathcal{I}}_{[\kappa],\{\alpha,\beta\}}^{\rho,\sigma} = \sum_{\omega=\rho}^{\infty} (q_{\text{T}}^2)^\omega \left[\tilde{\mathcal{G}}_{[\kappa],\{\alpha,\beta\}}^{\rho,\sigma,(\omega)} \Big|_c - \tilde{\mathcal{G}}_{[\kappa],\{\alpha,\beta\}}^{\rho,\sigma,(\omega)} \Big|_{c0}^{\langle\text{NS}\rangle} \right] + \sum_{\omega=\sigma}^{\infty} (q_{\text{T}}^2)^\omega \left[\tilde{\mathcal{G}}_{[\kappa],\{\alpha,\beta\}}^{\rho,\sigma,(\omega)} \Big|_{\bar{c}} - \tilde{\mathcal{G}}_{[\kappa],\{\alpha,\beta\}}^{\rho,\sigma,(\omega)} \Big|_{c\bar{0}}^{\langle\text{NS}\rangle} \right]. \quad (2.62)$$

Herein, we only show the expressions in the NS scheme for brevity, which can be straightforwardly converted into the FS ones through eq. (2.56). Referring back to eq. (2.42), we have now found a formulation in which the individual terms on the r.h.s. of eq. (2.62) are free of any dependence on the auxiliary scales $\nu_{n(\bar{n})}$ along the integration path. However, in return, they are now subject to the choice of rapidity regularisation scheme implemented through $\mathcal{R}(k_-, k_+, \tau)$. As will be discussed in sections 3.2 and 3.3, the regulator $\mathcal{R}(k_-, k_+, \tau)$ also depends on scales $\tilde{\nu}_n$ and $\tilde{\nu}_{\bar{n}}$ in practice, which bears resemblance to those in eq. (2.28) and can effectively concentrate the integrand in each sector onto its intrinsic domain, akin to the conventional dimensional regularisation [235].



(a) Subtrahends in the soft scaling.

(b) Subtrahends in the dual scaling.

Figure 1. Organisation of zero-bin subtrahends in different scalings. Every point in the map stands for a index-pair (λ, η) in eq. (2.61) which characterises the subtraction procedure entailed by the expansion of $\tilde{\mathcal{I}}_{[\kappa],\{\alpha,\beta\}}^{\lambda,\eta}$ with integer $\lambda, \eta \geq -1$ in the small q_T domain. As examples, the red stars highlight the subleading (NLP) power corrections, the blue triangles represent the sub-sub-leading (N²LP) ones, and the green dots indicate the sub-sub-sub-leading (N³LP) ones.

Finally, we can now analyse the scaling of k_{\pm} in each sector on the r.h.s. of eq. (2.62). Since the collinear functions here are derived by extrapolating the lower boundaries of eq. (2.31) and eq. (2.33), the integration variables in eq. (2.46) observe the same scaling rule as those in momentum space. More explicitly, we have $k_+ \sim \mathcal{O}(1)$ and $k_- \sim \mathcal{O}(q_T^2/m_H)$ for the n -collinear element and $k_+ \sim \mathcal{O}(q_T^2/m_H)$ and $k_- \sim \mathcal{O}(1)$ in the \bar{n} -collinear case. To determine the scaling in the subtraction terms of eq. (2.61), it merits noting that the integration variables k_{\pm} therein have been expanded in the arguments of both $F_{i/n,\beta_n}$ and $F_{j/\bar{n},\beta_{\bar{n}}}$, and also that the function $F_{j/\bar{n},\beta_{\bar{n}}}$ ($F_{i/n,\beta_n}$) in the “ $c0$ ” (“ $\bar{c}0$ ”) sector observes the same scaling pattern as that in the n -(\bar{n} -)collinear contribution of eq. (2.46). Therefore, we can interpret the variables k_{\pm} in eq. (2.61) from the dual scaling, expanding first the integrand with the collinear scaling and fixing the ω th-power correction, and then applying a second power expansion in line with soft scaling $k_{\pm} \sim \mathcal{O}(q_T)$ retaining all contributions below or equal to the (2ω) th-power.

It should be emphasised that at a lower power accuracy, the dual scaling can be reduced to the soft-only one especially in the case $\rho = \sigma = \chi$ with integer $\chi \geq -1$, which however does not hold in general. As an example, figure 1 illustrates the case $\chi = -1$, which is the minimum of χ allowed by the squared amplitudes in eq. (2.4) and thus concerns the leading power approximation in the small q_T domain. We observe that, on the lowest level, both of schemes consist of the origin $\lambda = \eta = -1$ and thus can be considered to be equivalent here. However, with the power accuracy growing, the soft scaling forces the indices λ and η to align along the diagonals, whereas the dual scaling organises the indices of the zero-bin subtrahend along rectangular edges, clearly separating the two. Those distinct patterns can subsequently evaluate to different zero-bin subtrahends for general choices of rapidity regulators, which therefore defies our interpretation of the integration variables of eq. (2.61) in a purely soft scaling prescription.

In order to systematically implement these scaling rules, we introduce the power expansion operator $\hat{\mathbf{T}}_i^{(\omega)}$, with the subscript i running over the sectors $\{c, \bar{c}, s\}$, acting on the object following it and projecting out the contribution at the ω th-power in line with the scalings indicated by i . In this way, the components of eq. (2.62) can be recast into,

$$\left(q_T^2\right)^{\omega} \tilde{\mathcal{G}}_{[\kappa],\{\alpha,\beta\}}^{\rho,\sigma,(\omega)} \Big|_c = \lim_{\tau \rightarrow 0} \int_0^{\tilde{k}_+^{\max}} \frac{dk_+}{k_+} \mathcal{R}(k_-, k_+, \tau) \hat{\mathbf{T}}_c^{(\omega)} I_{[\kappa],\{\alpha,\beta\}}^{\rho,\sigma},$$

$$\left(q_T^2 \right)^\omega \tilde{\mathcal{G}}_{[\kappa],\{\alpha,\beta\}}^{\rho,\sigma,(\omega)} \Big|_{\bar{c}} = \lim_{\tau \rightarrow 0} \int_0^{\frac{q_T^2}{k_+^{\min}}} \frac{dk_-}{k_-} \mathcal{R}(k_-, k_+, \tau) \hat{\mathbf{T}}_{\bar{c}}^{(\omega)} I_{[\kappa],\{\alpha,\beta\}}^{\rho,\sigma}, \quad (2.63)$$

and

$$\begin{aligned} \left(q_T^2 \right)^\omega \tilde{\mathcal{G}}_{[\kappa],\{\alpha,\beta\}}^{\rho,\sigma,(\omega)} \Big|_{c0} &= \theta(\omega - \sigma) \lim_{\tau \rightarrow 0} \int_0^\infty \frac{dk_+}{k_+} \mathcal{R}(k_-, k_+, \tau) \sum_{\bar{\omega}=(\rho+\sigma)}^{2\omega} \left(1 - \frac{\delta_{\bar{\omega}}^{2\omega}}{2} \right) \hat{\mathbf{T}}_s^{(\bar{\omega})} \hat{\mathbf{T}}_c^{(\omega)} I_{[\kappa],\{\alpha,\beta\}}^{\rho,\sigma}, \\ \left(q_T^2 \right)^\omega \tilde{\mathcal{G}}_{[\kappa],\{\alpha,\beta\}}^{\rho,\sigma,(\omega)} \Big|_{\bar{c}0} &= \theta(\omega - \rho) \lim_{\tau \rightarrow 0} \int_0^\infty \frac{dk_-}{k_-} \mathcal{R}(k_-, k_+, \tau) \sum_{\bar{\omega}=(\rho+\sigma)}^{2\omega} \left(1 - \frac{\delta_{\bar{\omega}}^{2\omega}}{2} \right) \hat{\mathbf{T}}_s^{(\bar{\omega})} \hat{\mathbf{T}}_{\bar{c}}^{(\omega)} I_{[\kappa],\{\alpha,\beta\}}^{\rho,\sigma}, \end{aligned} \quad (2.64)$$

where $I_{[\kappa],\{\alpha,\beta\}}^{\rho,\sigma}$ is the integrand of $\tilde{\mathcal{I}}_{[\kappa],\{\alpha,\beta\}}^{\rho,\sigma}$ defined in eq. (2.19),

$$I_{[\kappa],\{\alpha,\beta\}}^{\rho,\sigma} \equiv (k_-)^\rho (k_+)^\sigma F_{i/n,\beta_n}^{(\alpha_n)} \left(k_+ + m_H e^{-Y_H} \right) F_{j/\bar{n},\beta_{\bar{n}}}^{(\alpha_{\bar{n}})} \left(k_- + m_H e^{+Y_H} \right). \quad (2.65)$$

We note that after the re-arrangements of eqs. (2.48)–(2.52) and eqs. (2.57)–(2.59), the results in eqs. (2.63)–(2.64) present a form that is distinct from that observed in eqs. (2.31)–(2.33) as well as eqs. (2.40)–(2.41) obtained via the momentum cutoffs ν_n and $\nu_{\bar{n}}$. This is relevant in particular for the “ sc ” and “ $s\bar{c}$ ” sectors in eqs. (2.40)–(2.41), despite hybrid scaling having been used in the transitional range. As illustrated in eq. (2.34), the resulting coefficient $\tilde{\mathcal{I}}_{[\kappa],\{\alpha,\beta\}}^{\rho,\sigma,(\omega)}|_t$ invokes only the integrands at the same power accuracy once the scaling for the integration variable is given. Contrarily, the situation in eq. (2.64) is quite different, where, after applying the soft scaling, the results $\tilde{\mathcal{G}}_{[\kappa],\{\alpha,\beta\}}^{\rho,\sigma,(\omega)}|_{c0}$ and $\tilde{\mathcal{G}}_{[\kappa],\{\alpha,\beta\}}^{\rho,\sigma,(\omega)}|_{\bar{c}0}$ comprise not only corrections at the ω th-power, but also those on a lower level.

In order to interpret this structural difference, it merits recalling that in deriving eqs. (2.31) and (2.33) as well as eqs. (2.40) and (2.41) we have introduced a set of dynamic regions, see eq. (2.28), such that within these restricted phase space domains the assigned scalings are always effective before and after the phase space integration. However, in calculating the subtrahends in eq. (2.64), in particular after the combination with eqs. (2.57)–(2.59), all boundaries that separate the different scalings of the integration variables cancel out. As a result, the “ $c0$ ” and “ $\bar{c}0$ ” expressions of eq. (2.64) mainly comprise contributions from the rapidity extremities $k_\pm \rightarrow \pm 0$, correlated to the same positions of the collinear functions in eq. (2.63), rather than emphasising any integration segments in the physical domain. In light of this, the scaling laws implemented in eq. (2.64) should be conceived more of a prescription guiding us to organise the zero-bin subtrahends in order to subdue any unphysical asymptotic behaviour in the collinear sectors and averting the possibility of these sectors generating any non-trivial remainders for the resulting power series.

It is worth noting that the integrands in eq. (2.64) appear to contradict the homogeneity condition from the method of expansion by regions [177, 214–217]. In this method, the asymptotic behaviour of the Feynman or phase space integrals is associated with a set of regions along the integration path. From this one is able to expand the integrands before completing the integration and at a given power precision, the resulting power coefficients

only concern the expanded integrands of the same power accuracy, more specifically,

$$\tilde{\mathcal{F}}^{(\omega)} \sim \sum_i \int d\Phi \hat{\mathbf{T}}_i^{(\omega)} f, \quad (2.66)$$

where $\tilde{\mathcal{F}}^{(\omega)}$ denotes the ω th term in the power series, with f standing for a given integrand and Φ encoding a group of integration variables. In this paper, such a one-to-one correspondence between the power accuracy of the integrands and that of $\tilde{\mathcal{F}}^{(\omega)}$ will be referred to as the homogeneity of the asymptotic expansion hereafter.

On the contrary, a region analysis where the dimensional regulator uniquely governs the divergences incurred by the reduced integrands, such homogeneity is found to generally hold in a variety of kinematical limits, such as the off-shell large-momentum expansion and the large-mass limits with either an internal or external heavy parton [217]. The reason comes in part from the fact that the overlapping sectors for those asymptotic regimes, according to [177], admit the unbounded integrals over the multiple-expanded integrands, which, using dimensional regularisation, are all scaleless and thus vanish. In principle, if the homogeneity is also desired for the small q_T expansion, one can embed a special group of rapidity operators into eq. (2.64), such as the analytic [74, 76] and pure rapidity [113, 178] cases, from which, mimicking the dimensional regulator, the integrals in the zero-bin subtrahends of eq. (2.64) become scaleless and are thus eliminated. Subsequently, homogeneity is restored in the small q_T expansion and the power coefficients are thereby recast as,

$$\tilde{\mathcal{I}}_{[\kappa],\{\alpha,\beta\}}^{\rho,\sigma,(\omega)} = \tilde{\mathcal{G}}_{[\kappa],\{\alpha,\beta\}}^{\rho,\sigma,(\omega)} \Big|_c^{\langle \text{hom.rap.} \rangle} + \tilde{\mathcal{G}}_{[\kappa],\{\alpha,\beta\}}^{\rho,\sigma,(\omega)} \Big|_{\bar{c}}^{\langle \text{hom.rap.} \rangle}. \quad (2.67)$$

This work will dub this set of rapidity regulators the homogeneous ones, as labeled in the superscripts above. However, the above form is not generic. For instance, once the exponential regulator [79, 80] is put in place, both the “ $c0$ ” and “ $\bar{c}0$ ” sectors in eq. (2.64) will make non-trivial and indispensable contributions, from which all unphysical singularities generated in the collinear sectors of eq. (2.63) can be eliminated at each power, according to eq. (2.45). In this sense, the decomposition in eq. (2.67) can only be appropriate for the asymptotic expansion with a homogeneous regulator, while the generalised recipe, that will hold on a generic choice of rapidity regulators, is presented in eq. (2.62).

2.4.3 Comparison with existing results

We will now confront the zero-bin subtrahend derived in eqs. (2.62)–(2.64) with those proposed in the literature.

At LP, the zero-bin contribution at NLO involves only the master integral $\tilde{\mathcal{I}}_{[\kappa],\{\alpha,\beta\}}^{\rho,\sigma,(\omega)}$ with $\rho = \sigma = \omega = -1$ in the process $pp \rightarrow H + X$, and it has been demonstrated in [75, 163–166] that the zero-bin subtrahend can be constructed by taking the soft limit of the integrand. It follows that,

$$\frac{1}{q_T^2} \tilde{\mathcal{G}}_{[\kappa],\{\alpha,\beta\}}^{-1,-1,(-1)} \Big|_{c\bar{c}}^{\langle \text{NS} \rangle} \xrightarrow{\text{soft}} \lim_{\tau \rightarrow 0} \int_0^\infty \frac{dk_-}{k_-} \mathcal{R}(k_-, k_+, \tau) \frac{F_{i/n,\beta_n}^{(\alpha_n)}(m_H e^{-Y_H}) F_{j/\bar{n},\beta_{\bar{n}}}^{(\alpha_{\bar{n}})}(m_H e^{+Y_H})}{k_- k_+}. \quad (2.68)$$

This result can also be reproduced from eq. (2.64). At LP, the repeated application of the expansion operators in eq. (2.64) does not produce any power of the integration variables

k_{\pm} and therefore yields the same powers of k_{\pm} as that in eq. (2.68). Moreover, owing to the relation $2\omega = \bar{\omega} = -2$, the δ -functions in eq. (2.64) are both contributing a factor of $(1/2)$ from each sector, which add up to unity after combining the results. This thus leads to the exact same expression of eq. (2.68).

An alternative scheme to calculate the zero-bin subtraction up to NLP was proposed in [114, 115]. In this method, the asymptotic behaviour of the small q_T regime is assumed to be entirely governed by the n - and \bar{n} -collinear momenta. Subsequently, in order to remove the redundant overlapping contributions, each collinear ingredient is expanded in accordance with the scaling of the other one in the opposite direction and then their sum is averaged, more specifically,

$$\begin{aligned} \left(q_T^2\right)^\omega \tilde{\mathcal{G}}_{[\kappa],\{\alpha,\beta\}}^{\rho,\sigma,(\omega)} \Big|_{c\bar{c}}^{\langle\text{NS}\rangle} &\xrightarrow{\text{opp.col.}} \frac{\theta(\omega-\rho)\theta(\omega-\sigma)}{2} \lim_{\tau\rightarrow 0} \int_0^\infty \frac{dk_+}{k_+} \mathcal{R}(k_-, k_+, \tau) \\ &\times \left\{ \left(\sum_{\bar{\omega}=\sigma}^{\omega} \hat{\mathbf{T}}_{\bar{c}}^{(\bar{\omega})} \right) \hat{\mathbf{T}}_c^{(\omega)} + \left(\sum_{\bar{\omega}=\rho}^{\omega} \hat{\mathbf{T}}_c^{(\bar{\omega})} \right) \hat{\mathbf{T}}_{\bar{c}}^{(\omega)} \right. \\ &\left. + \hat{\mathbf{T}}_c^{(\omega)} \left(\sum_{\bar{\omega}=\sigma}^{\omega-1} \hat{\mathbf{T}}_{\bar{c}}^{(\bar{\omega})} \right) + \hat{\mathbf{T}}_{\bar{c}}^{(\omega)} \left(\sum_{\bar{\omega}=\rho}^{\omega-1} \hat{\mathbf{T}}_c^{(\bar{\omega})} \right) \right\} I_{[\kappa],\{\alpha,\beta\}}^{\rho,\sigma}. \end{aligned} \quad (2.69)$$

Using this result to calculate $I_{[\kappa],\{\alpha,\beta\}}^{-1,-1}$, we observe that only the first two terms in the curly brackets can give non-vanishing contributions at LP as the range of summation in the last two terms is more restricted. In addition, due to the fact that the product of two collinear expansion operators in the opposite collinear directions is equivalent to one single soft expansion operator in this case, eq. (2.69) evaluates to the identical expression to that in eq. (2.68).

At NLP, all terms of eq. (2.69) contribute to the zero-bin subtraction. While in the first two terms in the curly brackets the NLP collinear sectors have been expanded in line with the counting rule in the opposite direction, the last two terms recover the power corrections that did not contribute to the LP result, but re-enter the zero-bin subtraction procedure here. Thus, retaining all terms up to NLP, this yields,

$$\begin{aligned} \tilde{\mathcal{G}}_{[\kappa],\{\alpha,\beta\}}^{-1,-1,(0)} \Big|_{c\bar{c}}^{\langle\text{NS}\rangle} &\xrightarrow{\text{opp.col.}} \theta(\omega-\rho)\theta(\omega-\sigma) \lim_{\tau\rightarrow 0} \int_0^\infty \frac{dk_+}{k_+} \mathcal{R}(k_-, k_+, \tau) \left\{ 1 + \frac{1}{k_-} + \frac{1}{k_+} \right\} \\ &\times F_{i/n,\beta_n}^{(\alpha_n)} \left(m_H e^{-Y_H} \right) F_{j/\bar{n},\beta_{\bar{n}}}^{(\alpha_{\bar{n}})} \left(m_H e^{+Y_H} \right). \end{aligned} \quad (2.70)$$

This result agrees with the expectation from the dual scaling. Please note, LP-like terms have now entered the subtraction term at NLP, constituting the inhomogeneity we alluded to earlier. More explicitly, substituting the integrand $I_{[\kappa],\{\alpha,\beta\}}^{-1,-1}$ into eq. (2.64), we obtain,

$$\begin{aligned} \tilde{\mathcal{G}}_{[\kappa],\{\alpha,\beta\}}^{-1,-1,(0)} \Big|_{c_0} &= \theta(\omega-\sigma) \lim_{\tau\rightarrow 0} \int_0^\infty \frac{dk_+}{k_+} \mathcal{R}(k_-, k_+, \tau) \left\{ \frac{1}{2} + \frac{1}{k_+} \right\} F_{i/n,\beta_n}^{(\alpha_n)} \left(m_H e^{-Y_H} \right) F_{j/\bar{n},\beta_{\bar{n}}}^{(\alpha_{\bar{n}})} \left(m_H e^{+Y_H} \right), \\ \tilde{\mathcal{G}}_{[\kappa],\{\alpha,\beta\}}^{-1,-1,(0)} \Big|_{\bar{c}_0} &= \theta(\omega-\rho) \lim_{\tau\rightarrow 0} \int_0^\infty \frac{dk_-}{k_-} \mathcal{R}(k_-, k_+, \tau) \left\{ \frac{1}{2} + \frac{1}{k_-} \right\} F_{i/n,\beta_n}^{(\alpha_n)} \left(m_H e^{-Y_H} \right) F_{j/\bar{n},\beta_{\bar{n}}}^{(\alpha_{\bar{n}})} \left(m_H e^{+Y_H} \right). \end{aligned} \quad (2.71)$$

Recalling that additional constraints on the exponents ρ and σ have already been imposed in the definition of the power series in eq. (2.62), combining both contributions above precisely reproduces the results of eq. (2.70).

Furthermore, even though eq. (2.69) is obtained by summarising the asymptotic properties of the NLP ingredients in [114, 115], it is very interesting to note that eq. (2.69) is in fact still useful in organising the overlap removal for N²LP and beyond. To see this, we note that the collinear expansion operators $\widehat{\mathbf{T}}_c$ and $\widehat{\mathbf{T}}_{\bar{c}}$ commute. Hence, we can drop the factor of $\frac{1}{2}$ and recast the r.h.s. of eq. (2.69) below,

$$\begin{aligned}
 (q_{\mathbb{T}}^2)^\omega \widetilde{\mathcal{G}}_{[\kappa],\{\alpha,\beta\}}^{\rho,\sigma,(\omega)} \Big|_{c\bar{c}}^{(\text{NS})} &\xrightarrow{\text{opp.col.}} \theta(\omega-\rho)\theta(\omega-\sigma) \lim_{\tau \rightarrow 0} \int_0^\infty \frac{dk_+}{k_+} \mathcal{R}(k_-, k_+, \tau) \\
 &\times \left\{ \widehat{\mathbf{T}}_c^{(\omega)} \widehat{\mathbf{T}}_c^{(\omega)} + \widehat{\mathbf{T}}_c^{(\omega)} \left(\sum_{\bar{\omega}=\sigma}^{\omega-1} \widehat{\mathbf{T}}_c^{(\bar{\omega})} \right) + \widehat{\mathbf{T}}_c^{(\omega)} \left(\sum_{\bar{\omega}=\rho}^{\omega-1} \widehat{\mathbf{T}}_c^{(\bar{\omega})} \right) \right\} I_{[\kappa],\{\alpha,\beta\}}^{\rho,\sigma}.
 \end{aligned} \tag{2.72}$$

Plugging the expressions of eq. (2.65) into eq. (2.72), we then obtain,

$$\begin{aligned}
 \text{r.h.s. of eq. (2.72)} &= \theta(\omega-\rho)\theta(\omega-\sigma) \lim_{\tau \rightarrow 0} \int_0^\infty \frac{dk_+}{k_+} \mathcal{R}(k_-, k_+, \tau) \\
 &\times \left\{ k_-^\omega k_+^\omega \frac{F_{i/n,\beta_n}^{(\alpha_n+\omega-\sigma)}(m_H e^{-Y_H}) F_{j/\bar{n},\beta_{\bar{n}}}^{(\alpha_{\bar{n}}+\omega-\rho)}(m_H e^{+Y_H})}{(\omega-\sigma)! (\omega-\rho)!} \right. \\
 &\quad + k_-^{\omega-\sigma-1} \sum_{\eta=0}^{\omega-\sigma-1} k_+^{\sigma+\eta} \frac{F_{i/n,\beta_n}^{(\alpha_n+\eta)}(m_H e^{-Y_H}) F_{j/\bar{n},\beta_{\bar{n}}}^{(\alpha_{\bar{n}}+\omega-\rho)}(m_H e^{+Y_H})}{\eta! (\omega-\rho)!} \\
 &\quad \left. + k_-^{\omega} \sum_{\eta=0}^{\omega-\sigma-1} k_+^{\rho+\lambda} \frac{F_{i/n,\beta_n}^{(\alpha_n+\omega-\sigma)}(m_H e^{-Y_H}) F_{j/\bar{n},\beta_{\bar{n}}}^{(\alpha_{\bar{n}}+\lambda)}(m_H e^{+Y_H})}{\lambda! (\omega-\sigma)!} \right\}.
 \end{aligned} \tag{2.73}$$

Extracting a common factor of $(q_{\mathbb{T}}^2)^\omega$ from the curly bracket above, we observe its coincidence with the sum of eq. (2.61) and thus the equivalence with eq. (2.64).

We will now compare our results with the results obtained through employing the method of expansion by regions [177, 214–217] and focus in particular on the formalism proposed in [177]. Therein, the mathematical foundation behind the expansion by regions has been discussed via examples for the one-loop integrals in different kinematic limits. Of them, the analysis of the Feynman integrals in the Sudakov limit [177] is intimately related to the $q_{\mathbb{T}}$ spectra within the asymptotic regime. Therefore, after appropriate adaptations, the techniques proposed in [177] can also be exploited to compute the zero-bin subtraction here. In the following, we will elucidate this application.

The starting point of the formalism in [177] is to work out a group of dynamic regions that are able to encompass the entire phase space and also separately accommodate the contributions from all involved scales. In our case, this goal can be accomplished by the dynamic modes presented in eq. (2.28). The next task is to extrapolate the bounded integrals contained in each region so as to remove all auxiliary cutoff scales along the integration

paths. This procedure can be illustrated by using the expansion operators introduced in eqs. (2.63) and (2.64), i.e.

$$\tilde{\mathcal{I}}_{[\kappa],\{\alpha,\beta\}}^{\rho,\sigma} = \sum_{\omega} \left[\int_{\nu_n}^{\tilde{k}_+^{\max}} \hat{\mathbf{T}}_c^{(\omega)} + \int_{\frac{q_{\mathbb{T}}^2}{\nu_{\bar{n}}}}^{\nu_n} \hat{\mathbf{T}}_s^{(\omega)} + \int_{\tilde{k}_+^{\min}}^{\frac{q_{\mathbb{T}}^2}{\nu_{\bar{n}}}} \hat{\mathbf{T}}_{\bar{c}}^{(\omega)} \right] \frac{dk_+}{k_+} I_{[\kappa],\{\alpha,\beta\}}^{\rho,\sigma}, \quad (2.74)$$

and then extrapolating the integral boundaries ν_n and $\nu_{\bar{n}}$,

$$\begin{aligned} \sum_{\omega_c} \int_{\nu_n}^{\tilde{k}_+^{\max}} \hat{\mathbf{T}}_c^{(\omega_c)} &\rightarrow \lim_{\tau \rightarrow 0} \left[\sum_{\omega_c} \int_0^{\tilde{k}_+^{\max}} \mathcal{R} \hat{\mathbf{T}}_c^{(\omega_c)} - \sum_{\omega_c, \omega_s} \int_{\frac{q_{\mathbb{T}}^2}{\nu_{\bar{n}}}}^{\nu_n} \mathcal{R} \hat{\mathbf{T}}_s^{(\omega_s)} \hat{\mathbf{T}}_c^{(\omega_c)} - \sum_{\omega_c, \omega_{\bar{c}}} \int_0^{\frac{q_{\mathbb{T}}^2}{\nu_{\bar{n}}}} \mathcal{R} \hat{\mathbf{T}}_{\bar{c}}^{(\omega_{\bar{c}})} \hat{\mathbf{T}}_c^{(\omega_c)} \right], \\ \sum_{\omega_s} \int_{\frac{q_{\mathbb{T}}^2}{\nu_{\bar{n}}}}^{\nu_n} \hat{\mathbf{T}}_s^{(\omega_s)} &\rightarrow \lim_{\tau \rightarrow 0} \left[\sum_{\omega_s} \int_0^{\infty} \mathcal{R} \hat{\mathbf{T}}_s^{(\omega_s)} - \sum_{\omega_c, \omega_s} \int_{\nu_n}^{\infty} \mathcal{R} \hat{\mathbf{T}}_c^{(\omega_c)} \hat{\mathbf{T}}_s^{(\omega_s)} - \sum_{\omega_s, \omega_{\bar{c}}} \int_0^{\frac{q_{\mathbb{T}}^2}{\nu_{\bar{n}}}} \mathcal{R} \hat{\mathbf{T}}_{\bar{c}}^{(\omega_{\bar{c}})} \hat{\mathbf{T}}_s^{(\omega_s)} \right], \\ \sum_{\omega_{\bar{c}}} \int_{\tilde{k}_+^{\min}}^{\frac{q_{\mathbb{T}}^2}{\nu_{\bar{n}}}} \hat{\mathbf{T}}_{\bar{c}}^{(\omega_{\bar{c}})} &\rightarrow \lim_{\tau \rightarrow 0} \left[\sum_{\omega_{\bar{c}}} \int_{\tilde{k}_+^{\min}}^{\infty} \mathcal{R} \hat{\mathbf{T}}_{\bar{c}}^{(\omega_{\bar{c}})} - \sum_{\omega_{\bar{c}}, \omega_s} \int_{\frac{q_{\mathbb{T}}^2}{\nu_{\bar{n}}}}^{\nu_n} \mathcal{R} \hat{\mathbf{T}}_s^{(\omega_s)} \hat{\mathbf{T}}_{\bar{c}}^{(\omega_{\bar{c}})} - \sum_{\omega_c, \omega_{\bar{c}}} \int_{\nu_n}^{\infty} \mathcal{R} \hat{\mathbf{T}}_c^{(\omega_c)} \hat{\mathbf{T}}_{\bar{c}}^{(\omega_{\bar{c}})} \right]. \end{aligned} \quad (2.75)$$

Therein, in order to render the integrals still well-defined after extrapolating the boundaries, the rapidity regulator \mathcal{R} has been put in place. Since the discussion here is focused on the conservative rapidity regularisation prescription that preserves the expression of \mathcal{R} in all the involved sectors, in writing eq. (2.75), we pull all regulators \mathcal{R} in front of the expansion operators. We note that the r.h.s. of eq. (2.75) still depends on the cutoff scales ν_n and $\nu_{\bar{n}}$. This dependence can be eliminated through the following identity,

$$\begin{aligned} \sum_{\omega_c, \omega_{\bar{c}}, \omega_s} \int_0^{\infty} \mathcal{R} \hat{\mathbf{T}}_c^{(\omega_c)} \hat{\mathbf{T}}_s^{(\omega_s)} \hat{\mathbf{T}}_{\bar{c}}^{(\omega_{\bar{c}})} &\rightarrow \sum_{\omega_c, \omega_s} \int_0^{\frac{q_{\mathbb{T}}^2}{\nu_{\bar{n}}}} \mathcal{R} \hat{\mathbf{T}}_s^{(\omega_s)} \hat{\mathbf{T}}_c^{(\omega_c)} + \sum_{\omega_c, \omega_{\bar{c}}} \int_{\frac{q_{\mathbb{T}}^2}{\nu_{\bar{n}}}}^{\nu_n} \mathcal{R} \hat{\mathbf{T}}_{\bar{c}}^{(\omega_{\bar{c}})} \hat{\mathbf{T}}_c^{(\omega_c)} \\ &+ \sum_{\omega_{\bar{c}}, \omega_s} \int_{\nu_n}^{\infty} \mathcal{R} \hat{\mathbf{T}}_s^{(\omega_s)} \hat{\mathbf{T}}_{\bar{c}}^{(\omega_{\bar{c}})}. \end{aligned} \quad (2.76)$$

In its derivation, we have used the commutativity of the power projection operators $\hat{\mathbf{T}}_c$, $\hat{\mathbf{T}}_s$, and $\hat{\mathbf{T}}_{\bar{c}}$. Combining eq. (2.76) with eq. (2.75), we have,

$$\begin{aligned} \tilde{\mathcal{I}}_{[\kappa],\{\alpha,\beta\}}^{\rho,\sigma} &= \lim_{\tau \rightarrow 0} \left[\sum_{\omega_c} \int_0^{\tilde{k}_+^{\max}} \mathcal{R} \hat{\mathbf{T}}_c^{(\omega_c)} + \sum_{\omega_s} \int_0^{\infty} \mathcal{R} \hat{\mathbf{T}}_s^{(\omega_s)} + \sum_{\omega_{\bar{c}}} \int_{\tilde{k}_+^{\min}}^{\infty} \mathcal{R} \hat{\mathbf{T}}_{\bar{c}}^{(\omega_{\bar{c}})} \right. \\ &\quad - \sum_{\omega_c, \omega_s} \int_0^{\infty} \mathcal{R} \hat{\mathbf{T}}_c^{(\omega_c)} \hat{\mathbf{T}}_s^{(\omega_s)} - \sum_{\omega_c, \omega_{\bar{c}}} \int_0^{\infty} \mathcal{R} \hat{\mathbf{T}}_c^{(\omega_c)} \hat{\mathbf{T}}_{\bar{c}}^{(\omega_{\bar{c}})} - \sum_{\omega_s, \omega_{\bar{c}}} \int_0^{\infty} \mathcal{R} \hat{\mathbf{T}}_s^{(\omega_s)} \hat{\mathbf{T}}_{\bar{c}}^{(\omega_{\bar{c}})} \\ &\quad \left. + \sum_{\omega_c, \omega_s, \omega_{\bar{c}}} \int_0^{\infty} \mathcal{R} \hat{\mathbf{T}}_c^{(\omega_c)} \hat{\mathbf{T}}_s^{(\omega_s)} \hat{\mathbf{T}}_{\bar{c}}^{(\omega_{\bar{c}})} \right] \frac{dk_+}{k_+} I_{[\kappa],\{\alpha,\beta\}}^{\rho,\sigma}. \end{aligned} \quad (2.77)$$

Taking into account the facts that expanding in the collinear scalings following the soft power-projection operator $\hat{\mathbf{T}}_s$ can only result in delta functions as well as that two consecutive expansions in the collinear scalings are equivalent to one single expansion in the soft scaling

upon having summed all power contributions, we see that the doubly and triply expanded terms in eq. (2.77) are equal to an expansion in the soft scaling. To this end, we obtain,

$$\tilde{\mathcal{I}}_{[\kappa],\{\alpha,\beta\}}^{\rho,\sigma} = \sum_{\omega} \lim_{\tau \rightarrow 0} \left[\int_0^{\tilde{k}_+^{\max}} \mathcal{R} \hat{\mathbf{T}}_c^{(\omega)} + \int_{\tilde{k}_+^{\min}}^{\infty} \mathcal{R} \hat{\mathbf{T}}_{\tilde{c}}^{(\omega)} - \int_0^{\infty} \mathcal{R} \hat{\mathbf{T}}_s^{(\omega)} \right] \frac{dk_+}{k_+} I_{[\kappa],\{\alpha,\beta\}}^{\rho,\sigma}. \quad (2.78)$$

Comparing with eqs. (2.63) and (2.64), we observe that the first two terms in eq. (2.78) and the collinear functions in eq. (2.63) are equivalent. To explore the relationship of the third term in eq. (2.78) and the sum of eq. (2.64), we note that after bringing in the expression in eq. (2.65) the soft sector in eq. (2.78) evaluates to an infinite sum of the unbounded integrals, i.e.,

$$\sum_{\eta,\lambda=0}^{\infty} \lim_{\tau \rightarrow 0} \int_0^{\infty} \frac{dk_+}{k_+} \mathcal{R}(k_-, k_+, \tau) \frac{k_+^{\sigma+\eta} k_-^{\rho+\lambda}}{\eta! \lambda!} F_{i/n, \beta_n}^{(\alpha_n+\eta)}(m_H e^{-Y_H}) F_{j/\bar{n}, \beta_{\bar{n}}}^{(\alpha_{\bar{n}}+\lambda)}(m_H e^{+Y_H}), \quad (2.79)$$

which is exactly equal to the result from eq. (2.64) upon summing up all power contributions. Therefore, we can conclude at least the correspondence of eq. (2.78) and eqs. (2.63) and (2.64) on the cumulative level.

Notwithstanding, once a power-by-power comparison is being considered between both results, the analysis becomes more subtle. In [177], the analytic regulator is applied throughout the calculation of the Sudakov form factors. Implementing this scheme into eq. (2.77) (or eq. (2.78)), the integrals that are expanded in the soft scaling or comprise double or triple expansions all vanish. Then, eq. (2.77) and eq. (2.78) both reduce into the same decomposition we found in eq. (2.67) induced by the homogeneous regulators. However, if the inhomogeneous regularisation scheme is of one's particular interest, the soft function and the doubly and triply expanded constituents of eq. (2.77) can make non-trivial contributions at a given power accuracy, for which an unambiguous counting rule is required in order to produce the correct power coefficient $\tilde{\mathcal{I}}_{[\kappa],\{\alpha,\beta\}}^{\rho,\sigma,(\omega)}$.

2.5 Discussion and extrapolation

In the previous subsections, we have carried out the power expansion of the double-differential observable $d\sigma_H/dY_H dq_T^2$ in the low q_T domain. The result reads,

$$\frac{d\sigma_H}{dY_H dq_T^2} = \lambda_t^2 \sum_{\omega, \bar{\omega}} (q_T^2)^{\omega+\bar{\omega}} \sum_{[\kappa]} \sum_{\{\alpha,\beta\}, \rho, \sigma} \tilde{\mathcal{H}}_{[\kappa],\{\alpha,\beta\}}^{(\omega),\rho,\sigma}(m_H, Y_H, s) \left\{ \tilde{\mathcal{I}}_{[\kappa],\{\alpha,\beta\}}^{\rho,\sigma,(\bar{\omega})} + \Delta \tilde{\mathcal{I}}_{[\kappa],\{\alpha,\beta\}}^{\rho,\sigma,(\bar{\omega})} \right\}. \quad (2.80)$$

Therein, $\tilde{\mathcal{H}}_{[\kappa],\{\alpha,\beta\}}^{(\omega),\rho,\sigma}$ is a function of the hard scales m_H and s . Its expression has been presented in eq. (2.18) on a power-by-power basis. $\Delta \tilde{\mathcal{I}}_{[\kappa],\{\alpha,\beta\}}^{\rho,\sigma,(\bar{\omega})}$ accounts for the power corrections induced by the boundary conditions of the phase space integral. The results in the n -ultra-collinear limit can be extracted from eqs. (2.24)–(2.27), while those in the \bar{n} -direction can be derived by exchanging the light-cone coordinates in eqs. (2.26)–(2.27), as appropriate. Finally, eq. (2.80) contains $\tilde{\mathcal{I}}_{[\kappa],\{\alpha,\beta\}}^{\rho,\sigma,(\bar{\omega})}$ which comprises the contribution from the bulk of the phase space. In section 2.4.1 and section 2.4.2, we made use of two strategies to evaluate the expansion coefficients $\tilde{\mathcal{I}}_{[\kappa],\{\alpha,\beta\}}^{\rho,\sigma,(\bar{\omega})}$. In section 2.4.1, owing to the fact that our integration region comprises

multiple scales, we re-categorised the integration path via two of auxiliary cutoff scales, ν_n and $\nu_{\bar{n}}$. A dedicated method is applied for each subregion to perform the expansion within the low q_T domain. The quoted power series following this approach is illustrated in eq. (2.42). Then, in order to pave the way for future investigations of the power expansion at N²LO and beyond, we recombined the individual terms of eq. (2.42), eliminating any dependence on the auxiliary scales. The rearranged expansion coefficients are given in eq. (2.62). Equipped therewith, we are able to calculate the power series of $d\sigma_H/dY_H dq_T^2$ at an arbitrary power accuracy.

During our analysis, in order to facilitate the establishment of the relevant scaling relations, we concentrated on the central rapidity region where $e^{\pm Y_H} \sim \mathcal{O}(1)$. As it turns out, the expression in eq. (2.80) can also be extrapolated to the domain

$$\min\{\sqrt{s} - m_H e^{Y_H}, \sqrt{s} - m_H e^{-Y_H}\} > \max\{m_H e^{Y_H}, m_H e^{-Y_H}\}. \quad (2.81)$$

This extrapolation is straightforward to achieve in the kinematical reduction in section 2.2, since the expansion parameter therein is (q_T^2/m_H^2) .

Regarding $\Delta\tilde{\mathcal{I}}_{[\kappa],\{\alpha,\beta\}}^{\rho,\sigma}$, it is worth reminding the reader that the power expansion in section 2.3 primarily builds on the hierarchies,

$$\sqrt{s} - m_H e^{\pm Y_H} \gg |m_H - m_T| e^{\pm Y_H}, \quad m_H e^{\pm Y_H} \gg \frac{q_T^2}{\sqrt{s} - m_H e^{\mp Y_H}}. \quad (2.82)$$

Both relations are maintained by eq. (2.81) in the low q_T domain, and therefore the power expansion of $\Delta\tilde{\mathcal{I}}_{[\kappa],\{\alpha,\beta\}}^{\rho,\sigma}$ proceeds as before. A similar situation can be found in the interior contribution $\tilde{\mathcal{I}}_{[\kappa],\{\alpha,\beta\}}^{\rho,\sigma}$, in which the categorisation and the subsequent expansion base on the following relationship,

$$\sqrt{s} - m_H e^{-Y_H} > m_H e^{-Y_H} \gtrsim \nu_n \gg \frac{q_T^2}{\nu_{\bar{n}}} \gtrsim \frac{q_T^2}{m_H e^{Y_H}} > \frac{q_T^2}{\sqrt{s} - m_H e^{Y_H}}. \quad (2.83)$$

These inequalities ensure the integration variable k_{\pm} is always comparable to $m_H e^{\mp Y_H}$ in magnitude in the collinear sector, while that in the transitional domain is small enough to perform the power expansion. Eq. (2.83) is manifestly satisfied by the domain of eq. (2.81) for the small q_T regime, from which there exists a sufficiently wide window to introduce the auxiliary cutoff scales ν_n and $\nu_{\bar{n}}$. Hence, the subsequent power series of $\tilde{\mathcal{I}}_{[\kappa],\{\alpha,\beta\}}^{\rho,\sigma}$ can be derived as in section 2.4.

Following the above consideration, we can implement the expansion of eq. (2.80) within the full range of eq. (2.81). At the LHC with a colliding energy $\sqrt{s} = 13$ TeV, this interval corresponds to the rapidity region $|Y_H| \lesssim 4$ and, thus, enables a reliable power expansion in the bulk of the accessible phase space. Moving from $|Y_H| \approx 0$ to $|Y_H| \lesssim 4$, it is possible that novel hierarchies emerge from $\tilde{\mathcal{H}}_{[\kappa],\{\alpha,\beta\}}^{(\omega),\rho,\sigma}$ or any of the contributions in $\tilde{\mathcal{I}}_{[\kappa],\{\alpha,\beta\}}^{\rho,\sigma}$. For instance, $m_H e^{Y_H} \gg q_T \gg m_H e^{-Y_H}$ at $Y_H = 3.5$ and $q_T = 30$ GeV, which may alter the relative size of the coefficients at each power. It will not, however, impact the convergence of the power series of eq. (2.80) as a whole.

Eventually, it should be emphasised that our derivation of the power series expansion of the process $pp \rightarrow H + X$ primarily relies on the factorisation of the light-cone momenta in eq. (2.10). An analogous situation can also be found in the NLO squared amplitudes

for the Drell-Yan process viewed in terms of the decomposed scalar products in eq. (2.5). Therefore, our results for $\tilde{\mathcal{I}}_{[\kappa],\{\alpha,\beta\}}^{\rho,\sigma}$ and $\Delta\tilde{\mathcal{I}}_{[\kappa],\{\alpha,\beta\}}^{\rho,\sigma}$ obtained in this section are straightforwardly applicable onto the Drell-Yan process. After combining with its respective hard sector $\tilde{\mathcal{H}}$, it will in turn generate a power series via eq. (2.80) in the low q_T domain. Beside those two process classes, producing a single colour singlet boson, after appropriate generalisation of the kinematics, eq. (2.80) can in part also be used to describe the hadroproduction of the multiple colourless bosons, $pp \rightarrow B_1 + B_2 \dots B_n + X (n \geq 2)$, as well. We will elaborate on this procedure in appendix C.

3 Implementation up to N²LP

In this section, we will analyse the asymptotic behaviour of the q_T spectrum on the process $pp \rightarrow H + X$, and present the analytic expressions for the power corrections up to N²LP. As illustrated in eq. (2.80), the power expansion within the small q_T domain comprises two sectors, the interior contribution $\tilde{\mathcal{I}}_{[\kappa],\{\alpha,\beta\}}^{\rho,\sigma}$ and the boundary corrections $\Delta\tilde{\mathcal{I}}_{[\kappa],\{\alpha,\beta\}}^{\rho,\sigma}$. In the following, we will make use of three different methods to evaluate the interior sector. In section 3.1, the expressions in eqs. (2.30)–(2.33) and (2.40)–(2.41) that are derived via the momentum cutoff scales $\nu_{n(\bar{n})}$ in eq. (2.28) will be implemented. The results of eq. (2.46) and eq. (2.61) using a homogeneous regulator will be detailed in section 3.2 while an inhomogeneous prescription is used in section 3.3. It will be demonstrated that all three methods result in identical expressions for the interior contribution after combining all relevant terms. We expect the comparative study here can help the interpretation of the rapidity-divergence regularisation and present a viable prescription in the resummation beyond the leading power in the future.

3.1 Power expansion with momentum cutoffs

In line with the categorisation of phase space in eq. (2.28), the interior contributions are decomposed in terms of the collinear and transitional sectors, from which we can re-write eq. (2.80) here,

$$\frac{d\sigma_H}{dY_H dq_T^2} = \left. \frac{d\sigma_H^{\langle \text{m.c.} \rangle}}{dY_H dq_T^2} \right|_c + \left. \frac{d\sigma_H^{\langle \text{m.c.} \rangle}}{dY_H dq_T^2} \right|_{cs} + \left. \frac{d\sigma_H^{\langle \text{m.c.} \rangle}}{dY_H dq_T^2} \right|_{\bar{c}s} + \left. \frac{d\sigma_H^{\langle \text{m.c.} \rangle}}{dY_H dq_T^2} \right|_{\bar{c}} + \left. \frac{d\sigma_H}{dY_H dq_T^2} \right|_{b.c.}. \quad (3.1)$$

Therein, the ingredients with the subscripts “ c ” and “ \bar{c} ” account for the collinear pieces defined in eqs. (2.31) and (2.33), respectively, while those indicated by “ cs ” and “ $\bar{c}s$ ” encode the transitional elements from eqs. (2.40)–(2.41). In all these four terms, the superscript “m.c.” is introduced to manifest the fact that the momentum cutoffs ν_n and $\nu_{\bar{n}}$ are utilised during the power expansion. At last, we take account of the boundary corrections derived in section 2.3, termed “ $b.c.$ ”.

In the last section, the power expansions on those sectors are performed directly in the momentum space. To render their expressions more compact, we here recast them in terms of dimensionless parameters,

$$x_n \equiv \frac{m_H e^{-Y_H}}{\sqrt{s}} \equiv 1 - \bar{x}_n, \quad x_{\bar{n}} \equiv \frac{m_H e^{+Y_H}}{\sqrt{s}} \equiv 1 - \bar{x}_{\bar{n}}, \quad (3.2)$$

and those related to the integration variables,

$$k_+ \equiv m_H e^{-Y_H} \left(\frac{1 - z_n}{z_n} \right), \quad k_- \equiv m_H e^{+Y_H} \left(\frac{1 - z_{\bar{n}}}{z_{\bar{n}}} \right), \quad (3.3)$$

$$\nu_n \equiv m_H e^{-Y_H} \left(\frac{1 - \tilde{z}_n}{\tilde{z}_n} \right), \quad \nu_{\bar{n}} \equiv m_H e^{+Y_H} \left(\frac{1 - \tilde{z}_{\bar{n}}}{\tilde{z}_{\bar{n}}} \right). \quad (3.4)$$

Implementing this parameterisation is straightforward in the boundary corrections of eq. (2.24), the collinear sectors of eqs. (2.31) and (2.33), and the regular terms in the transitional contributions of eqs. (2.40)–(2.41). For contributions involving the star-distribution, e.g. eq. (2.38), we first make use of the method of integration by parts to reduce the higher ranked contributions to lower ones, and then introduce the dimensionless kinematic variables defined above to convert the star-distribution to the customary plus-distribution. Up to N²LP, the identities relevant to the reduction of the star-distributions read,

$$\begin{aligned} \int_0^\Lambda dx \left[\frac{1}{x^2} \right]_*^\nu f(x) &= \int_0^\Lambda dx \left[\frac{1}{x} \right]_*^\nu f'(x) - \frac{f(\Lambda)}{\Lambda} + f'(0) + \frac{f(0)}{\nu}, \\ \int_0^\Lambda dx \left[\frac{1}{x^3} \right]_*^\nu f(x) &= \frac{1}{2} \int_0^\Lambda dx \left[\frac{1}{x} \right]_*^\nu f''(x) - \frac{f(\Lambda)}{2\Lambda^2} - \frac{f'(\Lambda)}{2\Lambda} + \frac{3}{4} f''(0) + \frac{f'(0)}{\nu} + \frac{f(0)}{2\nu^2}, \end{aligned} \quad (3.5)$$

where $f(x)$ stands for a generic function sufficiently differentiable at $x = 0$. Regarding the transformation of the star-distributions to the plus distribution, the following relationships are used during our calculation,

$$\begin{aligned} \int_0^{\sqrt{s}x_n} dk_+ \left[\frac{1}{k_+} \right]_*^{\nu_n} f(k_+) &= \int_{x_n}^1 dz_n \left[\frac{1}{1 - z_n} \right]_+ f(z_n) + \int_{x_n}^1 \frac{dz_n}{z_n} f(z_n) + \ln \left[\frac{\sqrt{s}x_n}{\nu_n} \right] f(0), \\ \int_0^{\sqrt{s}x_{\bar{n}}} dk_- \left[\frac{1}{k_-} \right]_*^{\nu_{\bar{n}}} f(k_-) &= \int_{x_{\bar{n}}}^1 dz_{\bar{n}} \left[\frac{1}{1 - z_{\bar{n}}} \right]_+ f(z_{\bar{n}}) + \int_{x_{\bar{n}}}^1 \frac{dz_{\bar{n}}}{z_{\bar{n}}} f(z_{\bar{n}}) + \ln \left[\frac{\sqrt{s}x_{\bar{n}}}{\nu_{\bar{n}}} \right] f(0), \end{aligned} \quad (3.6)$$

where the plus-distribution is defined as,

$$\int_x^1 dz \left[\frac{1}{1 - z} \right]_+ f(z) = \int_x^1 dz \frac{f(z) - f(1)}{1 - z} - \int_0^x dz \frac{f(1)}{1 - z}. \quad (3.7)$$

Transitional domain. We have now all tools in place to present the respective expressions for each term on the r.h.s. of eq. (3.1). We begin with the transitional contributions that are associated with n -collinear and soft scalings,

$$\begin{aligned} \left. \frac{d\sigma_H^{\langle \text{m.c.} \rangle}}{dY_H dq_T^2} \right|_{cs} &\equiv \frac{\alpha_s^3 C_t^2}{192\pi^2 s v^2} \sum_{i,j=\{g,q,\bar{q}\}} \sum_{\omega=-1}^{\infty} \left(\frac{q_T^2}{m_H^2} \right)^\omega \int_{\tilde{z}_n}^1 dz_n \left[\mathbf{F}_{i/n} \left(\frac{x_n}{z_n} \right) \right]^\mathbf{T} \\ &\times \left\{ \mathbf{R}_{cs}^{(\omega),ij}(z_n) + \mathbf{P}_{cs}^{(\omega),ij} \left[\frac{1}{1 - z_n} \right]_+ + \mathbf{D}_{cs}^{(\omega),ij} \delta(1 - z_n) + \mathbf{B}_{cs}^{(\omega),ij}(\tilde{z}_n) \delta(\tilde{z}_n - z_n) \right\} \\ &\times \mathbf{F}_{j/\bar{n}}(x_{\bar{n}}). \end{aligned} \quad (3.8)$$

Therein, the q_T spectrum is expanded in the small parameter (q_T^2/m_H^2) on the r.h.s., and at each power of the resulting series, the coefficient comprises the convolution of the PDFs and the reduced squared amplitudes over the domain $z_n \in [\tilde{z}_n, 1]$. To facilitate the discussion, we here express the power series for each PDF in array form, more explicitly,

$$\begin{aligned} \left[\mathbf{F}_{i/n}(\xi_n) \right]^{\mathbf{T}} &\equiv \left[f_{i/n}(\xi_n), \xi_n f'_{i/n}(\xi_n), \frac{(\xi_n)^2}{2!} f''_{i/n}(\xi_n), \dots, \frac{(\xi_n)^k}{k!} f_{i/n}^{(k)}(\xi_n), \dots \right], \\ \mathbf{F}_{j/\bar{n}}(\xi_{\bar{n}}) &\equiv \left[f_{j/\bar{n}}(\xi_{\bar{n}}), \xi_{\bar{n}} f'_{j/\bar{n}}(\xi_{\bar{n}}), \frac{(\xi_{\bar{n}})^2}{2!} f''_{j/\bar{n}}(\xi_{\bar{n}}), \dots, \frac{(\xi_{\bar{n}})^k}{k!} f_{j/\bar{n}}^{(k)}(\xi_{\bar{n}}), \dots \right]^{\mathbf{T}}, \end{aligned} \quad (3.9)$$

where the superscript \mathbf{T} denotes the transposition operation. The shorthands $f_{i/n}^{(k)}$ and $f_{j/\bar{n}}^{(k)}$ are employed to represent the k -th derivative of the PDFs,

$$f_{i/n}^{(k)}(\tilde{\xi}_n) \equiv \left. \frac{\partial^k}{\partial \xi_n^k} f_{i/n}(\xi_n) \right|_{\xi_n = \tilde{\xi}_n}, \quad f_{j/\bar{n}}^{(k)}(\tilde{\xi}_{\bar{n}}) \equiv \left. \frac{\partial^k}{\partial \xi_{\bar{n}}^k} f_{j/\bar{n}}(\xi_{\bar{n}}) \right|_{\xi_{\bar{n}} = \tilde{\xi}_{\bar{n}}}. \quad (3.10)$$

Further, the reduced squared amplitudes $\mathbf{R}_{cs}^{(\omega),ij}$ are matrices in the rank of the PDF derivative encoded in $\mathbf{F}_{i/n}$. They characterise the ω th-power regular contributions from the transitional domain initiated by the partons i and j . For the partonic channel $gg \rightarrow Hg$, the results up to N²LP read,

$$\begin{aligned} \mathbf{R}_{cs}^{(-1),gg} &= -z_n + 1 - \frac{1}{z_n} + \frac{1}{z_n^2}, \\ \mathbf{R}_{cs}^{(0),gg} &= \begin{bmatrix} -\frac{3z_n^2}{2} - 4z_n - \frac{1}{2} + \frac{1}{2z_n^2} + \frac{5z_n}{2} + \frac{3}{2} + \frac{1}{2z_n} + \frac{1}{2z_n^2} \\ \frac{z_n^2}{2} + \frac{3z_n}{2} + \frac{1}{2z_n} & -z_n^2 - z_n - 1 \end{bmatrix}, \\ \mathbf{R}_{cs}^{(1),gg} &= \begin{bmatrix} -\frac{27z_n^3}{2} + \frac{3z_n^2}{8} - \frac{15z_n}{4} - \frac{19}{8} & \frac{27z_n^2}{4} + \frac{45z_n}{8} + \frac{29}{8} + \frac{5}{8z_n} & \frac{3z_n}{4} - \frac{3}{4} + \frac{3}{4z_n} + \frac{1}{4z_n^2} \\ & -\frac{1}{8z_n^2} & -6z_n^3 + 3z_n^2 \\ \frac{27z_n^3}{4} + \frac{13z_n^2}{8} + \frac{25z_n}{8} + \frac{7}{4} & -\frac{9z_n^2}{4} - \frac{11z_n}{4} - 3 + \frac{1}{4z_n} & 3z_n^3 \\ -\frac{9z_n^3}{4} - \frac{7z_n^2}{4} - \frac{5z_n}{2} - 2 & 0 & -z_n^3 - z_n^2 - z_n - 1 \end{bmatrix}. \end{aligned} \quad (3.11)$$

Here, all the entries that will vanish in the following are omitted for brevity. In the case of $i = q(\bar{q})$ and $j = g$, we have,

$$\begin{aligned} \mathbf{R}_{cs}^{(-1),q(\bar{q})g} &= \frac{2}{9} - \frac{4}{9z_n} + \frac{4}{9z_n^2}, \\ \mathbf{R}_{cs}^{(0),q(\bar{q})g} &= \begin{bmatrix} -\frac{2z_n}{9} + \frac{1}{3} + \frac{2}{9z_n^2} & -\frac{1}{9} + \frac{2}{9z_n} + \frac{2}{9z_n^2} \\ \frac{z_n}{9} - \frac{2}{9} + \frac{2}{9z_n} & 0 \end{bmatrix}, \\ \mathbf{R}_{cs}^{(1),q(\bar{q})g} &= \begin{bmatrix} \frac{z_n^2}{6} - \frac{z_n}{6} + \frac{1}{36} - \frac{1}{18z_n^2} & \frac{5z_n}{9} + \frac{1}{4} + \frac{5}{18z_n} + \frac{1}{18z_n^2} & \frac{4z_n}{9} + \frac{5}{18} + \frac{1}{3z_n} + \frac{1}{9z_n^2} \\ -\frac{z_n^2}{9} + \frac{5z_n}{36} - \frac{1}{18} + \frac{1}{18z_n} & -\frac{5z_n}{18} - \frac{2}{9} + \frac{1}{9z_n} & -\frac{2z_n}{9} - \frac{2}{9} \\ \frac{z_n^2}{18} - \frac{z_n}{9} + \frac{1}{9} & 0 & 0 \end{bmatrix}. \end{aligned} \quad (3.12)$$

Finally, those for the $q\bar{q}$ initial state read as follows,

$$\mathbf{R}_{cs}^{(-1),q\bar{q}} = 0, \quad \mathbf{R}_{cs}^{(0),q\bar{q}} = \frac{16}{27z_n} - \frac{16}{27}, \quad \mathbf{R}_{cs}^{(1),q\bar{q}} = \begin{bmatrix} \frac{16z_n}{27} - \frac{16}{27} & \frac{8}{27} + \frac{8}{27z_n} \\ \frac{8}{27} - \frac{8z_n}{27} & 0 \end{bmatrix}. \quad (3.13)$$

We next advance to the singular terms on the r.h.s. of eq. (3.1). $\mathbf{P}_{cs}^{(\omega)}$, consisting of only the constant coefficients, captures the contribution associated with the plus-distribution in eq. (3.7). Up to N²LP, they evaluate to,

$$\begin{aligned} \mathbf{P}_{cs}^{(-1),gg} &= 1, & \mathbf{P}_{cs}^{(0),gg} &= \begin{bmatrix} 4 & -\frac{1}{2} \\ -\frac{1}{2} & 1 \end{bmatrix}, & \mathbf{P}_{cs}^{(1),gg} &= \begin{bmatrix} 3 & -\frac{13}{8} & \frac{9}{4} \\ -\frac{13}{8} & \frac{13}{4} & 0 \\ \frac{9}{4} & 0 & 1 \end{bmatrix}, \\ \mathbf{P}_{cs}^{(-1),q(\bar{q})g} &= 0, & \mathbf{P}_{cs}^{(0),q(\bar{q})g} &= \begin{bmatrix} \frac{2}{9} & \frac{2}{9} \end{bmatrix}, & \mathbf{P}_{cs}^{(1),q(\bar{q})g} &= \begin{bmatrix} 0 & \frac{2}{9} & \frac{2}{9} \\ \frac{1}{9} & \frac{1}{3} & \frac{2}{9} \end{bmatrix}, \\ \mathbf{P}_{cs}^{(-1),q\bar{q}} &= 0, & \mathbf{P}_{cs}^{(0),q\bar{q}} &= 0, & \mathbf{P}_{cs}^{(1),q\bar{q}} &= 0. \end{aligned} \quad (3.14)$$

Herein, due to the finiteness of the squared amplitude of eq. (2.4) (qq) in the limit $k_{\pm} \rightarrow 0$, the $\mathbf{P}_{cs}^{(\omega),q\bar{q}}$ all vanish in the first few power corrections.

The remaining singular terms of eq. (2.4) are governed by the delta function and the coefficients $\mathbf{D}_{cs}^{(\omega)}$. Their expressions for LP, NLP, and N²LP are,

$$\begin{aligned} \mathbf{D}_{cs}^{(-1),gg} &= L_{cs} \mathbf{P}_{cs}^{(-1),gg}, & \mathbf{D}_{cs}^{(-1),q(\bar{q})g} &= \mathbf{D}_{cs}^{(-1),q\bar{q}} = \mathbf{D}_{cs}^{(0),q\bar{q}} = \mathbf{D}_{cs}^{(1),q\bar{q}} = 0, \\ \mathbf{D}_{cs}^{(0),gg} &= L_{cs} \mathbf{P}_{cs}^{(0),gg} + \begin{bmatrix} 3 & -3 \\ -1 & +1 \end{bmatrix}, & \mathbf{D}_{cs}^{(0),q(\bar{q})g} &= L_{cs} \mathbf{P}_{cs}^{(0),q(\bar{q})g}, \\ \mathbf{D}_{cs}^{(1),gg} &= L_{cs} \mathbf{P}_{cs}^{(1),gg} + \begin{bmatrix} 9 & -9 & 0 \\ -\frac{13}{2} & +\frac{7}{2} & -\frac{3}{2} \\ \frac{7}{2} & -\frac{1}{2} & \frac{3}{2} \end{bmatrix}, & \mathbf{D}_{cs}^{(1),q(\bar{q})g} &= L_{cs} \mathbf{P}_{cs}^{(1),q(\bar{q})g} + \begin{bmatrix} 0 & -\frac{4}{9} & -\frac{4}{9} \\ 0 & \frac{2}{9} & \frac{2}{9} \end{bmatrix}, \end{aligned} \quad (3.15)$$

where the logarithm $L_{cs} \equiv \ln[\sqrt{s}x_n/q_T]$ results from the logarithmic contributions in the transitional sectors of eqs. (2.40) and (3.6). We note that all L_{cs} dependences in $\mathbf{D}_{cs}^{(\omega)}$ are correlated to the coefficients $\mathbf{P}_{cs}^{(\omega)}$ at each power. To interpret this phenomenon, it merits recalling that in eq. (2.40), the coefficient function that is convoluted in the star-distribution reads $F_{i/n,\beta_n}^{(\alpha_n)} F_{j/\bar{n},\beta_{\bar{n}}}^{(\alpha_{\bar{n}}+\omega-\rho)}$, which, after reducing the rank with the help of eq. (3.5), is recast into $F_{i/n,\beta_n}^{(\alpha_n+\omega-\sigma)} F_{j/\bar{n},\beta_{\bar{n}}}^{(\alpha_{\bar{n}}+\omega-\rho)}$, corresponding to the coefficient of the logarithmic term. During the subsequent transformation in eq. (3.6), this correspondence is inherited by the coefficient associated with the plus distribution, which, within the parametrisation of eq. (3.8), correlates $\mathbf{P}_{cs}^{(\omega)}$ to the logarithmic terms in $\mathbf{D}_{cs}^{(\omega)}$.

The last constituent in eq. (3.8) is $\mathbf{B}_{cs}^{(\omega)}$. It accommodates the boundary terms on the r.h.s. of eq. (3.5), as a result of using an integration by parts in its derivation. The outputs for the first three orders read,

$$\begin{aligned} \mathbf{B}_{cs}^{(-1),gg} &= \mathbf{B}_{cs}^{(-1),q(\bar{q})g} = \mathbf{B}_{cs}^{(-1),q\bar{q}} = \mathbf{B}_{cs}^{(0),q(\bar{q})g} = \mathbf{B}_{cs}^{(0),q\bar{q}} = \mathbf{B}_{cs}^{(1),q\bar{q}} = 0, \\ \mathbf{B}_{cs}^{(0),gg} &= \left[-\frac{\tilde{z}_n^4}{\tilde{z}_n-1} \quad \frac{\tilde{z}_n^4}{\tilde{z}_n-1} \right], \\ \mathbf{B}_{cs}^{(1),gg} &= \begin{bmatrix} \frac{\tilde{z}_n^4[(11-6\tilde{z}_n)\tilde{z}_n-8]}{2(\tilde{z}_n-1)^2} & \frac{\tilde{z}_n^4(5\tilde{z}_n-4)}{2(\tilde{z}_n-1)^2} & \frac{\tilde{z}_n^4[(8-3\tilde{z}_n)\tilde{z}_n-6]}{2(\tilde{z}_n-1)^2} \\ \frac{\tilde{z}_n^5}{\tilde{z}_n-1} & 0 & \frac{\tilde{z}_n^5}{2(\tilde{z}_n-1)} \end{bmatrix}, \quad \mathbf{B}_{cs}^{(1),q(\bar{q})g} = \left[0 \quad \frac{2\tilde{z}_n^3}{9(\tilde{z}_n-1)} \quad \frac{2\tilde{z}_n^3}{9(\tilde{z}_n-1)} \right]. \end{aligned} \quad (3.16)$$

Since this contribution primarily arises from the reduction of the higher ranked star-distributions, $\mathbf{B}_{cs}^{(\omega),q\bar{q}}$ vanishes for $\omega \in [-1, 0, 1]$, similarly to the $\mathbf{P}_{cs}^{(\omega),q\bar{q}}$ earlier. The other part of the transitional region is subject to the \bar{n} -collinear and soft scalings, which can be organised in an analogous manner to eq. (3.8), more specifically,

$$\begin{aligned} \left. \frac{d\sigma_H^{(m.c.)}}{dY_H dq_T^2} \right|_{\bar{c}s} &\equiv \frac{\alpha_s^3 C_t^2}{192\pi^2 s v^2} \sum_{i,j=\{g,q,\bar{q}\}} \sum_{\omega=-1}^{\infty} \left(\frac{q_T^2}{m_H^2} \right)^\omega \int_{\tilde{z}_n}^1 dz_{\bar{n}} \left[\mathbf{F}_{i/n}(x_n) \right]^T \\ &\times \left\{ \mathbf{R}_{\bar{c}s}^{(\omega),ij}(z_{\bar{n}}) + \mathbf{P}_{\bar{c}s}^{(\omega),ij} \left[\frac{1}{1-z_{\bar{n}}} \right]_+ + \mathbf{D}_{\bar{c}s}^{(\omega),ij} \delta(1-z_{\bar{n}}) + \mathbf{B}_{\bar{c}s}^{(\omega),ij}(\tilde{z}_{\bar{n}}) \delta(\tilde{z}_{\bar{n}}-z_{\bar{n}}) \right\} \\ &\times \mathbf{F}_{j/\bar{n}} \left(\frac{x_{\bar{n}}}{z_{\bar{n}}} \right). \end{aligned} \quad (3.17)$$

Herein, eq. (3.17) comprises the matrices $\mathbf{R}_{\bar{c}s}$, $\mathbf{P}_{\bar{c}s}$, $\mathbf{D}_{\bar{c}s}$, and $\mathbf{B}_{\bar{c}s}$ to likewise encapsulate the different facets of partonic contributions, akin to those in eq. (3.8). Of them, the matrices for the partonic processes $gg \rightarrow Hg$ and $q\bar{q} \rightarrow Hg$ can be immediately derived from those appearing in eq. (3.8), as the squared amplitudes for these channels in eq. (2.4) (gg and qq) are symmetric under the exchange of their initial states, more explicitly,

$$\mathbf{X}_{\bar{c}s}^{(\omega),ij} = \left[\mathbf{X}_{cs}^{(\omega),ij} \right]^T \Bigg|_{\substack{z_n \rightarrow z_{\bar{n}}, \tilde{z}_n \rightarrow \tilde{z}_{\bar{n}} \\ L_{cs} \rightarrow L_{\bar{c}s}}}, \quad \text{where } \mathbf{X} \in \{\mathbf{R}, \mathbf{P}, \mathbf{D}, \mathbf{B}\} \text{ and } \{ij\} \in \{gg, q\bar{q}\}. \quad (3.18)$$

An analogous strategy can also be applied to evaluate the matrices $\mathbf{P}_{\bar{c}s}^{(\omega),q(\bar{q})g}$ that are induced by the initial state $q(\bar{q})g$. As discussed before, $\mathbf{P}_{\bar{c}s}^{(\omega),q(\bar{q})g}$ is associated with the coefficient of the logarithmic term of $\tilde{\mathcal{I}}_{[\bar{\kappa}],\{\alpha,\beta\}}^{\rho,\sigma}|_{\bar{c}s}$ in eq. (2.41), which, by comparison, is same as that from $\tilde{\mathcal{I}}_{[\bar{\kappa}],\{\alpha,\beta\}}^{\rho,\sigma}|_{cs}$ in eq. (2.40). To this end, we have,

$$\mathbf{P}_{\bar{c}s}^{(\omega),q(\bar{q})g} = \mathbf{P}_{cs}^{(\omega),q(\bar{q})g}. \quad (3.19)$$

This correspondence also holds for the logarithmic contributions in $\mathbf{D}_{\bar{c}s}^{(\omega),q(\bar{q})g}$,

$$\begin{aligned} \mathbf{D}_{\bar{c}s}^{(-1),q(\bar{q})g} &= 0, \\ \mathbf{D}_{\bar{c}s}^{(0),q(\bar{q})g} &= L_{\bar{c}s} \mathbf{P}_{cs}^{(0),q(\bar{q})g} + \left[-\frac{2}{9} \quad +\frac{2}{9} \right], \\ \mathbf{D}_{\bar{c}s}^{(1),q(\bar{q})g} &= L_{\bar{c}s} \mathbf{P}_{cs}^{(1),q(\bar{q})g} + \begin{bmatrix} 0 & 0 & \frac{2}{9} \\ -\frac{2}{9} & \frac{2}{9} & \frac{1}{3} \end{bmatrix}, \end{aligned} \quad (3.20)$$

where $L_{\bar{c}s} \equiv \ln[\sqrt{s}x_{\bar{n}}/q_T]$. Comparing with eq. (3.15), the constant terms in eq. (3.20) are very different, mirroring the asymmetry of the matrix element of $q(\bar{q}) + g \rightarrow H + q(\bar{q})$ in eq. (2.4) (gq) under the n -collinear and \bar{n} -collinear scalings.

Unsurprisingly, this asymmetric behaviour also emerges from the regular coefficients,

$$\begin{aligned} \mathbf{R}_{\bar{c}s}^{(-1),q(\bar{q})g} &= 0, \\ \mathbf{R}_{\bar{c}s}^{(0),q(\bar{q})g} &= \left[\frac{2}{9} + \frac{2}{9z_{\bar{n}}} - \frac{2}{9} \right], \\ \mathbf{R}_{\bar{c}s}^{(1),q(\bar{q})g} &= \begin{bmatrix} \frac{1}{9} - \frac{2z_{\bar{n}}}{9} & \frac{2z_{\bar{n}}}{9} - \frac{1}{9} - \frac{2z_{\bar{n}}}{9} - \frac{2}{9} \\ -\frac{2z_{\bar{n}}}{9} + \frac{1}{3} + \frac{1}{9z_{\bar{n}}} & \frac{2z_{\bar{n}}}{9} - \frac{1}{3} - \frac{2z_{\bar{n}}}{9} - \frac{2}{9} \end{bmatrix}, \end{aligned} \tag{3.21}$$

and the boundary corrections,

$$\mathbf{B}_{\bar{c}s}^{(-1),q(\bar{q})g} = 0, \quad \mathbf{B}_{\bar{c}s}^{(0),q(\bar{q})g} = \frac{2\tilde{z}_{\bar{n}}^2}{9(\tilde{z}_{\bar{n}} - 1)}, \quad \mathbf{B}_{\bar{c}s}^{(1),q(\bar{q})g} = \begin{bmatrix} -\frac{(\tilde{z}_{\bar{n}}-2)\tilde{z}_{\bar{n}}^2}{9(\tilde{z}_{\bar{n}}-1)} & \frac{\tilde{z}_{\bar{n}}^3}{9(\tilde{z}_{\bar{n}}-1)} \\ -\frac{\tilde{z}_{\bar{n}}^2[(\tilde{z}_{\bar{n}}-5)\tilde{z}_{\bar{n}}+5]}{9(\tilde{z}_{\bar{n}}-1)^2} & \frac{\tilde{z}_{\bar{n}}^3}{9(\tilde{z}_{\bar{n}}-1)} \end{bmatrix}. \tag{3.22}$$

Collinear and ultra-collinear regimes. The collinear contributions governed by eq. (2.31) and eq. (2.33) are formally aligned with the integrals from the transitional sectors as exhibited in eqs. (2.40)–(2.41). This correspondence even holds after reducing their rank using eq. (3.5) and transforming them with the help of eq. (3.6) if the plus distribution terms are treated to be regular functions and the boundary terms emerging from the integration by parts are all adapted to the collinear regimes as appropriate. The results then read,

$$\begin{aligned} \left. \frac{d\sigma_H^{(m.c.)}}{dY_H dq_T^2} \right|_{\bar{c}} &\equiv \frac{\alpha_s^3 C_t^2}{192\pi^2 s v^2} \sum_{i,j=\{g,q,\bar{q}\}} \sum_{\omega=-1}^{\infty} \left(\frac{q_T^2}{m_H^2} \right)^\omega \int_{x_n}^{\tilde{z}_n} dz_n \left[\mathbf{F}_{i/n} \left(\frac{x_n}{z_n} \right) \right]^T \\ &\times \left\{ \mathbf{R}_{\bar{c}s}^{(\omega),ij}(z_n) + \frac{\mathbf{P}_{\bar{c}s}^{(\omega),ij}}{1-z_n} + \mathbf{B}_{\bar{c}s}^{(\omega),ij}(z_n) \left[\delta(x_n - z_n) - \delta(\tilde{z}_n - z_n) \right] \right\} \\ &\times \mathbf{F}_{j/\bar{n}}(x_{\bar{n}}), \\ \left. \frac{d\sigma_H^{(m.c.)}}{dY_H dq_T^2} \right|_{\bar{c}} &\equiv \frac{\alpha_s^3 C_t^2}{192\pi^2 s v^2} \sum_{i,j=\{g,q,\bar{q}\}} \sum_{\omega=-1}^{\infty} \left(\frac{q_T^2}{m_H^2} \right)^\omega \int_{x_{\bar{n}}}^{\tilde{z}_{\bar{n}}} dz_{\bar{n}} \left[\mathbf{F}_{i/n}(x_n) \right]^T \\ &\times \left\{ \mathbf{R}_{\bar{c}s}^{(\omega),ij}(z_{\bar{n}}) + \frac{\mathbf{P}_{\bar{c}s}^{(\omega),ij}}{1-z_{\bar{n}}} + \mathbf{B}_{\bar{c}s}^{(\omega),ij}(z_{\bar{n}}) \left[\delta(x_{\bar{n}} - z_{\bar{n}}) - \delta(\tilde{z}_{\bar{n}} - z_{\bar{n}}) \right] \right\} \\ &\times \mathbf{F}_{j/\bar{n}} \left(\frac{x_{\bar{n}}}{z_{\bar{n}}} \right). \end{aligned} \tag{3.23}$$

Combining this result with the results from the moderate domain in eqs. (3.8) and (3.17), we observe that all the dependences on the parameters \tilde{z}_n and $\tilde{z}_{\bar{n}}$, which are associated with auxiliary cutoff scales ν_n and $\nu_{\bar{n}}$, drop out. This cancellation is in agreement with the vanishing derivatives in eqs. (2.43) and (2.44) as well as the expectation from a direct power expansion on the analytic expressions of the q_T spectrum (if they are known).

Finally, we move to the ultra-collinear contributions, which contains the maximal longitudinal momentum of an emitted parton allowed by the colliding energy. As discussed in

section 2.3, this sector stems from the power expansion on the boundary conditions in eq. (2.2). Therefore, the resulting expression will be proportional to the derivatives of the respective PDFs at the end point. Moreover, since, as defined in eqs. (2.22) and (2.23), the phase space integrals of this region are all restricted in the boundary strips of power-suppressed sizes, the ultra-collinear contribution will not invoke any singular behaviour in the low q_T region but can be relevant starting from NLP as a non-logarithmic power correction. The expression up to N²LP can be organised as,

$$\left. \frac{d\sigma_H}{dY_H dq_T^2} \right|_{b.c.} \equiv \frac{\alpha_s^3 C_t^2}{192\pi^2 s v^2} \sum_{i,j=\{g,q,\bar{q}\}} \sum_{\omega=-1}^{\infty} \left(\frac{q_T^2}{m_H^2} \right)^\omega \left\{ \left[\mathbf{F}_{i/n}(1) \right]^T \cdot \mathbf{B}_{uc}^{(\omega),ij}(x_n) \cdot \mathbf{F}_{j/\bar{n}}(x_{\bar{n}}) + \left[\mathbf{F}_{i/n}(x_n) \right]^T \cdot \mathbf{B}_{uc}^{(\omega),ij}(x_{\bar{n}}) \cdot \mathbf{F}_{j/\bar{n}}(1) \right\}. \quad (3.24)$$

Therein, the leading power coefficients all vanish,

$$\mathbf{B}_{uc}^{(-1),ij} = \mathbf{B}_{uc}^{(-1),ij} = 0. \quad (3.25)$$

The partonic matrices at the (sub-)subleading power induced by the \bar{n} -collinear mode evaluate to,

$$\begin{aligned} \mathbf{B}_{uc}^{(0),gg}(x_{\bar{n}}) &= \frac{[(x_{\bar{n}}-1)x_{\bar{n}}+1]^2}{2(x_{\bar{n}}-1)}, \\ \mathbf{B}_{uc}^{(1),gg}(x_{\bar{n}}) &= \begin{bmatrix} \frac{-3x_{\bar{n}}^6+11x_{\bar{n}}^5-12x_{\bar{n}}^4+17x_{\bar{n}}^3-10x_{\bar{n}}^2+x_{\bar{n}}-1}{8(x_{\bar{n}}-1)^2} & \frac{x_{\bar{n}}[(x_{\bar{n}}-1)x_{\bar{n}}+1]^2}{8(x_{\bar{n}}-1)} \\ -\frac{(x_{\bar{n}}+1)[(x_{\bar{n}}-1)x_{\bar{n}}+1]^2}{4(x_{\bar{n}}-1)^2} & 0 \end{bmatrix}, \\ \mathbf{B}_{uc}^{(0),q(\bar{q})g}(x_{\bar{n}}) &= \mathbf{B}_{uc}^{(0),q\bar{q}}(x_{\bar{n}}) = 0, \\ \mathbf{B}_{uc}^{(1),q(\bar{q})g}(x_{\bar{n}}) &= -\frac{x_{\bar{n}}}{9(x_{\bar{n}}-1)^2}, \\ \mathbf{B}_{uc}^{(1),q\bar{q}}(x_{\bar{n}}) &= \frac{8}{27}(x_{\bar{n}}-1)x_{\bar{n}}. \end{aligned} \quad (3.26)$$

Those from the n -collinear mode can be derived from the relation below,

$$\mathbf{B}_{uc}^{(\omega),ij}(x_n) = \left[\mathbf{B}_{uc}^{(\omega),ij}(x_{\bar{n}}) \right]^T \Big|_{x_{\bar{n}} \rightarrow x_n}, \quad \text{where } \omega \in \{-1, 0, +1\} \text{ and } \{ij\} \in \{gg, q\bar{q}\}, \quad (3.27)$$

together with,

$$\begin{aligned} \mathbf{B}_{uc}^{(0)q(\bar{q})g} &= \frac{1}{9}[-(x_n-2)x_n-2], \\ \mathbf{B}_{uc}^{(1)q(\bar{q})g} &= \begin{bmatrix} \frac{[x_n(2x_n-5)+5]x_n^2+2}{36(x_n-1)} & \frac{1}{18} \left(x_n^2 + \frac{2}{x_n-1} \right) \\ -\frac{1}{36}x_n[(x_n-2)x_n+2] & 0 \end{bmatrix}. \end{aligned} \quad (3.28)$$

We have presented here the analytic expressions of the first three terms in the power series of $d\sigma_H/(dY_H dq_T^2)$ in the vicinity of $q_T = 0$, using $pp \rightarrow H + X$ with the partonic channels

$gg \rightarrow Hg$, $q(\bar{q})g \rightarrow Hq(\bar{q})$, and $q\bar{q} \rightarrow Hg$ as an example. In addition, the q_T distribution also comprises the channels $gg(\bar{q}) \rightarrow Hq(\bar{q})$ and $\bar{q}q \rightarrow Hg$, for which the partonic matrices from the corresponding sectors can be derived from those in the $q(\bar{q})g \rightarrow Hq(\bar{q})$ and $q\bar{q} \rightarrow Hg$ processes by exchanging the labels $n \leftrightarrow \bar{n}$ as appropriate.

In the previous investigations on the process $pp \rightarrow H + X$, the ingredients contributing to the leading singular behaviour of the q_T distributions are known up to N³LO [100, 173–176, 179, 187, 189, 195–206]. Comparing the NLO expressions in [80, 174] derived with the exponential rapidity regulator with the leading terms of the sum of eqs. (3.8), (3.17), and (3.23), we find perfect agreement between the two upon performing an inverse Fourier transformation. In addition, the NLP power corrections have also been evaluated in [113] via the η - and pure rapidity regularisation schemes. Here as well, we have verified that the sum of eqs. (3.8), (3.17), and (3.23) can exactly reproduce the expressions in [113], except for the boundary terms encoded in the \mathbf{B}_{cs} matrix in eq. (3.8), $\mathbf{B}_{\bar{c}s}$ in eq. (3.17), and $\mathbf{B}_{uc,u\bar{c}}$ in eq. (3.24). The reason for the difference in the boundary terms is that all PDFs in [113] are assumed to vanish at end point, i.e. $f_{i/n}(1) = f_{j/\bar{n}}(1) = 0$, thereby setting all boundary corrections to zero by default. However, in this paper, all contributions from the boundary regions are retained for completeness and generality, and we find non-vanishing boundary terms at least in the PDF set MSHT20nlo_as118, which is used in section 4. Further details of this comparison can be found in appendix B.

3.2 Power expansion with the pure rapidity regulator

In this part, we re-derive the power series of $d\sigma_H/(dY_H dq_T^2)$ up to N²LP with the interior contribution evaluated from the rearranged ingredients, as illustrated in section 2.4.2. An appropriate regularisation scheme is required to be put in place to tame the rapidity divergences emerging from the domains $k_{\pm} \rightarrow 0$. In the following, the pure rapidity regularisation prescription proposed in [113, 178] will be employed to facilitate our calculation. In this regard, the regulator \mathcal{R} takes the form

$$\mathcal{R} = \left| \frac{\tilde{\nu}_n}{k_+} \frac{k_-}{\tilde{\nu}_{\bar{n}}} \right|^{\tau}. \quad (3.29)$$

Here $\tilde{\nu}_n$ and $\tilde{\nu}_{\bar{n}}$ represent two auxiliary scales, from which an effective cutoff can be imposed upon the rapidity of the emitted partons [113], akin to dimensional regularisation. In this paper, for simplicity, we take $\tilde{\nu}_n = \tilde{\nu}_{\bar{n}} = m_H$ throughout the calculation.

Applying eq. (3.29) onto the n -collinear function defined in eq. (2.46) concerns only the integrand with $\sigma \leq \omega$ in the limit $\tau \rightarrow 0$, more explicitly,

$$\begin{aligned}
 \left. \tilde{\mathcal{G}}_{[\kappa],\{\alpha,\beta\}}^{\rho,\sigma,(\omega)} \right|_c^{(\text{p.ra.})} &= \frac{\bar{\theta}(\omega-\sigma)}{(\omega-\rho)!} \int_0^{\tilde{k}_+^{\max}} \frac{dk_+}{k_+} (k_+)^{\sigma-\omega} F_{i/n,\beta_n}^{(\alpha_n)}(k_+ + m_H e^{-Y_H}) F_{j/\bar{n},\beta_{\bar{n}}}^{(\alpha_{\bar{n}}+\omega-\rho)}(m_H e^{+Y_H}) \\
 &\quad + \frac{\theta(\omega-\sigma)}{(\omega-\rho)!} \lim_{\tau \rightarrow 0} \int_0^{\tilde{k}_+^{\max}} \frac{dk_+}{k_+} (k_+)^{\sigma-\omega} \left| \frac{q_T^2}{k_+^2} \right|^{\tau} F_{i/n,\beta_n}^{(\alpha_n)}(k_+ + m_H e^{-Y_H}) F_{j/\bar{n},\beta_{\bar{n}}}^{(\alpha_{\bar{n}}+\omega-\rho)}(m_H e^{+Y_H}).
 \end{aligned} \quad (3.30)$$

To compute the second term on the r.h.s., we make use of the generalised star-distribution of eq. (2.38) to regularise all singular contributions, and then, within the pure rapidity

regularisation scheme, we complete the phase space integrals over those singular terms. The result reads,

$$\begin{aligned}
 & \theta(\omega - \sigma) \lim_{\tau \rightarrow 0} \int_0^{\tilde{k}_+^{\max}} \frac{dk_+}{k_+} (k_+)^{\sigma - \omega} \left| \frac{q_T^2}{k_+^2} \right|^\tau F_{i/n, \beta_n}^{(\alpha_n)}(k_+ + m_H e^{-Y_H}) F_{j/\bar{n}, \beta_{\bar{n}}}^{(\alpha_{\bar{n}} + \omega - \rho)}(m_H e^{+Y_H}) \\
 &= \theta(\omega - \sigma) \int_0^{\tilde{k}_+^{\max}} dk_+ \left[\frac{1}{k_+^{\omega - \sigma + 1}} \right]_*^{\nu_n} F_{i/n, \beta_n}^{(\alpha_n)}(k_+ + m_H e^{-Y_H}) F_{j/\bar{n}, \beta_{\bar{n}}}^{(\alpha_{\bar{n}} + \omega - \rho)}(m_H e^{+Y_H}) \\
 &+ \theta(\omega - \sigma - 1) \sum_{\eta=0}^{\omega - \sigma - 1} \frac{F_{i/n, \beta_n}^{(\alpha_n + \eta)}(m_H e^{-Y_H}) F_{j/\bar{n}, \beta_{\bar{n}}}^{(\alpha_{\bar{n}} + \omega - \rho)}(m_H e^{+Y_H}) \nu_n^{\sigma + \eta - \omega}}{\eta! (\sigma + \eta - \omega)} \\
 &+ \theta(\omega - \sigma) \left\{ \ln \left[\frac{\nu_n}{q_T} \right] - \frac{1}{2\tau} \right\} \frac{F_{i/n, \beta_n}^{(\alpha_n + \omega - \sigma)}(m_H e^{-Y_H}) F_{j/\bar{n}, \beta_{\bar{n}}}^{(\alpha_{\bar{n}} + \omega - \rho)}(m_H e^{+Y_H})}{(\omega - \sigma)!},
 \end{aligned} \tag{3.31}$$

where we have expanded in the small parameter τ and kept only contributions up to $\mathcal{O}(\tau^0)$. From eqs. (3.30) and (3.31), we note that except for the pole term, the recombined collinear sector here exactly reproduces the sum of eqs. (2.31) and (2.40) constructed via the explicit cutoffs. Likewise, the first term of eq. (3.30), proportional to $\bar{\theta}(\omega - \sigma)$, and the term containing the star-distribution in eq. (3.31) are equivalent to the sum of eq. (2.31) and the first two lines of eq. (2.40), as can be seen with the help of eq. (2.46) and the fact that the integrands in those sectors are all regular in the limit $k_+ \rightarrow 0$. In order to interpret the correspondence between the last two lines of eq. (2.40) and eq. (3.31), it is beneficial to recall that the ν_n -dependent terms in eq. (2.40) in fact stem from the boundary condition in the phase space integral of eq. (2.34), which, through applying the star distribution in eq. (2.38), is entirely inherited by the singular terms in eq. (3.31) and then mostly preserved in evaluating the k_+ integral within the pure rapidity regularisation scheme. Therefore, an analogous pattern is presented by the expressions in eqs. (3.30) and (3.31) and those in eq. (2.31) and eq. (2.40).

A similar strategy can also be used to calculate the \bar{n} -collinear term in eq. (2.46), which evaluates to,

$$\begin{aligned}
 \tilde{\mathcal{G}}_{[\kappa], \{\alpha, \beta\}}^{\rho, \sigma, (\omega)} \Big|_{\bar{c}}^{(\text{p.ra.})} &= \frac{\bar{\theta}(\omega - \rho)}{(\omega - \sigma)!} \int_0^{\frac{q_T^2}{k_+^{\min}}} \frac{dk_-}{k_-} k_-^{\rho - \omega} F_{i/n, \beta_n}^{(\alpha_n + \omega - \sigma)}(m_H e^{-Y_H}) F_{j/\bar{n}, \beta_{\bar{n}}}^{(\alpha_{\bar{n}})}(k_- + m_H e^{+Y_H}) \\
 &+ \frac{\theta(\omega - \rho)}{(\omega - \sigma)!} \int_0^{\frac{q_T^2}{k_+^{\min}}} dk_- \left[\frac{1}{k_-^{\omega - \rho + 1}} \right]_*^{\nu_{\bar{n}}} F_{i/n, \beta_n}^{(\alpha_n + \omega - \sigma)}(m_H e^{-Y_H}) F_{j/\bar{n}, \beta_{\bar{n}}}^{(\alpha_{\bar{n}})}(k_- + m_H e^{+Y_H}) \\
 &+ \frac{\theta(\omega - \rho - 1)}{(\omega - \sigma)!} \sum_{\lambda=0}^{\omega - \rho - 1} \frac{F_{i/n, \beta_n}^{(\alpha_n + \omega - \sigma)}(m_H e^{-Y_H}) F_{j/\bar{n}, \beta_{\bar{n}}}^{(\alpha_{\bar{n}} + \lambda)}(m_H e^{+Y_H}) \nu_{\bar{n}}^{\rho + \lambda - \omega}}{\lambda! (\rho + \lambda - \omega)} \\
 &+ \frac{\theta(\omega - \rho)}{(\omega - \sigma)!} \left\{ \ln \left[\frac{\nu_{\bar{n}}}{q_T} \right] + \frac{1}{2\tau} \right\} \frac{F_{i/n, \beta_n}^{(\alpha_n + \omega - \sigma)}(m_H e^{-Y_H}) F_{j/\bar{n}, \beta_{\bar{n}}}^{(\alpha_{\bar{n}} + \omega - \rho)}(m_H e^{+Y_H})}{(\omega - \rho)!}.
 \end{aligned} \tag{3.32}$$

In comparison with eq. (3.31), we note that the sign in front of the pole term is reversed. This indicates that the rapidity regulator in appraising the \bar{n} -collinear sector is in practice activated in a distinct extremal region than in the n -collinear case. Combining the n -collinear

function in eq. (3.31) with the \bar{n} -collinear piece of eq. (3.32), it is immediate to find that all poles cancel, fully reproducing our previous results summing eqs. (2.31) and (2.33) as well as eqs. (2.40) and (2.41) derived using the momentum cutoffs.

In fact, this agreement suggests that within the pure-rapidity regularisation scheme, the soft contribution of eq. (2.54) and zero-bin subtrahends of eq. (2.61) could be redundant. To confirm this, it is worth noting that the phase space integrals in these two functions are all unbounded by definition, such that applying the pure rapidity regulator here only results in vanishing quantities in the limit $\tau \rightarrow 0$. It thus leads to,

$$\tilde{\mathcal{G}}_{[\kappa],\{\alpha,\beta\}}^{\rho,\sigma,(\omega)} \Big|_s^{\langle\text{FS}\rangle, \langle\text{p.ra.}\rangle} = \tilde{\mathcal{G}}_{[\kappa],\{\alpha,\beta\}}^{\rho,\sigma,(\omega)} \Big|_{c0}^{\langle\text{NS}\rangle, \langle\text{p.ra.}\rangle} = \tilde{\mathcal{G}}_{[\kappa],\{\alpha,\beta\}}^{\rho,\sigma,(\omega)} \Big|_{\bar{c}0}^{\langle\text{NS}\rangle, \langle\text{p.ra.}\rangle} = 0. \quad (3.33)$$

In absence of the soft function and the zero-bin subtraction within the pure-rapidity regularisation scheme, we can then skip indulging in the inhomogeneous behaviour induced by the doubly and triply projected integrands of eq. (2.77). Similarly, we can also freely switch from Jantzen's formalism [177] in eq. (2.78) to our proposal in eq. (2.67) to perform the power expansion. This forms in part the reason why \mathcal{R} in eq. (3.29) is categorised to be one of the homogeneous regulators here.

Applying the expressions of eqs. (3.30)–(3.33) to eq. (2.62) or eq. (2.67), we arrive at the expression of the interior contribution and, in turn, the power expansion of $d\sigma_H/(dY_H dq_T^2)$. To make their expressions more compact, we recast them once again in terms of the dimensionless parameters defined in eq. (3.2) by means of the identities in eq. (3.5). Up to $N^2\text{LP}$, the results can be organised below,

$$\frac{d\sigma_H}{dY_H dq_T^2} = \frac{d\sigma_H}{dY_H dq_T^2} \Big|_{b.c.} + \frac{d\sigma_H^{\langle\text{p.ra.}\rangle}}{dY_H dq_T^2} \Big|_c + \frac{d\sigma_H^{\langle\text{p.ra.}\rangle}}{dY_H dq_T^2} \Big|_{\bar{c}}, \quad (3.34)$$

where the first term on the r.h.s. accounts for the boundary correction as illustrated in eq. (3.24). The second and third terms govern the n -collinear contributions in eqs. (3.30)–(3.31) and the \bar{n} -collinear case in eq. (3.32), respectively. Their expressions read,

$$\begin{aligned} \frac{d\sigma_H^{\langle\text{p.ra.}\rangle}}{dY_H dq_T^2} \Big|_c &\equiv \frac{\alpha_s^3 C_t^2}{192\pi^2 s v^2} \sum_{i,j=\{g,q,\bar{q}\}} \sum_{\omega=-1}^{\infty} \left(\frac{q_T^2}{m_H^2}\right)^\omega \int_{x_n}^1 dz_n \left[\mathbf{F}_{i/n} \left(\frac{x_n}{z_n}\right) \right]^{\mathbf{T}} \\ &\times \left\{ \mathbf{R}_{cs}^{(\omega),ij}(z_n) + \mathbf{P}_{cs}^{(\omega),ij} \left[\frac{1}{1-z_n} \right]_+ + \left(\mathbf{S}_c^{(\omega),ij} + \mathbf{D}_{cs}^{(\omega),ij} \right) \delta(1-z_n) \right. \\ &\left. + \mathbf{B}_{cs}^{(\omega),ij}(z_n) \delta(x_n - z_n) \right\} \mathbf{F}_{j/\bar{n}}(x_{\bar{n}}), \end{aligned} \quad (3.35)$$

and

$$\begin{aligned} \frac{d\sigma_H^{\langle\text{p.ra.}\rangle}}{dY_H dq_T^2} \Big|_{\bar{c}} &\equiv \frac{\alpha_s^3 C_t^2}{192\pi^2 s v^2} \sum_{i,j=\{g,q,\bar{q}\}} \sum_{\omega=-1}^{\infty} \left(\frac{q_T^2}{m_H^2}\right)^\omega \int_{x_{\bar{n}}}^1 dz_{\bar{n}} \left[\mathbf{F}_{i/n}(x_n) \right]^{\mathbf{T}} \\ &\times \left\{ \mathbf{R}_{\bar{c}s}^{(\omega),ij}(z_{\bar{n}}) + \mathbf{P}_{\bar{c}s}^{(\omega),ij} \left[\frac{1}{1-z_{\bar{n}}} \right]_+ + \left(\mathbf{S}_{\bar{c}}^{(\omega),ij} + \mathbf{D}_{\bar{c}s}^{(\omega),ij} \right) \delta(1-z_{\bar{n}}) \right. \\ &\left. + \mathbf{B}_{\bar{c}s}^{(\omega),ij}(z_{\bar{n}}) \delta(x_{\bar{n}} - z_{\bar{n}}) \right\} \mathbf{F}_{j/\bar{n}} \left(\frac{x_{\bar{n}}}{z_{\bar{n}}}\right), \end{aligned} \quad (3.36)$$

where the matrices \mathbf{R} , \mathbf{P} , \mathbf{D} , and \mathbf{B} have been previously displayed in section 3.1. The novel ingredients here are \mathbf{S}_c and $\mathbf{S}_{\bar{c}}$, characterising the pole terms in eqs. (3.31) and (3.32). The coefficients of these singularities in the n -(\bar{n} -)collinear sector are of opposite (same) sign, but otherwise identical, to those associated with the logarithmic contributions. The latter are, as discussed in section 3.1, associated with the partonic matrices in front of the plus distributions. Hence, we can now express \mathbf{S}_c and $\mathbf{S}_{\bar{c}}$ in terms of \mathbf{P}_{cs} in eqs. (3.14), more specifically,

$$\mathbf{S}_c^{(\omega),ij} = -\mathbf{S}_{\bar{c}}^{(\omega),ij} = -\frac{1}{2\tau} \mathbf{P}_{cs}^{(\omega),ij}, \quad \text{where } \omega \in \{-1, 0, 1\} \text{ and } \{ij\} = \{gg, q(\bar{q})g, q\bar{q}\}. \quad (3.37)$$

3.3 Power expansion with the exponential rapidity regulator

In order to explore the pattern of the power expansion of $d\sigma_H/(dY_H dq_T^2)$ in a more generic way, in the following we re-appraise the interior region with the aid of the exponential regulator [79, 80]. As will be illustrated below, the zero-bin subtrahends at this moment are non-trivial and play an important role in the cancellation of the pole terms, at variance to those derived in section 3.2. We will use the $\langle \text{NS} \rangle$ prescription here and make use of eq. (2.61) to establish them.

The exponential regulator takes the form,

$$\mathcal{R} = \exp(-\tau b_0 k_0), \quad (3.38)$$

where $b_0 = 2e^{-\gamma_E}$. At LP, where non-Abelian exponentiation [80, 173] holds, this type of regularisation scheme has been extensively utilised to calculate the fixed-order ingredients related to q_T resummation. For instance, the leading power beam and soft functions are now available up to N³LO [79, 80, 173–176], while the anomalous dimensions are available at N⁴LO accuracy [207, 208]. In the following, we will implement this method to the NLO q_T spectrum up to N²LP, for the first time. Our deliberations may also be useful for future analyses of power suppressed contribution at N²LO and beyond, within an inhomogeneous regularisation scheme.

We start our discussion by considering the collinear sectors of eq. (2.46). Applying the exponential regularisation method here follows an analogous pattern to our steps leading up to eqs. (3.30) and (3.31). First, we use the star-distribution of eq. (2.38) to separate the regular and singular terms in the limit $k_{\pm} \rightarrow 0$. The regular terms maximally preserve the form of eq. (2.46), while the singular ones contain rapidity divergences under the phase space integral necessitating the exponential regulator. Here we use the functions $\Upsilon_n^{(h)}$ and $\Upsilon_{\bar{n}}^{(h)}$ to collect those singular contributions in the n - and \bar{n} -collinear sectors, respectively. Within the exponential regularisation scheme, their expressions read,

$$\Upsilon_n^{(h)} \equiv \lim_{\tau \rightarrow 0} \int_0^{\nu_n} dk_+ \frac{e^{-\tau b_0 k_0}}{k_+^{h+1}}, \quad \Upsilon_{\bar{n}}^{(h)} \equiv \lim_{\tau \rightarrow 0} \int_0^{\nu_{\bar{n}}} dk_- \frac{e^{-\tau b_0 k_0}}{k_-^{h+1}} = \Upsilon_n^{(h)} \Big|_{\nu_n \rightarrow \nu_{\bar{n}}}. \quad (3.39)$$

As for the first few ranks, $\Upsilon_n^{(h)}$ evaluates to,

$$\begin{aligned} \Upsilon_n^{(0)} &= \ln \left[\frac{\nu_n}{q_T} \right] - L_\tau, & \Upsilon_n^{(1)} &= \frac{1}{q_T^2 \tilde{\tau}} - \frac{1}{\nu_n}, & \Upsilon_n^{(2)} &= \frac{1}{q_T^4 \tilde{\tau}^2} - \frac{1}{2\nu_n^2} - \frac{1}{q_T^2}, \\ \Upsilon_n^{(3)} &= \frac{2}{q_T^6 \tilde{\tau}^3} - \frac{1}{3\nu_n^3} - \frac{1}{q_T^4 \tilde{\tau}}, & \dots & \dots & \dots \end{aligned} \quad (3.40)$$

where $L_\tau = \ln(q_T \tau)$ and $\tilde{\tau} = \tau e^{-\gamma_E}$. The expression of $\Upsilon_{\bar{n}}^{(h)}$ can be derived from $\Upsilon_n^{(h)}$ by the replacement $n \leftrightarrow \bar{n}$. Thus equipped, we are now poised to establish the collinear contribution

of eq. (2.46) within the exponential regularisation scheme, more explicitly

$$\begin{aligned}
 \tilde{\mathcal{G}}_{[\kappa],\{\alpha,\beta\}}^{\rho,\sigma,(\omega)} \Big|_c^{(\text{exp})} &= \frac{\bar{\theta}(\omega-\sigma)}{(\omega-\rho)!} \int_0^{\tilde{k}_+^{\text{max}}} \frac{dk_+}{k_+} (k_+)^{\sigma-\omega} F_{i/n,\beta_n}^{(\alpha_n)} \left(k_+ + m_H e^{-Y_H} \right) F_{j/\bar{n},\beta_{\bar{n}}}^{(\alpha_{\bar{n}}+\omega-\rho)} \left(m_H e^{+Y_H} \right) \\
 &+ \frac{\theta(\omega-\sigma)}{(\omega-\rho)!} \int_0^{\tilde{k}_+^{\text{max}}} dk_+ \left[\frac{1}{k_+^{\omega-\sigma+1}} \right]_*^{\nu_n} F_{i/n,\beta_n}^{(\alpha_n)} \left(k_+ + m_H e^{-Y_H} \right) F_{j/\bar{n},\beta_{\bar{n}}}^{(\alpha_{\bar{n}}+\omega-\rho)} \left(m_H e^{+Y_H} \right) \\
 &+ \frac{\theta(\omega-\sigma-1)}{(\omega-\rho)!} \sum_{\eta=0}^{\omega-\sigma-1} \frac{F_{i/n,\beta_n}^{(\alpha_n+\eta)} \left(m_H e^{-Y_H} \right) F_{j/\bar{n},\beta_{\bar{n}}}^{(\alpha_{\bar{n}}+\omega-\rho)} \left(m_H e^{+Y_H} \right)}{\eta!} \Upsilon_n^{(\omega-\sigma-\eta)} \\
 &+ \frac{\theta(\omega-\sigma)}{(\omega-\rho)!} \frac{F_{i/n,\beta_n}^{(\alpha_n+\omega-\sigma)} \left(m_H e^{-Y_H} \right) F_{j/\bar{n},\beta_{\bar{n}}}^{(\alpha_{\bar{n}}+\omega-\rho)} \left(m_H e^{+Y_H} \right)}{(\omega-\sigma)!} \Upsilon_n^{(0)}, \tag{3.41}
 \end{aligned}$$

$$\begin{aligned}
 \tilde{\mathcal{G}}_{[\kappa],\{\alpha,\beta\}}^{\rho,\sigma,(\omega)} \Big|_{\bar{c}}^{(\text{exp})} &= \frac{\bar{\theta}(\omega-\rho)}{(\omega-\sigma)!} \int_0^{\frac{q_T^2}{\tilde{k}_+^{\text{min}}}} \frac{dk_-}{k_-} k_-^{\rho-\omega} F_{i/n,\beta_n}^{(\alpha_n+\omega-\sigma)} \left(m_H e^{-Y_H} \right) F_{j/\bar{n},\beta_{\bar{n}}}^{(\alpha_{\bar{n}})} \left(k_- + m_H e^{+Y_H} \right) \\
 &+ \frac{\theta(\omega-\rho)}{(\omega-\sigma)!} \int_0^{\frac{q_T^2}{\tilde{k}_+^{\text{min}}}} dk_- \left[\frac{1}{k_-^{\omega-\rho+1}} \right]_*^{\nu_{\bar{n}}} F_{i/n,\beta_n}^{(\alpha_n+\omega-\sigma)} \left(m_H e^{-Y_H} \right) F_{j/\bar{n},\beta_{\bar{n}}}^{(\alpha_{\bar{n}})} \left(k_- + m_H e^{+Y_H} \right) \\
 &+ \frac{\theta(\omega-\rho-1)}{(\omega-\sigma)!} \sum_{\lambda=0}^{\omega-\rho-1} \frac{F_{i/n,\beta_n}^{(\alpha_n+\omega-\sigma)} \left(m_H e^{-Y_H} \right) F_{j/\bar{n},\beta_{\bar{n}}}^{(\alpha_{\bar{n}}+\lambda)} \left(m_H e^{+Y_H} \right)}{\lambda!} \Upsilon_{\bar{n}}^{(\omega-\rho-\lambda)} \\
 &+ \frac{\theta(\omega-\rho)}{(\omega-\sigma)!} \frac{F_{i/n,\beta_n}^{(\alpha_n+\omega-\sigma)} \left(m_H e^{-Y_H} \right) F_{j/\bar{n},\beta_{\bar{n}}}^{(\alpha_{\bar{n}}+\omega-\rho)} \left(m_H e^{+Y_H} \right)}{(\omega-\rho)!} \Upsilon_{\bar{n}}^{(0)}. \tag{3.42}
 \end{aligned}$$

By comparison with the expressions in eqs. (3.30)–(3.32) evaluated in the pure-rapidity regularisation scheme, the above expressions possess the same regular contributions in the first two lines, as the regulator has no relevance in the absence of rapidity divergences. In their third lines, aside from identical ν_n and $\nu_{\bar{n}}$ dependences residing in $\Upsilon_{n(\bar{n})}$ compared to those in eqs. (3.31)–(3.32), the power series in terms of q_T and $\tilde{\tau}$ is appearing. This behaviour stems from the definition of the exponential regulator in eq. (3.38), comprising the temporal component $k^0 = k_+ + (q_T^2/k_+)$ as a whole. In deriving the n -collinear function, for instance, its second part (q_T^2/k_+) suppresses the rapidity divergences, thereby yielding the leading singularity in the limit $\tilde{\tau} \rightarrow 0$, whilst the first part k_+ gives rise to corrections of $\mathcal{O}(\tilde{\tau})$ and in turn generates subleading singular terms and the constant contributions, as exhibited in eqs. (3.40). Ultimately, confronting the fourth line of eqs. (3.31)–(3.32) to the results in eqs. (3.41)–(3.42), we observe that addition logarithms $L_\tau = \ln(q_T\tau)$ emerge in the exponential regularisation scheme. In the limit $\tau \rightarrow 0$, those logarithms in practice play an equivalent role to the pole term in eqs. (3.31)–(3.32).

Combining the collinear functions we have derived using the exponential regulator above, a cancellation of all pole terms is not found, at variance with our earlier findings for eqs. (3.30)–(3.32). This therefore calls for the zero-bin subtraction procedure derived in eq. (2.61) to remove all overlapping contributions. Implementing the exponential regulator in eq. (2.61) prompts the k_\pm -integrals over the interval $k_\pm \in [0, \infty]$, which are encoded by the function $\Upsilon_{zb}^{(h)}$ in this paper, more specifically,

$$\Upsilon_{zb}^{(h)} \equiv \lim_{\tau \rightarrow 0} \int_0^\infty dk_\pm \frac{e^{-\tau b_0 k_0}}{(k_\pm)^{h+1}}. \tag{3.43}$$

The results for the first few ranks read,

$$\Upsilon_{zb}^{(0)} = -2L_\tau, \quad \Upsilon_{zb}^{(1)} = \frac{1}{q_\tau^2 \tilde{\tau}}, \quad \Upsilon_{zb}^{(2)} = \frac{1}{q_\tau^4 \tilde{\tau}^2} - \frac{1}{q_\tau^2}, \quad \Upsilon_{zb}^{(3)} = \frac{2}{q_\tau^6 \tilde{\tau}^3} - \frac{1}{q_\tau^4 \tilde{\tau}}, \quad \dots \quad (3.44)$$

With the help of eq. (3.43), the zero-bin subtrahends in the exponential regularisation can be written as,

$$\begin{aligned} \tilde{\mathcal{G}}_{[\kappa],\{\alpha,\beta\}}^{\rho,\sigma,(\omega)} \Big|_{c0}^{(NS),(\text{exp})} &= \theta(\omega-\sigma) \sum_{\eta=0}^{\omega-\sigma} \frac{F_{i/n,\beta_n}^{(\alpha_n+\eta)} (m_H e^{-Y_H}) F_{j/\bar{n},\beta_{\bar{n}}}^{(\alpha_{\bar{n}}+\omega-\rho)} (m_H e^{+Y_H})}{\eta! (\omega-\rho)!} \left(1 - \frac{\delta_\omega^{\sigma+\eta}}{2}\right) \Upsilon_{zb}^{(\omega-\sigma-\eta)}, \\ \tilde{\mathcal{G}}_{[\kappa],\{\alpha,\beta\}}^{\rho,\sigma,(\omega)} \Big|_{c\bar{0}}^{(NS),(\text{exp})} &= \theta(\omega-\rho) \sum_{\lambda=0}^{\omega-\rho} \frac{F_{i/n,\beta_n}^{(\alpha_n+\omega-\sigma)} (m_H e^{-Y_H}) F_{j/\bar{n},\beta_{\bar{n}}}^{(\alpha_{\bar{n}}+\lambda)} (m_H e^{+Y_H})}{\lambda! (\omega-\sigma)!} \left(1 - \frac{\delta_\omega^{\rho+\lambda}}{2}\right) \Upsilon_{zb}^{(\omega-\rho-\lambda)}. \end{aligned} \quad (3.45)$$

At leading power $\omega = -1$, where the integrand of eq. (2.65) with $\rho = \sigma = -1$ is the relevant contributor, the sum of the contribution above amounts to the leading soft function in eq. (2.54), agreeing with the assertion made in [79]. Nevertheless, it is worth emphasising that this coincidence will not hold in general. At NLP, for instance, the zero-bin subtrahends here comprise the terms

$$\begin{aligned} \tilde{\mathcal{G}}_{[\kappa],\{\alpha,\beta\}}^{-1,-1,(0)} \Big|_{c0}^{(NS),(\text{exp})} + \tilde{\mathcal{G}}_{[\kappa],\{\alpha,\beta\}}^{-1,-1,(0)} \Big|_{c\bar{0}}^{(NS),(\text{exp})} &= F_{i/n}^{(\alpha_n+1)} F_{j/\bar{n}}^{(\alpha_{\bar{n}}+1)} \Upsilon_{zb}^{(0)} \\ &\quad + F_{i/n}^{(\alpha_n)} F_{j/\bar{n}}^{(\alpha_{\bar{n}}+1)} \Upsilon_{zb}^{(1)} + F_{i/n}^{(\alpha_n+1)} F_{j/\bar{n}}^{(\alpha_{\bar{n}})} \Upsilon_{zb}^{(1)}. \end{aligned} \quad (3.46)$$

Recalling the definition in eq. (2.54), the soft sector at the same power accuracy reads,

$$\tilde{\mathcal{G}}_{[\kappa],\{\alpha,\beta\}}^{-1,-1,(0)} \Big|_s^{(FS)} = F_{i/n}^{(\alpha_n+1)} F_{j/\bar{n}}^{(\alpha_{\bar{n}}+1)} \Upsilon_{zb}^{(0)} + \frac{F_{i/n}^{(\alpha_n)} F_{j/\bar{n}}^{(\alpha_{\bar{n}}+2)}}{2} \Upsilon_{zb}^{(2)} + \frac{F_{i/n}^{(\alpha_n+2)} F_{j/\bar{n}}^{(\alpha_{\bar{n}})}}{2} \Upsilon_{zb}^{(2)}. \quad (3.47)$$

Comparing those two expressions, with the exception of the first term on the r.h.s. of eq. (3.47), the other constituents in eq. (3.47) both differ from those in eq. (3.46). This discrepancy highlights the structural differences between the soft function and zero-bin subtrahends beyond leading power. Indeed, both of them contain unbounded integrals over integrands expanded in line with soft scaling. However, the soft function consists of all ingredients at a given power, whereas the zero-bin subtrahends concern only those associated with the collinear functions from the lowest power accuracy up to the current power under consideration.

Combining the results in eq. (3.45) with their corresponding collinear ingredients in eqs. (3.41) and (3.42), we observe that all the τ -dependences will drop out as they should, from which we can separately reproduce the n - and \bar{n} -collinear contributions in eqs. (2.31)–(2.33) and eqs. (2.40)–(2.41) derived via the momentum cutoffs, more explicitly,

$$\begin{aligned} \tilde{\mathcal{G}}_{[\kappa],\{\alpha,\beta\}}^{\rho,\sigma,(\omega)} \Big|_c^{(\text{exp})} - \tilde{\mathcal{G}}_{[\kappa],\{\alpha,\beta\}}^{\rho,\sigma,(\omega)} \Big|_{c0}^{(NS),(\text{exp})} &= \tilde{\mathcal{I}}_{[\kappa],\{\alpha,\beta\}}^{\rho,\sigma,(\omega)} \Big|_c + \tilde{\mathcal{I}}_{[\kappa],\{\alpha,\beta\}}^{\rho,\sigma,(\omega)} \Big|_{cs}, \\ \tilde{\mathcal{G}}_{[\kappa],\{\alpha,\beta\}}^{\rho,\sigma,(\omega)} \Big|_{c\bar{0}}^{(\text{exp})} - \tilde{\mathcal{G}}_{[\kappa],\{\alpha,\beta\}}^{\rho,\sigma,(\omega)} \Big|_{c\bar{0}}^{(NS),(\text{exp})} &= \tilde{\mathcal{I}}_{[\kappa],\{\alpha,\beta\}}^{\rho,\sigma,(\omega)} \Big|_{c\bar{0}} + \tilde{\mathcal{I}}_{[\kappa],\{\alpha,\beta\}}^{\rho,\sigma,(\omega)} \Big|_{c\bar{0}cs}. \end{aligned} \quad (3.48)$$

Now we are ready to use the zero-bin subtracted collinear contributions to evaluate the internal region in eq. (2.62) and in turn the q_T spectrum. Akin to the previous subsections, to make our results more compact, we rewrite the momentum space expressions in eqs. (3.41)–(3.42) and eq. (3.45) in terms of the dimensionless parameters defined in eq. (3.2). Up to N²LP, this kind of transformation can be always achieved through eqs. (3.5) and (3.6). Collectively, we express the result below,

$$\frac{d\sigma_H}{dY_H dq_T^2} = \frac{d\sigma_H}{dY_H dq_T^2} \Big|_{b.c.} + \frac{d\sigma_H^{(\text{exp})}}{dY_H dq_T^2} \Big|_c - \frac{d\sigma_H^{(\text{exp})}}{dY_H dq_T^2} \Big|_{c_0} + \frac{d\sigma_H^{(\text{exp})}}{dY_H dq_T^2} \Big|_{\bar{c}} - \frac{d\sigma_H^{(\text{exp})}}{dY_H dq_T^2} \Big|_{\bar{c}_0}, \quad (3.49)$$

where the term with the subscript “*b.c.*” indicates the ultra-collinear contributions as presented in eq. (3.24). The following four terms in eq. (3.49), marked by the superscripts “(exp)”, stand for the collinear sectors and their corresponding zero-bin subtrahends evaluated within the exponential regularisation scheme. Of them, the constituents dressed with the subscripts “*c*” and “ \bar{c} ” are induced by eq. (3.41) and eq. (3.42), respectively. Their expressions read,

$$\begin{aligned} \frac{d\sigma_H^{(\text{exp})}}{dY_H dq_T^2} \Big|_c &\equiv \frac{\alpha_s^3 C_t^2}{192\pi^2 s v^2} \sum_{i,j=\{g,q,\bar{q}\}} \sum_{\omega=-1}^{\infty} \left(\frac{q_T^2}{m_H^2}\right)^\omega \int_{x_n}^1 dz_n \left[\mathbf{F}_{i/n} \left(\frac{x_n}{z_n}\right) \right]^{\mathbf{T}} \\ &\cdot \left\{ \mathbf{R}_{cs}^{(\omega),ij}(z_n) + \mathbf{P}_{cs}^{(\omega),ij} \left[\frac{1}{1-z_n} \right]_+ + \left(\mathbf{T}_c^{(\omega),ij} + \mathbf{D}_{cs}^{(\omega),ij} \right) \delta(1-z_n) + \mathbf{B}_c^{(\omega),ij}(z_n) \delta(x_n - z_n) \right\} \\ &\cdot \mathbf{F}_{j/\bar{n}}(x_{\bar{n}}), \end{aligned} \quad (3.50)$$

$$\begin{aligned} \frac{d\sigma_H^{(\text{exp})}}{dY_H dq_T^2} \Big|_{\bar{c}} &\equiv \frac{\alpha_s^3 C_t^2}{192\pi^2 s v^2} \sum_{i,j=\{g,q,\bar{q}\}} \sum_{\omega=-1}^{\infty} \left(\frac{q_T^2}{m_H^2}\right)^\omega \int_{x_{\bar{n}}}^1 dz_{\bar{n}} \left[\mathbf{F}_{i/n}(x_n) \right]^{\mathbf{T}} \\ &\cdot \left\{ \mathbf{R}_{\bar{c}s}^{(\omega),ij}(z_{\bar{n}}) + \mathbf{P}_{\bar{c}s}^{(\omega),ij} \left[\frac{1}{1-z_{\bar{n}}} \right]_+ + \left(\mathbf{T}_{\bar{c}}^{(\omega),ij} + \mathbf{D}_{\bar{c}s}^{(\omega),ij} \right) \delta(1-z_{\bar{n}}) + \mathbf{B}_{\bar{c}s}^{(\omega),ij}(z_{\bar{n}}) \delta(x_{\bar{n}} - z_{\bar{n}}) \right\} \\ &\cdot \mathbf{F}_{j/\bar{n}} \left(\frac{x_{\bar{n}}}{z_{\bar{n}}} \right). \end{aligned} \quad (3.51)$$

Here the partonic matrices \mathbf{R} , \mathbf{P} , \mathbf{D} , and \mathbf{B} are same as those in eq. (3.8) and eq. (3.17). The new ingredients are \mathbf{T}_c and $\mathbf{T}_{\bar{c}}$, accommodating all the τ -dependences from Υ_n and $\Upsilon_{\bar{n}}$ in eq. (3.39) and (3.40). Up to N²LP, the results for \mathbf{T}_c read,

$$\begin{aligned} \mathbf{T}_c^{(-1),q(\bar{q})g} &= \mathbf{T}_c^{(-1),q\bar{q}} = \mathbf{T}_c^{(0),q\bar{q}} = \mathbf{T}_c^{(1),q\bar{q}} = 0, \\ \mathbf{T}_c^{(-1),gg} &= -L_\tau \mathbf{P}_c^{(-1),gg}, \quad \mathbf{T}_c^{(0),q(\bar{q})g} = -L_\tau \mathbf{P}_c^{(0),q(\bar{q})g}, \\ \mathbf{T}_c^{(0),gg} &= -L_\tau \mathbf{P}_c^{(0),gg} + \left[-\frac{r_n}{q_T \bar{\tau}} \quad \frac{r_n}{q_T \bar{\tau}} \right], \\ \mathbf{T}_c^{(1),gg} &= -L_\tau \mathbf{P}_c^{(1),gg} + \left[\begin{array}{cc} \frac{3r_n^2}{q_T^2 \bar{\tau}^2} - 3r_n^2 - \frac{7r_n}{2q_T \bar{\tau}} - \frac{r_n^2}{q_T^2 \bar{\tau}^2} + r_n^2 + \frac{7r_n}{2q_T \bar{\tau}} \frac{r_n^2}{q_T^2 \bar{\tau}^2} - r_n^2 & \\ + \frac{5r_n}{2q_T \bar{\tau}} & -\frac{r_n}{2q_T \bar{\tau}} \quad \frac{r_n}{q_T \bar{\tau}} \end{array} \right], \\ \mathbf{T}_c^{(1),q(\bar{q})g} &= -L_\tau \mathbf{P}_c^{(1),q(\bar{q})g} + \left[0 \quad \frac{2r_n}{9q_T \bar{\tau}} \quad \frac{2r_n}{9q_T \bar{\tau}} \right], \end{aligned} \quad (3.52)$$

where $r_n = x_n \sqrt{s}/q_T$ and $r_{\bar{n}} = x_{\bar{n}} \sqrt{s}/q_T$. As for the partonic processes $gg \rightarrow Hg$ and $q\bar{q} \rightarrow Hg$, the expressions for $\mathbf{T}_{\bar{c}}$ can be derived by \mathbf{T}_c via the following relationship,

$$\mathbf{T}_{\bar{c}}^{(\omega),gg} = \left[\mathbf{T}_c^{(\omega),gg} \right]^{\mathbf{T}} \Big|_{r_n \rightarrow r_{\bar{n}}}, \quad \mathbf{T}_{\bar{c}}^{(\omega),q\bar{q}} = \left[\mathbf{T}_c^{(\omega),q\bar{q}} \right]^{\mathbf{T}} \Big|_{r_n \rightarrow r_{\bar{n}}}. \quad (3.53)$$

For those induced by the channel $q(\bar{q})g \rightarrow Hq(\bar{q})$, they evaluate to

$$\begin{aligned} \mathbf{T}_{\bar{c}}^{(-1),q(\bar{q})g} &= 0, & \mathbf{T}_{\bar{c}}^{(0),q(\bar{q})g} &= -L_\tau \mathbf{P}_{\bar{c}}^{(0),q(\bar{q})g} + \frac{2r_{\bar{n}}}{9q_T \bar{\tau}}, \\ \mathbf{T}_{\bar{c}}^{(1),q(\bar{q})g} &= -L_\tau \mathbf{P}_{\bar{c}}^{(1),q(\bar{q})g} + \left[\begin{array}{cc} \frac{r_{\bar{n}}}{9q_T \bar{\tau}} & \frac{r_{\bar{n}}}{9q_T \bar{\tau}} \\ \frac{2r_{\bar{n}}^2}{9q_T^2 \bar{\tau}^2} - \frac{2r_{\bar{n}}^2}{9} + \frac{r_{\bar{n}}}{3q_T \bar{\tau}} & \frac{2r_{\bar{n}}}{9q_T \bar{\tau}} \end{array} \right]. \end{aligned} \quad (3.54)$$

On the other hand, eq. (3.49) also includes the components “ $c0$ ” and “ $\bar{c}0$ ”, accounting for the zero-bin subtraction terms in eq. (3.45). Their results are,

$$\begin{aligned} \left. \frac{d\sigma_H^{(\text{exp})}}{dY_H dq_T^2} \right|_{c0} &\equiv \frac{\alpha_s^3 C_t^2}{192\pi^2 s v^2} \sum_{i,j=\{g,q,\bar{q}\}} \sum_{\omega=-1}^{\infty} \left(\frac{q_T^2}{m_H^2} \right)^\omega \left[\mathbf{F}_{i/n}(x_n) \right]^{\mathbf{T}} \cdot \mathbf{T}_c^{(\omega),ij} \cdot \mathbf{F}_{j/\bar{n}}(x_{\bar{n}}), \\ \left. \frac{d\sigma_H^{(\text{exp})}}{dY_H dq_T^2} \right|_{\bar{c}0} &\equiv \frac{\alpha_s^3 C_t^2}{192\pi^2 s v^2} \sum_{i,j=\{g,q,\bar{q}\}} \sum_{\omega=-1}^{\infty} \left(\frac{q_T^2}{m_H^2} \right)^\omega \left[\mathbf{F}_{i/n}(x_n) \right]^{\mathbf{T}} \cdot \mathbf{T}_{\bar{c}}^{(\omega),ij} \cdot \mathbf{F}_{j/\bar{n}}(x_{\bar{n}}). \end{aligned} \quad (3.55)$$

Since Υ_{zb} in eqs. (3.43) and (3.44) exactly reproduces all the τ -dependent contributions from Υ_n and $\Upsilon_{\bar{n}}$ in eqs. (3.39) and (3.40), respectively, the partonic matrices \mathbf{T}_c and $\mathbf{T}_{\bar{c}}$ governing the zero-bin subtrahends here are identical to those in the collinear sectors in eqs. (3.50) and (3.51).

4 Numerical results

Having introduced all building blocks in the previous sections, we will now present numerical results for the q_T spectrum for the process $pp \rightarrow H + X$ at LHC by the means of the power expansion derived in section 3. Since we have shown that this power series is equivalent whether it is computed using momentum cutoffs to regulate rapidity divergences, as in eq. (3.1), the pure-rapidity regulator in eq. (3.34), or the exponential rapidity regulator in eq. (3.49), any one can be employed. We would like to stress again, though, that although individual constituents are dependent on the rapidity regularisation scheme, the sum of all sectors is identical in all three choices with no scheme-dependent power-suppressed terms remaining. Hence, it is scheme-independent sum of sectors that we implement.

During our calculation, we take the mass m_H of the Higgs boson and the vacuum expectation value v from PDG [236]. As to Wilson coefficient C_t , although it is known up to four-loop order [185, 187–192], we only consider its LO contribution here in accordance with the perturbative accuracy of the amplitudes presented in eqs. (2.4). In this paper, we use the MSHT20nlo_as118 [237] PDF set, with the associated value and evolution of α_s , interfaced through LHAPDF [238, 239]. We set the renormalisation scale to $\mu_R = m_H$, entering our calculation only as the scale we evaluate the strong coupling at. In implementing MSHT20nlo_as118 for eq. (3.1) particular attention should be paid to the fact that the PDFs and their higher order derivatives are both involved in the power correction expansion, as illustrated in eq. (3.9). As LHAPDF does not offer direct access to the PDFs’ derivatives, in this work, we make use of the method of [212, 213] and fit MSHT20nlo_as118 in terms of Chebyshev polynomials at the factorisation scale $\mu_F = m_H$ first, from which the derivatives

of the PDFs can be evaluated analytically. The virtue of this strategy is that the robustness of the PDFs’ derivatives is maintained in regards to the fitted PDFs throughout our numerical calculation, which, as a matter of fact, is one of prerequisites for our validation procedure. To examine our fitted PDFs, we compare the q_T distributions generated by SHERPA [240–242] and RIVET [243, 244] with LHAPDF against those from the fitted ones, finding only per-mill level discrepancies between them. The above ansatz, however, proves challenging once dynamical scales are considered and, potentially, different solutions must be sought.

Equipped with those inputs, we are capable of calculating the power series of the q_T distribution via eq. (3.1). In the following, we will emphasis three types of results, i.e.,

$$\begin{aligned}
 \left. \frac{d\sigma_H^{\langle \text{asy} \rangle}}{dY_H dq_T^2} \right|_{\text{LP}} &= \sum_m \frac{\Delta_{\text{LP}}^{(m)}}{q_T^2} (L_H)^m, \\
 \left. \frac{d\sigma_H^{\langle \text{asy} \rangle}}{dY_H dq_T^2} \right|_{\text{NLP}} &= \sum_m \frac{\Delta_{\text{LP}}^{(m)}}{q_T^2} (L_H)^m + \sum_m \Delta_{\text{NLP}}^{(m)} (L_H)^m, \\
 \left. \frac{d\sigma_H^{\langle \text{asy} \rangle}}{dY_H dq_T^2} \right|_{\text{N}^2\text{LP}} &= \sum_m \frac{\Delta_{\text{LP}}^{(m)}}{q_T^2} (L_H)^m + \sum_m \Delta_{\text{NLP}}^{(m)} (L_H)^m + \sum_m q_T^2 \Delta_{\text{N}^2\text{LP}}^{(m)} (L_H)^m,
 \end{aligned} \tag{4.1}$$

where the superscript “asy” signifies the truncated asymptotic series in the low q_T domain. $\Delta_{\text{N}^k\text{LP}}$ stands for the partonic contribution at the k -th power convoluted with PDFs and their derivatives, which can be extracted from the power coefficients in eq. (3.1), eq. (3.34), or eq. (3.49). In eq. (4.1), the q_T spectrum at LP encodes the most singular behavior in the low q_T domain, consisting of the first term of the power series in eq. (2.8). The NLP result in eq. (4.1) includes also the first power correction term, comprising the first two constituents of eq. (2.8) in total. Our most precise result is calculated at N^2LP , given in the last line of eq. (4.1). It includes the contributions from Δ_{LP} up to $\Delta_{\text{N}^2\text{LP}}$ in eq. (2.8). Moreover, in order to deliver a quantitative assessment of the quality of these approximate results, we also showcase the exact fixed-order q_T distribution below as a benchmark. It is derived based on eq. (2.1) and dubbed “F.O.” hereafter.

We start the discussion of our results by considering the q_T spectrum at central rapidities, setting $Y_H = 0$ for definitiveness. Figure 2 therefore details a comparison of our power-expanded approximate result of sections 2 and 3 including terms up to LP (blue), NLP (red), and N^2LP (green) to its exact fixed-order counter-part (black) for all three partonic channels, $gg \rightarrow Hg$ (left), $q(\bar{q})g \rightarrow Hq(\bar{q})$ (center), and $q\bar{q} \rightarrow Hg$ (right). Generally, the main plot focusses on the absolute values of the q_T distribution, while the ratio plot shows the ratio of each of the approximate results to the exact one, allowing to judge the quality of the individual approximation. We will retain this pattern of visualisation throughout this section.

Examining our results in more detail, we begin by discussing the $gg \rightarrow Hg$ subprocess, shown in figure 2(a). This process dominates the inclusive cross section and any improvements in the quality of the power-expanded approximation will be exceedingly beneficial to the description of the inclusive q_T spectrum. Due to the presence of singular terms, see eq. (2.8), the q_T spectrum is divergent as $q_T \rightarrow 0$, hence we limit our deliberations to $q_T > 1 \text{ GeV}$. In this limit, the LP contribution is, of course, dominant and the approximated calculations, independent of the number of higher-power terms included, reproduce the exact result.

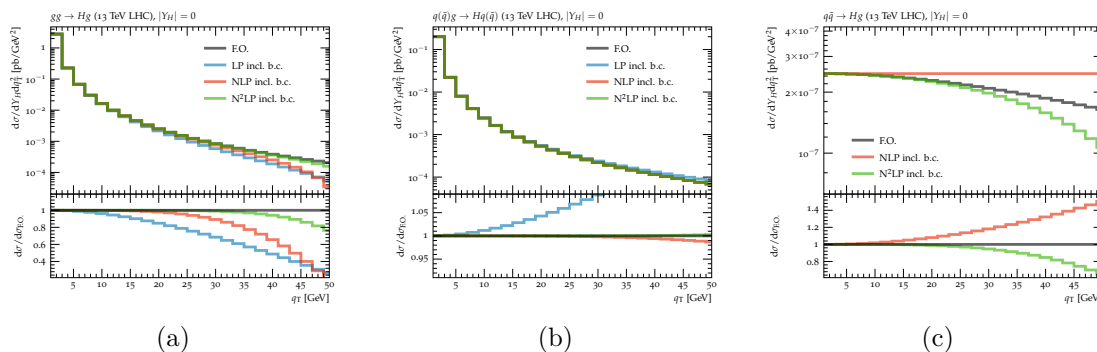


Figure 2. Comparisons of the q_T spectra between the exact fixed-order calculation (black) and approximations constructed using the power expansion up to LP (blue), NLP (red), and N²LP (green) for different partonic processes at $|Y_H| = 0$. While the upper plot contains the absolute differential cross sections, the lower plot contains the ratios of the approximations w.r.t. the exact fixed-order result. Throughout we include the boundary corrections \mathbf{B}_{cs} , $\mathbf{B}_{\bar{c}s}$, and $\mathbf{B}_{uc(\bar{c})}$.

Nevertheless, departing from the low q_T domain towards higher values of our observable, the power corrections manifest themselves progressively. More specifically, the LP-only result deteriorates in quality the quickest, failing to describe the exact spectrum by about 4% at $q_T = 10$ GeV and increasing to about 30% near $q_T = 30$ GeV. Including the NLP terms alleviates this deviation somewhat, decreasing it to about 1% at $q_T = 10$ GeV and about 10% at $q_T = 30$ GeV. The best approximation provided in this work, including terms up to N²LP, reproduces the q_T spectrum on level of 1% up to values in excess of 30 GeV, leaving higher-power corrections to contribute more than percent level only for $q_T \gtrsim 40$ GeV.

Figure 2(b) now shows the contributions from the partonic channel characterised by $q(\bar{q})g$ initial states. This channel contributes on the 10% level to the inclusive spectrum. Our results here in general demonstrate an analogous behaviour to those of $gg \rightarrow Hg$ in the vicinity of $q_T = 0$ GeV, including the presence of a divergence for $q_T \rightarrow 0$ as well as the mutual agreement between the fixed-order and approximate curves in that limit. However, advancing to the intermediate q_T range, distinct features are found between the two in regard to the relative magnitudes of subleading and sub-subleading power corrections. While in figure 2(a), these two terms observe convergent but still comparable magnitudes, respectively accounting for 20% and 10% contributions of the full theory in the vicinity of $q_T = 30$ GeV, the NLP terms in figure 2(b) play a dominant role and relegate the terms at N²LP and beyond to an almost insignificant role.

Moving onto the last partonic process contributing at our accuracy, $q\bar{q} \rightarrow Hg$, depicted in figure 2(c), a very different scenario presents itself. For lack of the LP contributions and the associated singularity at $q_T \rightarrow 0$, the fixed-order and approximate results here both approach constants in the low q_T region. In particular, the NLP spectrum here takes the leading role and remains constant throughout the q_T interval of our interest. The N²LP corrections, meanwhile, exhibit the linear dependences on the variable q_T as the logarithmic contributions in eqs. (3.14) and (3.15) vanish. Comparing with the fixed-order spectrum, the NLP and N²LP results both yield the correct regular behaviour in the small q_T range but give oscillatorily converging power corrections for moderate q_T . For instance, the NLP

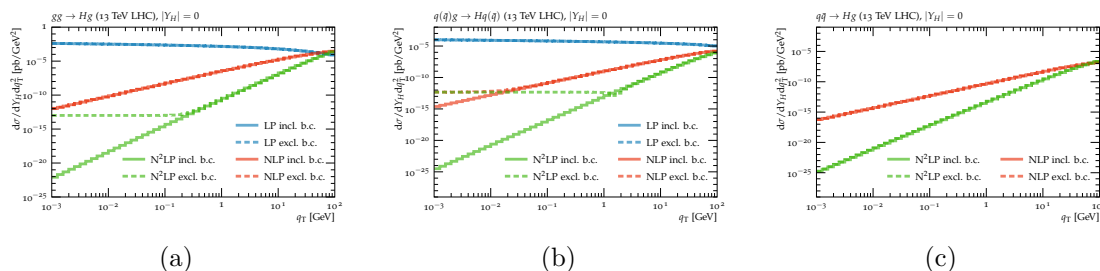


Figure 3. Difference of the exact spectra and the approximations for the three different partonic processes at $|Y_H| = 0$. The solid (dashed) lines present the results including (excluding) the boundary corrections \mathbf{B}_{cs} in eq. (3.8), $\mathbf{B}_{\bar{c}s}$ in eq. (3.17), and $\mathbf{B}_{uc(\bar{c})}$ in eq. (3.24). The blue, red, and green lines detail the LP, NLP, and N^2 LP approximations, respectively.

approximation overshoots the full theory by about 20% near $q_T = 30$ GeV, whilst incorporating N^2 LP corrections underestimates the exact one by a few percent here.

In pursuit of further examining the higher-power correction terms derived in section 3, we look into the differences between the fixed order results and the approximate ones. We note at this point that although we have already seen that their respective ratios approach unity in the limit $q_T \rightarrow 0$, finite differences in this limit play an important role when the approximants are used to subtract or replace the exact spectrum in higher-order calculations where the divergences cancel against the virtual corrections in the $q_T = 0$ bin. Similarly, while the ratio tests above emphasise the relative sizes between the full theory and the sum of all corrections to each power considered, their differences allow to examine the individual term of the power series. To this end, according to the power series in eq. (2.8) as well as the definitions in eq. (4.1), the differences between the two are expected to take the following asymptotic behaviour,

$$\begin{aligned}
 \left. \frac{d\sigma_H^{\langle \text{F.O.} \rangle}}{dY_H dq_T^2} - \frac{d\sigma_H^{\langle \text{asy} \rangle}}{dY_H dq_T^2} \right|_{\text{LP}} &= \sum_m \Delta_{\text{NLP}}^{(m)} (L_H)^m + \dots, \\
 \left. \frac{d\sigma_H^{\langle \text{F.O.} \rangle}}{dY_H dq_T^2} - \frac{d\sigma_H^{\langle \text{asy} \rangle}}{dY_H dq_T^2} \right|_{\text{NLP}} &= \sum_m q_T^2 \Delta_{\text{N}^2\text{LP}}^{(m)} (L_H)^m + \dots, \\
 \left. \frac{d\sigma_H^{\langle \text{F.O.} \rangle}}{dY_H dq_T^2} - \frac{d\sigma_H^{\langle \text{asy} \rangle}}{dY_H dq_T^2} \right|_{\text{N}^2\text{LP}} &= \sum_m q_T^4 \Delta_{\text{N}^3\text{LP}}^{(m)} (L_H)^m + \dots.
 \end{aligned}
 \tag{4.2}$$

The numerical results for the magnitudes of these missing, or yet uncalculated, higher-power corrections are presented in figure 3 for all three partonic processes at $Y_H = 0$. Therein, the solid lines denote our results including both the interior contribution from section 2.4 and the boundary correction discussed in section 2.3. Due to the presence of the logarithmic contributions in eqs. (3.15) and (3.20), the differences between the exact q_T spectra and its LP approximations (blue solid line) experience mild enhancements in magnitude in the low q_T regime, agreeing with the expectation in eq. (4.2).³ After incorporating the NLP corrections, as exhibited in the red solid line, the difference between the full theory and our

³In fact, the difference between the LP expression and the exact result forms an integrable divergence as $q_T \rightarrow 0$. This integrable divergence is removed once NLP corrections are introduced.

NLP-correct approximation starts to decrease as $q_T \rightarrow 0$ for all three partonic channels. This echoes again, our NLP expectation of eq. (4.2) that, starting at this order, the difference vanishes in this limit. This also demonstrates that at least up to NLP, the power coefficients of the q_T distribution can be reproduced as appropriate by the expressions in section 3. Similarly, including the power corrections up to N²LP results, detailed by the green line, results in the difference vanishing twice as fast.

On the other hand, figure 3 also depicts our results for which we have removed the boundary contributions of eq. (3.24), induced by expanding the integral boundaries of eq. (2.2) as well as those in eq. (3.8) and eq. (3.17) which arise from integrating the preceding expressions by parts, in dashed lines. Since those boundary corrections will start at NLP accuracy, our LP result (blue) remains unchanged. At NLP, these boundary impacts play only a small role in both the gg and $q\bar{q}$ channels, but manifest themselves in the $q(\bar{q})g$ -initiated process for $q_T \lesssim \mathcal{O}(10^{-2})$. The resulting expression then ceases to reproduce the entire NLP coefficient of eq. (2.8), halting the $\propto q_T^2$ behaviour we would expect the difference with the exact result to exhibit. At N²LP, the sensitivity of the result to the presence of these boundary contributions is even larger, being noticeable already for q_T of $\mathcal{O}(10^{-1})$ in the gg -initiated and $\mathcal{O}(1)$ for the $q(\bar{q})g$ -initiated partonic channels. In both cases, the respective power accuracy is lost in that domain, and only LP accuracy is maintained, exemplifying the necessity of the boundary corrections.

It is worth noting that despite their indispensable effects in reproducing the power coefficients at a given power, at least up to N²LP, those boundary terms can only generate constant corrections of comparably small magnitude. They may therefore not play a role of phenomenological interest when the larger q_T region, where power corrections are larger by construction, is being investigated, and our results may form the basis of a subleading power resummation. However, it should be stressed that, from a theoretical point of view, the emergence of the boundary corrections highlights one of the main differences between the asymptotic expansion of loop integrals and phase space integrals in the small q_T regime. While the loop integrals generally involve unbounded integrals and, thus, only incur relevant power expansions of the integrand within a variety of scalings, the expansion of phase space integrals in the small, but finite, q_T regime additionally induces phase space boundaries through eq. (2.2), from which the appearance of hierarchies $q_T \ll m_H$ (and the application of the integration by parts identities) will introduce a novel type of power corrections associated with the PDFs at the end point, as shown in eqs. (2.24) and (3.6).

To scrutinise the power correction at N²LP, we investigate the differences between the weighted q_T distribution in the full theory and the power-expanded approximations below. From eqs. (2.8) as well as (4.1), we expect these differences to exhibit the following asymptotic properties,

$$\begin{aligned}
 \left. \frac{1}{q_T^2} \frac{d\sigma_H^{\langle \text{F.O.} \rangle}}{dY_H dq_T^2} - \frac{1}{q_T^2} \frac{d\sigma_H^{\langle \text{asy} \rangle}}{dY_H dq_T^2} \right|_{\text{LP}} &= \sum_m \frac{1}{q_T^2} \Delta_{\text{NLP}}^{(m)} (L_H)^m + \dots, \\
 \left. \frac{1}{q_T^2} \frac{d\sigma_H^{\langle \text{F.O.} \rangle}}{dY_H dq_T^2} - \frac{1}{q_T^2} \frac{d\sigma_H^{\langle \text{asy} \rangle}}{dY_H dq_T^2} \right|_{\text{NLP}} &= \sum_m \Delta_{\text{N}^2\text{LP}}^{(m)} (L_H)^m + \dots, \\
 \left. \frac{1}{q_T^2} \frac{d\sigma_H^{\langle \text{F.O.} \rangle}}{dY_H dq_T^2} - \frac{1}{q_T^2} \frac{d\sigma_H^{\langle \text{asy} \rangle}}{dY_H dq_T^2} \right|_{\text{N}^2\text{LP}} &= \sum_m q_T^2 \Delta_{\text{N}^3\text{LP}}^{(m)} (L_H)^m + \dots.
 \end{aligned}
 \tag{4.3}$$

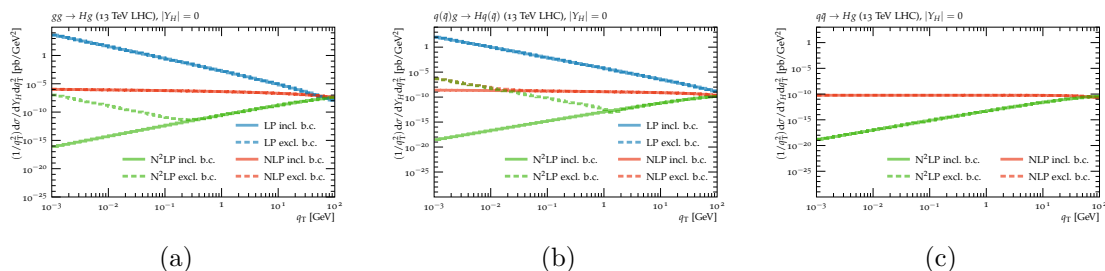


Figure 4. Difference of the weighted exact spectra and the approximations for the three different partonic processes at $|Y_H| = 0$. The solid (dashed) lines present the results including (excluding) the boundary corrections \mathbf{B}_{CS} in eq. (3.8), $\mathbf{B}_{\bar{c}S}$ in eq. (3.17), and $\mathbf{B}_{uc(\bar{c})}$ in eq. (3.24). The blue, green, and red lines detail the LP, NLP, N^2 LP approximations, respectively.

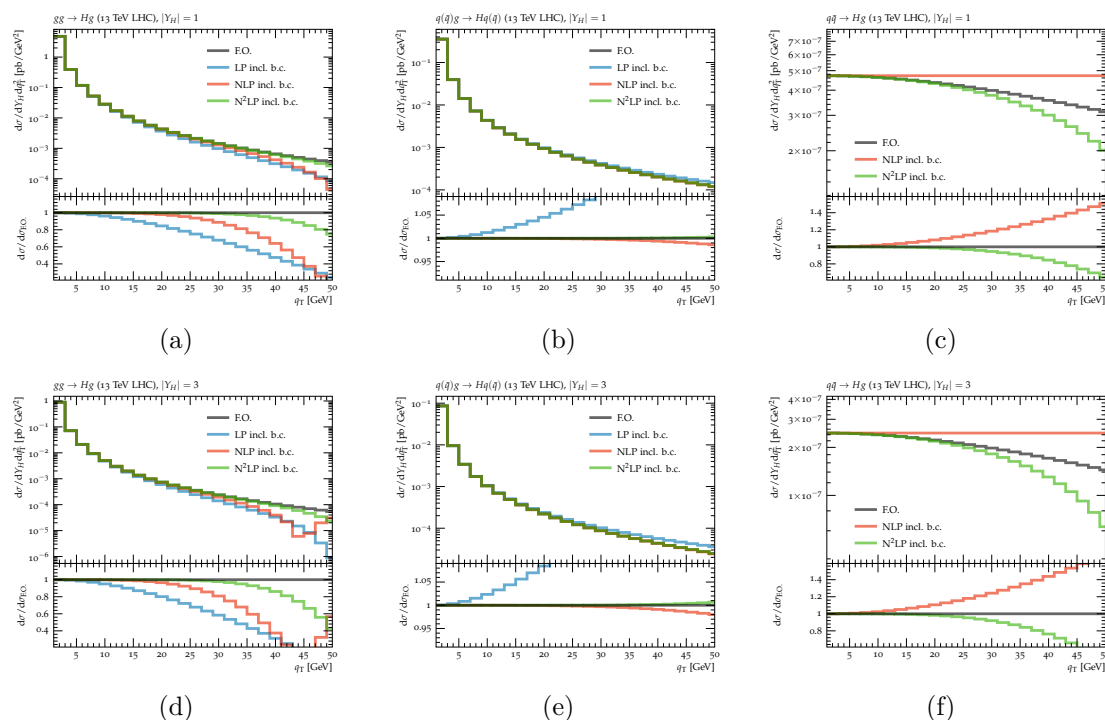


Figure 5. Comparisons of the q_T spectra between the exact fixed-order calculation (black) and approximations constructed using the power expansion up to LP (blue), NLP (red), and N^2 LP (green) for different partonic processes at $|Y_H| = 1$ (top) and $|Y_H| = 3$ (bottom). Throughout we include the boundary corrections \mathbf{B}_{CS} , $\mathbf{B}_{\bar{c}S}$, and $\mathbf{B}_{uc(\bar{c})}$.

Comparing with eqs. (4.2), the remainders on the r.h.s. of eq. (4.3) are generally one power lower. Their numeric results are displayed in figure 4. Our attention is immediately drawn to the observation that the difference between the exact and approximate weighted spectrum diverges at LP as $q_T \rightarrow 0$ whereas it approaches a constant at NLP. Only once the N^2 LP corrections are taken into account, including the boundary terms, does the difference of the weighted spectra vanish in the $q_T \rightarrow 0$ limit, in line with the N^2 LP expectation of eq. (4.3) justifying (at least the first three terms of) our power series derived in section 3.

In the previous figures we have focussed on the q_T spectra at central rapidities, $|Y_H| = 0$, where $e^{\pm Y_H} \sim \mathcal{O}(1)$. We now increase the rapidity of the Higgs boson to affect the scaling

of the relevant light cone momenta k_{\pm} , associated momentum fractions of eq. (3.2), and phase space boundaries of eq. (2.2). To this end, figure 5 displays the q_T spectra at $|Y_H| = 1$ and $|Y_H| = 3$. We observe that the q_T distributions at $|Y_H| = 1$ generally observe similar patterns to those at $|Y_H| = 0$ from figure 2 for all three partonic channels, as $e^{\pm Y_H}$ is still more or less of $\mathcal{O}(1)$. At $|Y_H| = 3$, where $e^{|Y_H|}$ is now of $\mathcal{O}(10)$, even though ability of the LP approximation to reproduce the exact result is further reduced in the moderate domain, the higher power corrections are still convergent as before. More specifically, nearing $q_T = 30$ GeV, the LP contribution to the process $gg \rightarrow Hg$ accounts for less than 60% of the full theory, which is raised to nearly 80% after including the NLP corrections and about 97% with the N²LP terms. A marked difference, even at N²LP, w.r.t. the central rapidity region is only observed at very high q_T around 50 GeV. We would like to note that the non-monotonous behaviour of the NLP result in figure 5(d) around $q_T \sim 45$ GeV is caused by a changing sign of the NLP approximants.

Finally, to assess the coefficients at each power, we investigate the difference between the exact (weighted) q_T spectra and their approximations on different levels of the power expansion in figure 6. We find that the power series appraised in section 3 is capable of reproducing the asymptotic behaviour of the full theory for both $|Y_H| = 1$ and $|Y_H| = 3$. Moreover, an interesting phenomenon can be observed here: the ranges that are sensitive to the boundary corrections grow with increasing rapidity $|Y_H|$ for all three partonic processes. For instance, the N²LP accurate computation, represented by the green curves, shows discrepancies between the solid and dashed lines, which are driven by the boundary corrections, arise below $q_T \approx 0.4$ GeV in the $|Y_H| = 1$ case in the gg channel but already below $q_T \approx 1$ GeV in the $|Y_H| = 3$ case. To interpret this behaviour, it merits recalling that in the central rapidity regime where $e^{\pm Y_H} \sim \mathcal{O}(1)$, the momentum fractions x_n and $x_{\bar{n}}$ in eq. (3.2) both approach zero. Hence, while the interior contribution experiences no suppression from the PDFs, the boundary correction in eq. (2.24) does, suppressing it in the majority of the phase space. However, nearing the rapidity extremes $Y_H \rightarrow \pm 4.5$, one of x_n and $x_{\bar{n}}$ approaches unity. Now, the interior contribution will be suppressed by one of the PDFs, analogous to that in eq. (2.24), thereby losing its predominant role, relatively enlarging the boundary terms.

5 Conclusions

In this paper, we constructed a systematic and mathematically well-defined framework to construct a small- q_T expansion at NLO up to arbitrary power accuracy. This framework is applicable to all possible conservative regulators of the emerging rapidity divergences, and we have shown that the results are identical for three radically different choices. In our power expansion we have refactored all q_T dependences from the transition amplitudes and PDFs, except for those residing in the integration path and phase space boundaries. To achieve this, we have divided the phase space into two sectors, the interior of the integration domain and the segments in the vicinity of the integration boundaries.

The contributions originating from the integration boundaries, which we have evaluated in this paper for the first time, are always associated with the PDF of the beam at the opposite side and, ultimately, give rise to power suppressed constant corrections at NLO. We have summarised their analytic expressions in eqs. (2.26) and (2.27). The analysis of the

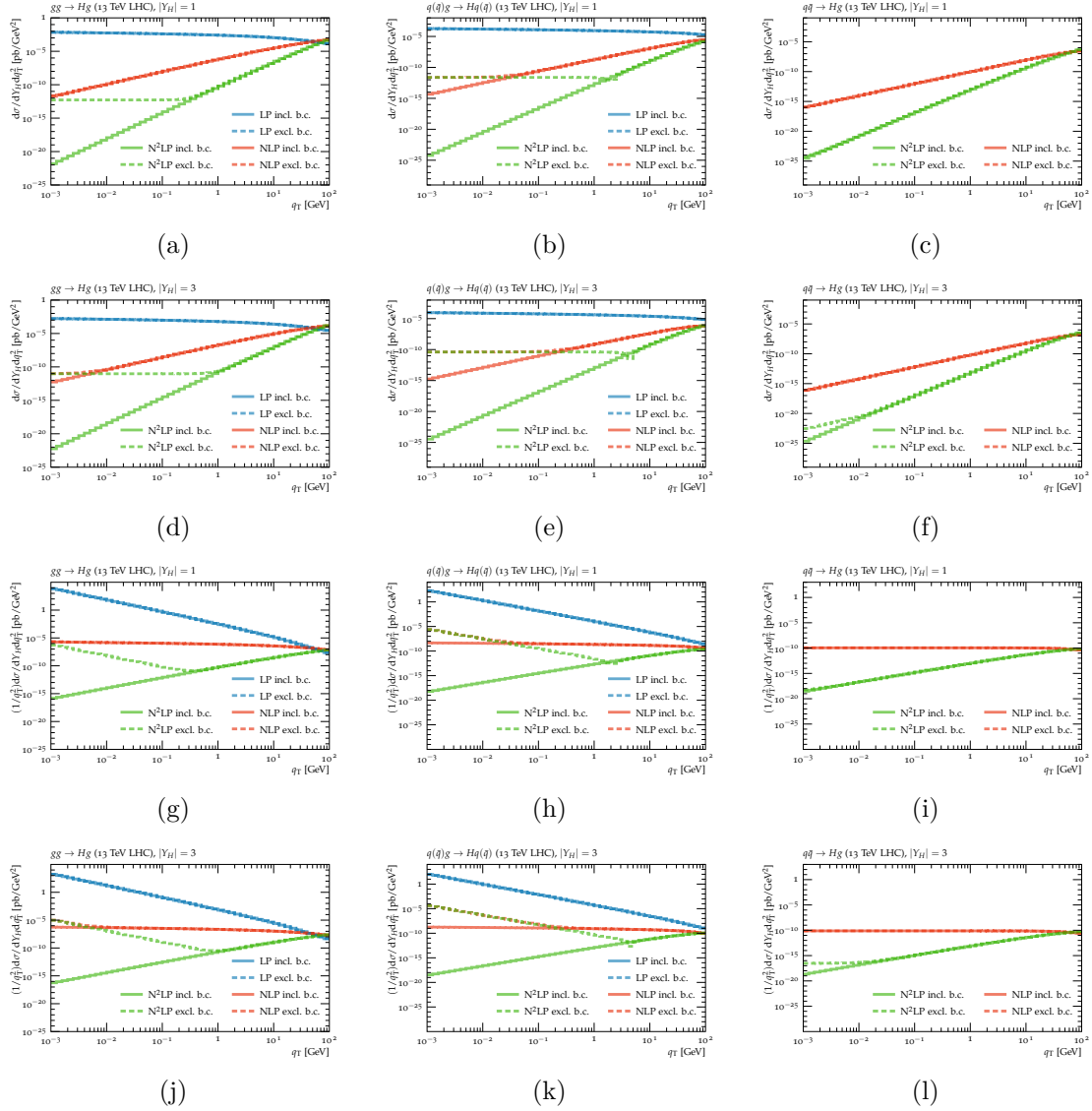


Figure 6. Differences of the q_T (1st & 2nd row) and weighted q_T (3rd & 4th row) spectra between the exact fixed-order calculation and the approximations for the three different partonic processes at $|Y_H| = 1$ (1st & 3rd row) and $|Y_H| = 3$ (2nd & 4th row). The solid (dashed) lines present the results including (excluding) the boundary corrections \mathbf{B}_{cs} in eq. (3.8), $\mathbf{B}_{\bar{c}s}$ in eq. (3.17), and $\mathbf{B}_{uc(\bar{c})}$ in eq. (3.24). The blue, green, and red lines detail the LP, NLP, and N²LP approximations, respectively.

contributions from the interior domain, on the other hand, is more involved due to the number of scales that are enclosed in the phase space integral. To derive the asymptotic series of the interior contributions, we have introduced a set of auxiliary cutoff scales to disentangle the scale hierarchies and in turn perform the appropriate power expansion. The recombination of all artificially separated contributions at each power removes all dependence on the auxiliary scales, such that the final result is independent of them. In any case, the contributions from the interior domain are comprised of three sectors, the n - and \bar{n} -collinear domains, and the zero-bin subtrahends. At a given ω -th power, for example, the two collinear contributions

can be derived by expanding the integrands according to the respective collinear scaling of the integration variable and projecting onto the ω -th power contributions. Conversely, the zero-bin subtrahends are organised by dual-scalings, in which a second expansion of the ω -th power collinear functions needs to be performed according to the soft scaling, giving contributions from the lowest power precision up to the ω -th power. This algorithm is presented in eqs. (2.63) and (2.64) in terms of the expansion operators.

To demonstrate the applicability of our algorithm, two additional fundamentally different rapidity regulators, the pure-rapidity and exponential regulators, in addition to the above cutoff scale regulator, have been embedded into eqs. (2.63)–(2.64) in order to calculate the power corrections from the interior domain up to N²LP accuracy, which we present here for the first time. We found that even though substantial differences emerge from the individual sectors in those two regularisation schemes, after summing all contributions both results produce the same power series as we have obtained via the momentum cutoffs. Together with the correction terms induced by the kinematical variables and the integral boundaries, we have derived analytic expressions for the expanded q_T distribution for Higgs hadroproduction up to N²LP, following eq. (2.80).

To validate our results, we confronted the resulting power series approximation to the full QCD calculation at the same order. We have shown that our expanded q_T spectra can satisfactorily replicate the desired qualities of the full theory for all contributing partonic channels at three different rapidity slices, $|Y_H| = 0, 1, 3$. In particular, when including N²LP corrections, the approximate predictions can capture the exact ones within (sub)percent level accuracy up to $q_T = 30$ GeV. In addition, to explore the relationship between the sizes of the different ingredients at a given power, we produced results without accounting for contributions stemming from the integral boundaries, a situation that may arise if PDFs and their derivatives are considered to vanish at the opposite in these regions. We found that the boundary contributions are generally small at q_T larger than a few GeV, but can play a decisive role as $q_T \rightarrow 0$. Here, their omission effectively degrades the NLP and N²LP results to LP accuracy. To give an example, the N²LP corrections in the partonic process $q(\bar{q})g \rightarrow Hq(\bar{q})$ are driven by the boundary corrections already at $q_T \lesssim 10$ GeV at $Y_H = 3$.

At last, it is worth emphasising that although Higgs hadroproduction is used as an example here to illustrate the capabilities and practicability of our results in eq. (2.80), the algorithm developed in this paper is expected to be directly applicable to the Drell-Yan family of processes and other colour-singlet processes containing similar denominators in the transition amplitudes. Furthermore, during our investigation, except for the indispensable ansatz made on the analytic properties of the PDFs, the power expansions are all carried out following a mathematically well-defined manner. Therefore, we expect the conclusions from this work can not only serve as a robust recipe to derive the power series of the q_T distribution at NLO, but also offer the theoretical baseline for exploring the asymptotic properties of contributions at higher perturbative order.

Acknowledgments

MS is funded by the Royal Society through a University Research Fellowship (URF\R1\180549 and URF\R\231031) and a Royal Society Enhancement Award (RGF\EA\181033, CEC19\100349, and RF\ERE\210397).

A Application and adaptation of the dissipative regulators

Here we will demonstrate that, after suitable adaptation, our zero-bin subtrahends in eqs. (2.64) can also be utilised in the power expansion governed by the dissipative regulators. In the followings, we will illustrate this by implementing the Δ - and η -regulators.

A.1 The Δ -regulator

The Δ -regulator was proposed in [166] to regulate the rapidity divergence in the massive Sudakov factor, which was afterwards generalised in [75, 171, 172, 179] for fulfilling the restrictions from the non-abelian exponentiation theorem in higher-perturbative order calculation. The method behind this regularisation scheme is to shift the mass of the mediating particles in the transition amplitudes by an infinitesimal amount, such that when approaching the rapidity extrema, i.e. $y_k \rightarrow \pm\infty$, the involved propagators can never go on-shell and thus are always insulated from the rapidity divergences.

The Δ -regulator is dedicated to the rapidity divergences at LP, as extra residual momenta can be generated during the expansion of the squared amplitudes beyond LP [114], which are singular in the limit $y_k \rightarrow \pm\infty$ and stay unprotected by the Δ -regulator. To this end, in the following discussion, we will focus on the LP contribution only.

At LP, the zero-bin subtraction for the small q_T expansion primarily concerns the process $gg \rightarrow Hg$ up to NLO, which, as presented in eq. (2.4), corresponds to the integrand $I_{[\kappa],\{\alpha,\beta\}}^{-1,-1}$ based on the definition in eq. (2.65). Applying the Δ -regulator onto eq. (2.65) with $\rho = \sigma = -1$ amounts to re-weighting the squared amplitudes by a factor of,

$$\mathcal{R}(k_-, k_+, \tau) = \frac{q_T^2}{(k_+ + \tau)(k_- + \tau)}, \quad (\text{A.1})$$

where τ denotes an infinitesimal parameter, $\tau > 0$. It is seen that \mathcal{R} in eq. (A.1) indeed satisfies the criteria of eq. (2.47), which keeps void for the rapidity-safe integrands but becomes activated for the singular transition amplitudes.

Substituting eq. (A.1) into eqs. (2.63) and (2.64) and then truncating out the corrections beyond LP, it yields,

$$\begin{aligned} \tilde{\mathcal{G}}_{[\kappa],\{\alpha,\beta\}}^{-1,-1,(-1)} \Big|_c^{\langle\Delta\rangle} &= \int_0^{\tilde{k}_+^{\max}} dk_+ \left[\frac{1}{k_+} \right]_*^{\nu_n} F_{i/N,\beta_1}^{(\beta_2)}(k_+ + m_H e^{-Y_H}) F_{j/\bar{N},\alpha_1}^{(\alpha_2)}(m_H e^{+Y_H}) \\ &\quad + F_{i/N,\beta_1}^{(\beta_2)}(m_H e^{-Y_H}) F_{j/\bar{N},\alpha_1}^{(\alpha_2)}(m_H e^{+Y_H}) \ln \left[\frac{\nu_n}{\tau} \right], \end{aligned} \quad (\text{A.2})$$

$$\begin{aligned} \tilde{\mathcal{G}}_{[\kappa],\{\alpha,\beta\}}^{-1,-1,(-1)} \Big|_{\bar{c}}^{\langle\Delta\rangle} &= \int_0^{\frac{q_T^2}{\tilde{k}_+^{\min}}} dk_- \left[\frac{1}{k_-} \right]_*^{\nu_{\bar{n}}} F_{i/N,\beta_1}^{(\beta_2)}(m_H e^{-Y_H}) F_{j/\bar{N},\alpha_1}^{(\alpha_2)}(k_- + m_H e^{+Y_H}) \\ &\quad + F_{i/N,\beta_1}^{(\beta_2)}(m_H e^{-Y_H}) F_{j/\bar{N},\alpha_1}^{(\alpha_2)}(m_H e^{+Y_H}) \ln \left[\frac{\nu_{\bar{n}}}{\tau} \right], \end{aligned} \quad (\text{A.3})$$

and

$$\tilde{\mathcal{G}}_{[\kappa],\{\alpha,\beta\}}^{-1,-1,(-1)} \Big|_{c0}^{\langle\text{NS}\rangle,\langle\Delta\rangle} = \tilde{\mathcal{G}}_{[\kappa],\{\alpha,\beta\}}^{-1,-1,(-1)} \Big|_{\bar{c}0}^{\langle\text{NS}\rangle,\langle\Delta\rangle} = F_{i/N,\beta_1}^{(\beta_2)}(m_H e^{-Y_H}) F_{j/\bar{N},\alpha_1}^{(\alpha_2)}(m_H e^{+Y_H}) \ln \left[\frac{q_T}{\tau} \right]. \quad (\text{A.4})$$

It is immediate to find that the difference between eqs. (A.2)–(A.3) and eq. (A.4) exactly replicates the leading power outputs in eqs. (2.31)–(2.33) and eqs. (2.40)–(2.41) derived via momentum cutoffs, those in eqs. (3.30)–(3.32) by means of the pure-rapidity regulator, or those in eqs. (3.41)–(3.45) from the exponential one, after setting $\omega = \rho = \sigma = -1$ therein.

A.2 The η -regulator

The η -regulator was devised by [77, 78] to facilitate the establishment of the rapidity renormalisation group equations in the SCET_{II}-based analysis of the jet broadening and q_T distributions. Akin to the analytic regularisation prescription [74, 76], the η -regulator concerns the momenta of the emitted partons raised by the power of τ as well. However, in place of the light-cone component k_+ or k_- entailed in [74, 76], the η -regulator puts the magnitude of the longitudinal one into the base, namely,

$$\mathcal{R}(k_-, k_+, \tau) = |k_- - k_+|^{-\tau}. \tag{A.5}$$

Implementing the η -regularisation scheme is rather subtle. In its original definition [77, 78] and the recent review of [113], the calculation on the collinear sector calls for the expansions of both the rapidity regulator in eq. (A.5) and the integrand of eq. (2.65), which, based on the notation in eq. (2.63), requires that \mathcal{R} always appears to the right hand side of $\widehat{\mathbf{T}}_c^{(\omega)}$ and $\widehat{\mathbf{T}}_c^{(\omega)}$. In doing this, a set of evanescent power corrections can be generated from eq. (A.5), which are proportional to τ (or its higher powers) and will make non-trivial contributions in combination with the pole terms. Those evanescent influences have not been taken into account during the derivation of eqs. (2.63)–(2.64), and therefore, it is not straightforward to apply eq. (A.5) here until appropriate adaptations are put in place.

In the following, we will introduce one of strategies to adapt the η -regulator to our formalism in eqs. (2.63)–(2.64). Considering that the main obstacle hindering this application comes from evanescent contributions, it could be beneficial to maintain the regulator in eq. (A.5) always to the left of the operators $\widehat{\mathbf{T}}_c^{(\omega)}$ and $\widehat{\mathbf{T}}_c^{(\omega)}$ in practical calculations. In this way, eq. (A.5) abides by the criteria of eq. (2.47) and can still serve as a qualified rapidity-divergence regularisation scheme at any power accuracy. Furthermore, since the η -regulator at this moment does not participate into the expansion governed by $\widehat{\mathbf{T}}_c^{(\omega)}$ and $\widehat{\mathbf{T}}_c^{(\omega)}$, one can save efforts in coping with the evanescent contribution.

Now applying the η -regulator onto eqs. (2.63)–(2.64) becomes immediate, which evaluates to,

$$\begin{aligned} \widetilde{\mathcal{G}}_{[\kappa], \{\alpha, \beta\}}^{\rho, \sigma, (\omega)} \Big|_c^{(\eta)} &= \frac{\bar{\theta}(\omega - \sigma)}{(\omega - \rho)!} \int_0^{\bar{k}_+^{\max}} \frac{dk_+}{k_+} (k_+)^{\sigma - \omega} F_{i/N, \beta_1}^{(\beta_2)} \left(k_+ + m_H e^{-Y_H} \right) F_{j/\bar{N}, \alpha_1}^{(\alpha_2 + \omega - \rho)} \left(m_H e^{+Y_H} \right) \\ &+ \frac{\theta(\omega - \sigma)}{(\omega - \rho)!} \int_0^{\bar{k}_+^{\max}} dk_+ \left[\frac{1}{k_+^{\omega - \sigma + 1}} \right]_*^{\nu_n} F_{i/N, \beta_1}^{(\beta_2)} \left(k_+ + m_H e^{-Y_H} \right) F_{j/\bar{N}, \alpha_1}^{(\alpha_2 + \omega - \rho)} \left(m_H e^{+Y_H} \right) \\ &+ \frac{\theta(\omega - \sigma - 1)}{(\omega - \rho)!} \sum_{\eta=0}^{\omega - \sigma - 1} \frac{F_{i/N, \beta_1}^{(\beta_2 + \eta)} \left(m_H e^{-Y_H} \right) F_{j/\bar{N}, \alpha_1}^{(\alpha_2 + \omega - \rho)} \left(m_H e^{+Y_H} \right)}{\eta!} \frac{\nu_n^{\sigma + \eta - \omega}}{\sigma + \eta - \omega} \\ &+ \frac{\theta(\omega - \sigma)}{(\omega - \rho)!} \frac{F_{i/N, \beta_1}^{(\beta_2 + \omega - \sigma)} \left(m_H e^{-Y_H} \right) F_{j/\bar{N}, \alpha_1}^{(\alpha_2 + \omega - \rho)} \left(m_H e^{+Y_H} \right)}{(\omega - \sigma)!} \left\{ \ln \left[\frac{\nu_n}{q_T^2} \right] + \frac{1}{\tau} \right\}, \end{aligned} \tag{A.6}$$

$$\begin{aligned}
 \tilde{\mathcal{G}}_{[\kappa],\{\alpha,\beta\}}^{\rho,\sigma,(\omega)} \Big|_{\bar{c}}^{(\eta)} &= \frac{\bar{\theta}(\omega-\rho)}{(\omega-\sigma)!} \int_0^{\frac{q_T^2}{\bar{k}_+^{\min}}} \frac{dk_-}{k_-} k_-^{\rho-\omega} F_{i/N,\beta_1}^{(\beta_2+\omega-\sigma)} \left(m_H e^{-Y_H} \right) F_{j/\bar{N},\alpha_1}^{(\alpha_2)} \left(k_- + m_H e^{+Y_H} \right) \\
 &+ \frac{\theta(\omega-\rho)}{(\omega-\sigma)!} \int_0^{\frac{q_T^2}{\bar{k}_+^{\min}}} dk_- \left[\frac{1}{k_-^{\omega-\rho+1}} \right]_*^{\nu_{\bar{n}}} F_{i/N,\beta_1}^{(\beta_2+\omega-\sigma)} \left(m_H e^{-Y_H} \right) F_{j/\bar{N},\alpha_1}^{(\alpha_2)} \left(k_- + m_H e^{+Y_H} \right) \\
 &+ \frac{\theta(\omega-\rho-1)}{(\omega-\sigma)!} \sum_{\lambda=0}^{\omega-\rho-1} \frac{F_{i/N,\beta_1}^{(\beta_2+\omega-\sigma)} \left(m_H e^{-Y_H} \right) F_{j/\bar{N},\alpha_1}^{(\alpha_2+\lambda)} \left(m_H e^{+Y_H} \right)}{\lambda!} \frac{\nu_{\bar{n}}^{\rho+\lambda-\omega}}{\rho+\lambda-\omega} \\
 &+ \frac{\theta(\omega-\rho)}{(\omega-\sigma)!} \frac{F_{i/N,\beta_1}^{(\beta_2+\omega-\sigma)} \left(m_H e^{-Y_H} \right) F_{j/\bar{N},\alpha_1}^{(\alpha_2+\omega-\rho)} \left(m_H e^{+Y_H} \right)}{(\omega-\rho)!} \left\{ \ln \left[\frac{\nu_{\bar{n}}}{q_T^2} \right] + \frac{1}{\tau} \right\}, \tag{A.7}
 \end{aligned}$$

together with the subtraction terms,

$$\tilde{\mathcal{G}}_{[\kappa],\{\alpha,\beta\}}^{\rho,\sigma,(\omega)} \Big|_{c0}^{(NS),(\eta)} = \theta(\omega-\sigma) \frac{F_{i/N,\beta_1}^{(\beta_2+\omega-\sigma)} \left(m_H e^{-Y_H} \right) F_{j/\bar{N},\alpha_1}^{(\alpha_2+\omega-\rho)} \left(m_H e^{+Y_H} \right)}{(\omega-\sigma)! (\omega-\rho)!} \left\{ \ln \left[\frac{1}{q_T} \right] + \frac{1}{\tau} \right\}, \tag{A.8}$$

$$\tilde{\mathcal{G}}_{[\kappa],\{\alpha,\beta\}}^{\rho,\sigma,(\omega)} \Big|_{\bar{c}0}^{(NS),(\eta)} = \theta(\omega-\rho) \frac{F_{i/N,\beta_1}^{(\beta_2+\omega-\sigma)} \left(m_H e^{-Y_H} \right) F_{j/\bar{N},\alpha_1}^{(\alpha_2+\omega-\rho)} \left(m_H e^{+Y_H} \right)}{(\omega-\sigma)! (\omega-\rho)!} \left\{ \ln \left[\frac{1}{q_T} \right] + \frac{1}{\tau} \right\}. \tag{A.9}$$

Subtracting eqs. (A.8)–(A.9) from eqs. (A.6)–(A.7), it reproduces the results in eqs. (2.31)–(2.33) and eqs. (2.40)–(2.41) obtained from momentum cutoffs, and also those in section 3 by means of pure-rapidity and exponential regularisation schemes.

B Comparison of the NLP results with the previous literature

Subleading power corrections of the process $pp \rightarrow H+X$ have been investigated in [113] as well by means of the η - and pure rapidity regulators. Here we take the partonic process $q\bar{q} \rightarrow Hg$ as an illustrative example to compare the expressions in [113] and those in eq. (3.8), (3.17), and (3.23). Over the course, we will particularly emphasise the interior contributions encoded by the partonic matrices \mathbf{P} , \mathbf{D} , and \mathbf{R} , as the boundary corrections in \mathbf{B} are related to the PDFs at the opposite end, which are all assumed to be vanishing in [113].

In [113], the analytic results for the channel $q\bar{q} \rightarrow Hg$ entail the expanded amplitudes of eq. (2.4) sandwiched by the (derivatives of) PDFs. Recasting their expressions into matrix form according to the bases in eq. (3.9) and also synchronising the pre-factors in line with eq. (3.8), we obtain

$$\widehat{\mathbf{P}}_{cs}^{(0),q\bar{q}} = \widehat{\mathbf{P}}_{\bar{c}s}^{(0),q\bar{q}} = \widehat{\mathbf{D}}_{cs}^{(0),q\bar{q}} = \widehat{\mathbf{D}}_{\bar{c}s}^{(0),q\bar{q}} = 0, \tag{B.1}$$

$$\widehat{\mathbf{R}}_{cs}^{(0),q\bar{q}} = \begin{bmatrix} -\frac{32}{27} + \frac{16}{27z_n} + \frac{16}{27z_n^2} \\ \frac{16}{27} - \frac{32}{27z_n} + \frac{16}{27z_n^2} \end{bmatrix}, \tag{B.2}$$

$$\widehat{\mathbf{R}}_{\bar{c}s}^{(0),q\bar{q}} = \begin{bmatrix} -\frac{32}{27} + \frac{16}{27z_n} + \frac{16}{27z_n^2} & \frac{16}{27} - \frac{32}{27z_n} + \frac{16}{27z_n^2} \end{bmatrix}, \tag{B.3}$$

where the hatted bold matrices encode the results of [113]. It is immediate to see that the matrices in eq. (B.1) associated with the plus distribution and delta function are all zero, echoing the outputs from this work in eqs. (3.15), (3.14), and (3.18), whereas, due to the emergence of the extra off-diagonal entries in eqs. (B.2)–(B.3), the regular contributions from [113] appear to observe distinct patterns from ours in eq. (3.13) and eq. (3.18).

As a matter of fact, this kind of difference can be resolved by applying the method of integration by parts as appropriate. From eq. (3.9), the off-diagonal terms in eqs. (B.2)–(B.3) always invoke the derivatives of one of the PDFs, which, via the integration by parts, can be in turn transformed into the PDFs multiplied by the derivatives of the original integrands, up to a few of boundary terms, more specifically,

$$\int_{x_n}^1 dz_n \frac{x_n}{z_n} f'_{i/N} \left(\frac{x_n}{z_n} \right) f_{j/\bar{N}}(x_{\bar{n}}) g(z_n) = \int_{x_n}^1 dz_n f_{i/N} \left(\frac{x_n}{z_n} \right) f_{j/\bar{N}}(x_{\bar{n}}) \frac{\partial g(z_n)}{\partial \ln(z_n)} - f_{i/N}(x_n) f_{j/\bar{N}}(x_{\bar{n}}) g_n(1) + b.c., \quad (\text{B.4})$$

$$\int_{x_{\bar{n}}}^1 dz_{\bar{n}} f_{i/N}(x_n) \frac{x_{\bar{n}}}{z_{\bar{n}}} f'_{j/\bar{N}} \left(\frac{x_{\bar{n}}}{z_{\bar{n}}} \right) g_{\bar{n}}(z_{\bar{n}}) = \int_{x_{\bar{n}}}^1 dz_{\bar{n}} f_{i/N}(x_n) f_{j/\bar{N}} \left(\frac{x_{\bar{n}}}{z_{\bar{n}}} \right) \frac{\partial g_{\bar{n}}(z_{\bar{n}})}{\partial \ln(z_{\bar{n}})} - f_{i/N}(x_n) f_{j/\bar{N}}(x_{\bar{n}}) g_{\bar{n}}(1) + b.c., \quad (\text{B.5})$$

where $g_n(z_n)$ and $g_{\bar{n}}(z_{\bar{n}})$ represent the two regular functions with finite derivatives across the domains $z_n \in [x_n, 1]$ and $z_{\bar{n}} \in [x_{\bar{n}}, 1]$, respectively.

Applying those two relations onto eqs. (B.2)–(B.3), the off-diagonal entries therein are both eliminated, replicating our results in eq. (3.13) and eq. (3.18). Analogous strategy can also be utilised in comparing the expressions of the processes $gg \rightarrow Hg$ and $q(\bar{q})g \rightarrow Hq(\bar{q})$.

C Small q_T expansion for multi-boson hadroproduction

Here we will demonstrate that, after appropriate generalisations, the method presented in this paper in section 2 can also be used in the power expansion on the hadroproduction of multiple colour-singlet bosons, i.e. $pp \rightarrow \{B_n\} + X$. Here a set of electroweak (or Higgs) bosons are collected within the set $\{B_n\} \equiv \{B_1, B_2, B_3, \dots, B_n\}$ ($n \geq 2$).

We start with the analysis of the fixed-order results. According the QCD factorization, the differential q_T distributions at NLO can be expressed as,

$$\frac{d\sigma_B}{d\Phi_n d^2\vec{q}_T} = \frac{1}{2^{4n} \pi^{3n-1} s^2} \sum_{i,j} \int_{k_+^{\min}}^{k_+^{\max}} \frac{dk_+}{k_+} \frac{f_{i/n}(\xi_n)}{\xi_n} \frac{f_{j/\bar{n}}(\xi_{\bar{n}})}{\xi_{\bar{n}}} \overline{\sum_{\text{col,pol}}} |\mathcal{M}(i+j \rightarrow \{B_n\} + k)|^2. \quad (\text{C.1})$$

Now q_T represents the transverse momentum of the whole colourless system $\{B_n\}$. The differential $d\Phi_n$ collects the differentials for the rapidity y_i and transverse momentum \vec{k}_{\perp}^i of the i th boson,

$$d\Phi_n = \left(\prod_{i=1}^n dy_i \right) \left(\prod_{i=1}^{n-1} d^2\vec{k}_{\perp}^i \right). \quad (\text{C.2})$$

Here only the transverse momenta of the first $n - 1$ partons have been spelled out, as the last one is subjected to the momentum conservation condition,

$$\vec{k}_\perp^n = \vec{q}_T - \sum_{i=1}^{n-1} \vec{k}_\perp^i. \quad (\text{C.3})$$

On the r.h.s. of eq. (C.1), the integrand concerns the momentum fractions ξ_n and $\xi_{\bar{n}}$, which can be determined by the momentum conservation condition on the longitudinal direction,

$$\xi_n = \frac{1}{\sqrt{s}} \left(k_+ + \sum_{i=1}^n m_{\text{T}}^i e^{-y_i} \right), \quad \xi_{\bar{n}} = \frac{1}{\sqrt{s}} \left(k_- + \sum_{i=1}^n m_{\text{T}}^i e^{+y_i} \right). \quad (\text{C.4})$$

Here k_\pm stands for the light-cone components of the emitted colourful particle as defined in eq. (2.6). m_{T}^i reveals the transverse mass for the i th boson. According to the conditions $\xi_n \leq 1$ and $\xi_{\bar{n}} \leq 1$, we can then evaluate the boundaries for the k_+ -integral in eq. (C.1),

$$k_+^{\text{max}} = \sqrt{s} - \sum_{i=1}^n m_{\text{T}}^i e^{-y_i}, \quad k_-^{\text{max}} = \frac{q_{\text{T}}^2}{k_+^{\text{min}}} = \sqrt{s} - \sum_{i=1}^n m_{\text{T}}^i e^{+y_i}. \quad (\text{C.5})$$

The calculation on eq. (C.1) also entails the squared amplitudes for the ensuing partonic process $i + j \rightarrow \{B_n\} + k$. On the tree level, the Feynman diagrams presiding over this transition can be categorised into two groups: (A) topologies in which the final colour-singlet bosons are not directly connected to final colourful particle; (B) topologies in which at least one of the final colour-singlet bosons is emitted from the final QCD parton. The representative circumstances on those two topologies have been illustrated in figure 7 and figure 8. The topology (A) is, for instance, expected to govern the partonic channel $q\bar{q} \rightarrow \{B_n\} + g$ with $\{B_n\}$ comprising only the electroweak vector bosons. In the other circumstances, the contributions from topology (B) can be relevant and therefore have to be addressed as appropriate. However, it merits noting that in topology (B), the emission off the QCD parton will leave all the propagators in the ensuing Feynman diagrams away from the threshold by $\mathcal{O}(m_B^i)$, where m_B^i indicates the mass of the i th final colourless boson, such that the leading singular behaviour of the process $pp \rightarrow \{B_n\} + X$ is entirely captured by the configuration (A).

Without any loss of generality, the matrix elements induced by those two topologies can be recast in the following forms,

$$\begin{aligned} & \overline{\sum_{\text{col,pol}}} |\mathcal{M}(i+j \rightarrow \{B_n\} + k)|^2 \Big|_{(\text{A})} \\ &= \sum_{F \in \mathbf{T}_A} \lambda_{ijk}(F) \left[\prod_{n=1}^{\text{card}[I_F]} \left(p_i - \sum_{l \in I_F^{(n)}} k_l \right)^{-2} \right] \left[\prod_{m=1}^{\text{card}[J_F]} \left(p_j - \sum_{l \in J_F^{(m)}} k_l \right)^{-2} \right] \sum_{\rho, \sigma} k_-^\rho k_+^\sigma \left(\tilde{\mathcal{K}}_\perp \cdot \tilde{\mathcal{E}}_F^{\rho\sigma} \right), \end{aligned} \quad (\text{C.6})$$

$$\begin{aligned} & \overline{\sum_{\text{col,pol}}} |\mathcal{M}(i+j \rightarrow \{B_n\} + k)|^2 \Big|_{(\text{B})} \\ &= \sum_{F \in \mathbf{T}_B} \lambda_{ijk}(F) \left[\prod_{n=1}^{\text{card}[I_F]} \left(p_i - \sum_{l \in I_F^{(n)}} k_l \right)^{-2} \right] \left[\prod_{m=1}^{\text{card}[J_F]} \left(p_j - \sum_{l \in J_F^{(m)}} k_l \right)^{-2} \right] \left[\prod_{h=1}^{\text{card}[K_F]} \left(k_+ + \sum_{l \in K_F^{(h)}} k_l \right)^{-2} \right] \\ & \times \sum_{\rho, \sigma} k_-^\rho k_+^\sigma \left(\tilde{\mathcal{K}}_\perp \cdot \tilde{\mathcal{E}}_F^{\rho\sigma} \right). \end{aligned} \quad (\text{C.7})$$

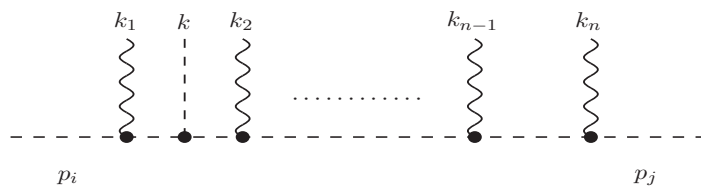


Figure 7. Representative diagram of the topology that the final colour-singlet bosons are all directly connected to the initial partons. Here the dashed lines stand for the colourful particles, while wave lines indicate the colour-singlet bosons.



Figure 8. Representative diagram of the topology that the final colour-singlet bosons are in part connected to the final QCD parton. Here the dashed lines stand for the colourful particles, while wave lines indicate the colour-singlet bosons.

Here F denotes the Feynman diagrams driving the process $i + j \rightarrow \{B_n\} + k$, which, at LO, belongs to either topology \mathbf{T}_A or \mathbf{T}_B . $\lambda_{ijk}(F)$ collects the coupling constants, colour factors, and average factors for the initial states and the final identical particles. I_F and J_F encode two sets of colourless particles emitted from the initial partons i and j , respectively. For instance, if the squared amplitudes are induced by the configuration in figure 7 and its complex conjugate, we have $I_F = \{I_F^{(1)}, I_F^{(2)}\}$ with $I_F^{(1,2)} = B_1$ and $J_F = \{J_F^{(1)}, J_F^{(2)}, J_F^{(3)}, J_F^{(4)}, \dots\}$ with $J_F^{(1,2)} = B_n$, $J_F^{(3,4)} = \{B_{n-1}, B_n\}$, etc. The number of the elements in each set is evaluated by the cardinality operator **card**. With the help of I_F and J_F , one can specify the expressions of the denominators in a given Feynman diagram as presented in the square brackets in eqs. (C.6)–(C.7).

To express the numerators of the squared amplitudes, we introduce the arrays $\tilde{\mathcal{K}}_\perp$ and $\tilde{\mathcal{E}}_F^{\rho\sigma}$,

$$\tilde{\mathcal{K}}_\perp = [1, (\vec{q}_T)_{i_1}, (\vec{q}_T)_{i_2} (\vec{q}_T)_{j_2}, (\vec{q}_T)_{i_3} (\vec{q}_T)_{j_3} (\vec{q}_T)_{k_3}, \dots], \quad (\text{C.8})$$

$$\begin{aligned} (\tilde{\mathcal{E}}_F^{\rho\sigma})^{\mathbf{T}} = & \left[E_F^{\rho\sigma, (0)}, \sum_l (\vec{k}_\perp^l)_{i_1} E_{F,l}^{\rho\sigma, (1s)} + \sum_l (\vec{k}_\perp^l)_{i_1} E_{F,l}^{\rho\sigma, (1A)}, \epsilon_\perp^{i_2 j_2} E_F^{\rho\sigma, (2AA)} \right. \\ & + \sum_{l_1, l_2} (\vec{k}_\perp^{l_1})_{i_2} (\vec{k}_\perp^{l_2})_{j_2} E_{F, l_1, l_2}^{\rho\sigma, (2SS)} + \sum_{l_1, l_2} (\vec{k}_\perp^{l_1})_{i_2} (\vec{k}_\perp^{l_2})_{j_2} E_{F, l_1, l_2}^{\rho\sigma, (2AS)} \\ & \left. + \sum_{l_1, l_2} (\vec{k}_\perp^{l_1})_{i_2} (\vec{k}_\perp^{l_2})_{j_2} E_{F, l_1, l_2}^{\rho\sigma, (2SA)}, \dots \right]. \quad (\text{C.9}) \end{aligned}$$

Here $\tilde{\mathcal{K}}_\perp$ consists of the tensors constructed by the momentum \vec{q}_T in different ranks, while $\tilde{\mathcal{E}}_F^{\rho\sigma}$ collects those formed by k_i^μ with $i \in [1, n]$. To accommodate the asymmetric behaviour induced by the Dirac traces that contain γ_5 , we introduce $\epsilon_\perp^{\rho\sigma} = \epsilon^{\mu\nu\rho\sigma} n_\mu \bar{n}_\nu$ and $(\vec{k}_\perp)^\rho = \epsilon_\perp^{\rho\sigma} \vec{k}_\perp^{\sigma}$ in eq. (C.9), where $\epsilon^{\mu\nu\rho\sigma}$ denotes the customary anti-symmetric tensor. The coefficients $E_{F, \{l\}}^{\rho\sigma, (m)}$ in charge of tensor structures as specified in “(m)” encode the hard scales $m_T^i e^{\pm y_i}$, $(\vec{k}_\perp^i \cdot \vec{k}_\perp^j)$, and $(\vec{k}_\perp^i \cdot \vec{k}_\perp^j)$.

In the following, we will show that the q_T spectra induced by the topology (A) can be all expanded following the method developed in section 2. First of all, it should be noted that in eq. (C.6), all the dependences on the integration variable k_{\pm} have been taken out from the numerator, while the denominators, after evaluating the scalar products, present only the linear dependences on k_{\pm} , more explicitly,

$$\left(p_i - \sum_{l \in X} k_l\right)^2 \equiv (p_i - k_X)^2 = -m_T^X e^{y_X} \left(k_+ + \sum_{l \notin X} m_T^l e^{-y_l} + \frac{|\vec{k}_{\perp}^X|^2}{m_T^X e^{y_X}}\right), \quad (\text{C.10})$$

$$\left(p_j - \sum_{l \in X} k_l\right)^2 \equiv (p_j - k_X)^2 = -m_T^X e^{-y_X} \left(k_- + \sum_{l \notin X} m_T^l e^{y_l} + \frac{|\vec{k}_{\perp}^X|^2}{m_T^X e^{-y_X}}\right). \quad (\text{C.11})$$

Therein, k_X represents the total momentum of the particles belong to the set X , from which we are able to calculate the transverse mass m_T^X and rapidity y_X for this colourless system.

The factorised form in eqs. (C.10)–(C.11) then allows us to recategorise the dominators in eq. (C.6) according to their k_{\pm} -dependences, more explicitly,

$$\begin{aligned} \left. \frac{d\sigma_B}{d\Phi_n d^2\vec{q}_T} \right|_{(\text{A})} &= \sum_{F \in \mathbf{T}_A} \sum_{\rho, \sigma} \left(\tilde{\mathcal{K}}_{\perp} \cdot \tilde{\mathcal{H}}_F^{\rho\sigma} \right) \int_{k_+^{\min}}^{k_+^{\max}} \frac{dk_+}{k_+} (k_-)^{\rho} (k_+)^{\sigma} \hat{F}_{i/n, \{\beta_n\}}^{\{0\}}(k_+, \{Q_n\}, \{I_F\}) \\ &\quad \times \hat{F}_{j/\bar{n}, \{\beta_{\bar{n}}\}}^{\{0\}}(k_-, \{Q_{\bar{n}}\}, \{J_F\}), \end{aligned} \quad (\text{C.12})$$

where the novel array $\tilde{\mathcal{H}}_F^{\rho\sigma}$ emerges, which is defined analogously to eq. (C.9) but can absorb extra hard scales as a result of the denominator decomposition in eqs. (C.10)–(C.11). Within the integral, all the k_{\pm} reliances from the PDFs and denominators of the squared amplitudes have been collected in the generalised functions $\hat{F}_{i/n, \{\beta_n\}}^{\{\alpha_n\}}$ and $\hat{F}_{j/\bar{n}, \{\beta_{\bar{n}}\}}^{\{\alpha_{\bar{n}}\}}$,

$$\begin{aligned} &\hat{F}_{i/n, \{\beta_n\}}^{\{\alpha_n\}}(k_+, \{Q_n\}, \{I_F\}) \\ &\equiv \frac{\partial^{\alpha_n^{(-1)}}}{\partial(k_+)^{\alpha_n^{(-1)}}} \left\{ \prod_{l=0}^{\text{card}[I_F]} \frac{\partial^{\alpha_n^{(l)}}}{\partial(Q_n^{(l)})^{\alpha_n^{(l)}}} \right\} \left[\frac{f_{i/n} \left(\frac{k_+ + Q_n^{(0)}}{\sqrt{s}} \right)}{k_+ + Q_n^{(0)}} \right] \prod_{h=1}^{\text{card}[I_F]} \left(k_+ + Q_n^{(h)} \right)^{-\beta_n^{(h)}}, \end{aligned} \quad (\text{C.13})$$

$$\begin{aligned} &\hat{F}_{j/\bar{n}, \{\beta_{\bar{n}}\}}^{\{\alpha_{\bar{n}}\}}(k_-, \{Q_{\bar{n}}\}, \{J_F\}) \\ &\equiv \frac{\partial^{\alpha_{\bar{n}}^{(-1)}}}{\partial(k_-)^{\alpha_{\bar{n}}^{(-1)}}} \left\{ \prod_{l=0}^{\text{card}[J_F]} \frac{\partial^{\alpha_{\bar{n}}^{(l)}}}{\partial(Q_{\bar{n}}^{(l)})^{\alpha_{\bar{n}}^{(l)}}} \right\} \left[\frac{f_{j/\bar{n}} \left(\frac{k_- + Q_{\bar{n}}^{(0)}}{\sqrt{s}} \right)}{k_- + Q_{\bar{n}}^{(0)}} \right] \prod_{h=1}^{\text{card}[J_F]} \left(k_- + Q_{\bar{n}}^{(h)} \right)^{-\beta_{\bar{n}}^{(h)}}, \end{aligned} \quad (\text{C.14})$$

where $\{Q_n, Q_{\bar{n}}\}$ signify two sets of hard scales. $Q_n^{(0)}$ and $Q_{\bar{n}}^{(0)}$ can be extracted from the fractions in eq. (C.4), while $Q_n^{(l)}$ and $Q_{\bar{n}}^{(l)}$ with $l \geq 1$ are derived by matching onto eqs. (C.10)–(C.11). In comparison with the functions $F_{i/n, \beta_n}^{(\alpha_n)}$ and $F_{j/\bar{n}, \beta_{\bar{n}}}^{(\alpha_{\bar{n}})}$ in eq. (2.12), eqs. (C.13)–(C.14) here observe structural similarity but call for more indices to accommodate the input scales, such as $\alpha_n^{(h)}$ presiding over the orders of the derivatives of the kinematics variables and $\beta_n^{(h)}$ controlling the exponents of the various denominators $(k_{\pm} + Q_n^{(h)})$. Equipped with those

results, in eq. (C.12), we manage to transform the q_T distribution into its k_+/k_- -factorised formulation as in eq. (2.11), for which the power expansion can be carried out by repeating the procedures in section 2.2, section 2.3, and section 2.4.

However, if the contribution related to \mathbf{T}_B is of one's concern, the small q_T expansion becomes more involved. To see this, it is worth recalling that extra type of propagators appear from the third square bracket of eq. (C.7), which prompts the quadratic dependences on k_{\pm} upon evaluating the scalar products,

$$\left(k + \sum_{l \in X} k_l\right)^2 \equiv (k + k_X)^2 = k_+ m_T^X e^{y_X} + k_- m_T^X e^{-y_X} + m_X^2 - 2\vec{q}_T \cdot \vec{k}_{\perp}^X. \quad (\text{C.15})$$

At this moment, it is not straightforward to derive the factorised form for the squared amplitudes of eq. (C.7) as in eq. (C.12), which therefore defies an immediate implementation of the frameworks in section 2. Promisingly, the power series of the \mathbf{T}_B -induced contributions can also be derived via a set of dynamic regions from the phase space. However, more considerations and efforts should be paid to work out a group of auxiliary cutoffs that are capable of unambiguously and consistently separating all the relevant scales embedded by eq. (C.15). Hence, we postpone this part of discussion to the further investigations.

Open Access. This article is distributed under the terms of the Creative Commons Attribution License ([CC-BY4.0](https://creativecommons.org/licenses/by/4.0/)), which permits any use, distribution and reproduction in any medium, provided the original author(s) and source are credited.

References

- [1] ATLAS collaboration, *Measurement of the transverse momentum and ϕ_{η}^* distributions of Drell-Yan lepton pairs in proton-proton collisions at $\sqrt{s} = 8$ TeV with the ATLAS detector*, *Eur. Phys. J. C* **76** (2016) 291 [[arXiv:1512.02192](https://arxiv.org/abs/1512.02192)] [[INSPIRE](#)].
- [2] ATLAS collaboration, *Measurement of the W-boson mass in pp collisions at $\sqrt{s} = 7$ TeV with the ATLAS detector*, *Eur. Phys. J. C* **78** (2018) 110 [*Erratum ibid.* **78** (2018) 898] [[arXiv:1701.07240](https://arxiv.org/abs/1701.07240)] [[INSPIRE](#)].
- [3] ATLAS collaboration, *Measurement of the transverse momentum distribution of Drell-Yan lepton pairs in proton-proton collisions at $\sqrt{s} = 13$ TeV with the ATLAS detector*, *Eur. Phys. J. C* **80** (2020) 616 [[arXiv:1912.02844](https://arxiv.org/abs/1912.02844)] [[INSPIRE](#)].
- [4] ATLAS collaboration, *A precise measurement of the Z-boson double-differential transverse momentum and rapidity distributions in the full phase space of the decay leptons with the ATLAS experiment at $\sqrt{s} = 8$ TeV*, [arXiv:2309.09318](https://arxiv.org/abs/2309.09318) [[INSPIRE](#)].
- [5] CMS collaboration, *Measurement of the Z boson differential cross section in transverse momentum and rapidity in proton-proton collisions at 8 TeV*, *Phys. Lett. B* **749** (2015) 187 [[arXiv:1504.03511](https://arxiv.org/abs/1504.03511)] [[INSPIRE](#)].
- [6] CMS collaboration, *Measurement of the weak mixing angle using the forward-backward asymmetry of Drell-Yan events in pp collisions at 8 TeV*, *Eur. Phys. J. C* **78** (2018) 701 [[arXiv:1806.00863](https://arxiv.org/abs/1806.00863)] [[INSPIRE](#)].
- [7] CMS collaboration, *Measurement of the differential Drell-Yan cross section in proton-proton collisions at $\sqrt{s} = 13$ TeV*, *JHEP* **12** (2019) 059 [[arXiv:1812.10529](https://arxiv.org/abs/1812.10529)] [[INSPIRE](#)].

- [8] CMS collaboration, *Measurements of differential Z boson production cross sections in proton-proton collisions at $\sqrt{s} = 13$ TeV*, *JHEP* **12** (2019) 061 [[arXiv:1909.04133](#)] [[INSPIRE](#)].
- [9] CMS collaboration, *Measurements of the W boson rapidity, helicity, double-differential cross sections, and charge asymmetry in pp collisions at $\sqrt{s} = 13$ TeV*, *Phys. Rev. D* **102** (2020) 092012 [[arXiv:2008.04174](#)] [[INSPIRE](#)].
- [10] LHCb collaboration, *Measurement of the W boson mass*, *JHEP* **01** (2022) 036 [[arXiv:2109.01113](#)] [[INSPIRE](#)].
- [11] D0 collaboration, *Measurement of the W Boson Mass with the D0 Detector*, *Phys. Rev. Lett.* **108** (2012) 151804 [[arXiv:1203.0293](#)] [[INSPIRE](#)].
- [12] CDF collaboration, *Precise measurement of the W-boson mass with the CDF II detector*, *Phys. Rev. Lett.* **108** (2012) 151803 [[arXiv:1203.0275](#)] [[INSPIRE](#)].
- [13] CDF and D0 collaborations, *Combination of CDF and D0 W-Boson Mass Measurements*, *Phys. Rev. D* **88** (2013) 052018 [[arXiv:1307.7627](#)] [[INSPIRE](#)].
- [14] CDF collaboration, *High-precision measurement of the W boson mass with the CDF II detector*, *Science* **376** (2022) 170 [[INSPIRE](#)].
- [15] ATLAS collaboration, *Fiducial and differential cross sections of Higgs boson production measured in the four-lepton decay channel in pp collisions at $\sqrt{s} = 8$ TeV with the ATLAS detector*, *Phys. Lett. B* **738** (2014) 234 [[arXiv:1408.3226](#)] [[INSPIRE](#)].
- [16] CMS collaboration, *Measurement of differential and integrated fiducial cross sections for Higgs boson production in the four-lepton decay channel in pp collisions at $\sqrt{s} = 7$ and 8 TeV*, *JHEP* **04** (2016) 005 [[arXiv:1512.08377](#)] [[INSPIRE](#)].
- [17] ATLAS collaboration, *Measurement of inclusive and differential cross sections in the $H \rightarrow ZZ^* \rightarrow 4\ell$ decay channel in pp collisions at $\sqrt{s} = 13$ TeV with the ATLAS detector*, *JHEP* **10** (2017) 132 [[arXiv:1708.02810](#)] [[INSPIRE](#)].
- [18] CMS collaboration, *Measurement and interpretation of differential cross sections for Higgs boson production at $\sqrt{s} = 13$ TeV*, *Phys. Lett. B* **792** (2019) 369 [[arXiv:1812.06504](#)] [[INSPIRE](#)].
- [19] ATLAS collaboration, *Measurements of the Higgs boson inclusive and differential fiducial cross sections in the 4ℓ decay channel at $\sqrt{s} = 13$ TeV*, *Eur. Phys. J. C* **80** (2020) 942 [[arXiv:2004.03969](#)] [[INSPIRE](#)].
- [20] ATLAS collaboration, *Measurements of the Higgs boson inclusive and differential fiducial cross-sections in the diphoton decay channel with pp collisions at $\sqrt{s} = 13$ TeV with the ATLAS detector*, *JHEP* **08** (2022) 027 [[arXiv:2202.00487](#)] [[INSPIRE](#)].
- [21] ATLAS collaboration, *Measurement of the total and differential Higgs boson production cross-sections at $\sqrt{s} = 13$ TeV with the ATLAS detector by combining the $H \rightarrow ZZ^* \rightarrow 4\ell$ and $H \rightarrow \gamma\gamma$ decay channels*, *JHEP* **05** (2023) 028 [[arXiv:2207.08615](#)] [[INSPIRE](#)].
- [22] ATLAS collaboration, *Measurements of differential cross sections of Higgs boson production through gluon fusion in the $H \rightarrow WW^* \rightarrow e\nu\mu\nu$ final state at $\sqrt{s} = 13$ TeV with the ATLAS detector*, *Eur. Phys. J. C* **83** (2023) 774 [[arXiv:2301.06822](#)] [[INSPIRE](#)].
- [23] ATLAS collaboration, *Fiducial and differential cross-section measurements for the vector-boson-fusion production of the Higgs boson in the $H \rightarrow WW^* \rightarrow e\nu\mu\nu$ decay channel at 13 TeV with the ATLAS detector*, *Phys. Rev. D* **108** (2023) 072003 [[arXiv:2304.03053](#)] [[INSPIRE](#)].

- [24] CMS collaboration, *Measurements of inclusive and differential cross sections for the Higgs boson production and decay to four-leptons in proton-proton collisions at $\sqrt{s} = 13$ TeV*, *JHEP* **08** (2023) 040 [[arXiv:2305.07532](#)] [[INSPIRE](#)].
- [25] K. Melnikov and F. Petriello, *Electroweak gauge boson production at hadron colliders through $O(\alpha_s^2)$* , *Phys. Rev. D* **74** (2006) 114017 [[hep-ph/0609070](#)] [[INSPIRE](#)].
- [26] S. Catani et al., *Vector boson production at hadron colliders: a fully exclusive QCD calculation at NNLO*, *Phys. Rev. Lett.* **103** (2009) 082001 [[arXiv:0903.2120](#)] [[INSPIRE](#)].
- [27] S. Camarda et al., *DYTurbo: Fast predictions for Drell-Yan processes*, *Eur. Phys. J. C* **80** (2020) 251 [*Erratum ibid.* **80** (2020) 440] [[arXiv:1910.07049](#)] [[INSPIRE](#)].
- [28] C. Duhr, F. Dulat and B. Mistlberger, *Drell-Yan Cross Section to Third Order in the Strong Coupling Constant*, *Phys. Rev. Lett.* **125** (2020) 172001 [[arXiv:2001.07717](#)] [[INSPIRE](#)].
- [29] C. Duhr and B. Mistlberger, *Lepton-pair production at hadron colliders at N^3 LO in QCD*, *JHEP* **03** (2022) 116 [[arXiv:2111.10379](#)] [[INSPIRE](#)].
- [30] X. Chen et al., *Dilepton Rapidity Distribution in Drell-Yan Production to Third Order in QCD*, *Phys. Rev. Lett.* **128** (2022) 052001 [[arXiv:2107.09085](#)] [[INSPIRE](#)].
- [31] X. Chen et al., *Third-Order Fiducial Predictions for Drell-Yan Production at the LHC*, *Phys. Rev. Lett.* **128** (2022) 252001 [[arXiv:2203.01565](#)] [[INSPIRE](#)].
- [32] T. Neumann and J. Campbell, *Fiducial Drell-Yan production at the LHC improved by transverse-momentum resummation at N^4 LL_p+ N^3 LO*, *Phys. Rev. D* **107** (2023) L011506 [[arXiv:2207.07056](#)] [[INSPIRE](#)].
- [33] J. Baglio, C. Duhr, B. Mistlberger and R. Szafron, *Inclusive production cross sections at N^3 LO*, *JHEP* **12** (2022) 066 [[arXiv:2209.06138](#)] [[INSPIRE](#)].
- [34] A. Gehrmann-De Ridder et al., *Precision phenomenology with fiducial cross sections in the triple-differential Drell-Yan process*, *JHEP* **05** (2023) 002 [[arXiv:2301.11827](#)] [[INSPIRE](#)].
- [35] S. Dawson, *Radiative corrections to Higgs boson production*, *Nucl. Phys. B* **359** (1991) 283 [[INSPIRE](#)].
- [36] A. Djouadi, M. Spira and P.M. Zerwas, *Production of Higgs bosons in proton colliders: QCD corrections*, *Phys. Lett. B* **264** (1991) 440 [[INSPIRE](#)].
- [37] M. Spira, A. Djouadi, D. Graudenz and P.M. Zerwas, *Higgs boson production at the LHC*, *Nucl. Phys. B* **453** (1995) 17 [[hep-ph/9504378](#)] [[INSPIRE](#)].
- [38] R.V. Harlander and W.B. Kilgore, *Next-to-next-to-leading order Higgs production at hadron colliders*, *Phys. Rev. Lett.* **88** (2002) 201801 [[hep-ph/0201206](#)] [[INSPIRE](#)].
- [39] C. Anastasiou and K. Melnikov, *Higgs boson production at hadron colliders in NNLO QCD*, *Nucl. Phys. B* **646** (2002) 220 [[hep-ph/0207004](#)] [[INSPIRE](#)].
- [40] V. Ravindran, J. Smith and W.L. van Neerven, *NNLO corrections to the total cross-section for Higgs boson production in hadron hadron collisions*, *Nucl. Phys. B* **665** (2003) 325 [[hep-ph/0302135](#)] [[INSPIRE](#)].
- [41] C. Anastasiou et al., *Higgs Boson Gluon-Fusion Production in QCD at Three Loops*, *Phys. Rev. Lett.* **114** (2015) 212001 [[arXiv:1503.06056](#)] [[INSPIRE](#)].
- [42] C. Anastasiou et al., *High precision determination of the gluon fusion Higgs boson cross-section at the LHC*, *JHEP* **05** (2016) 058 [[arXiv:1602.00695](#)] [[INSPIRE](#)].

- [43] B. Mistlberger, *Higgs boson production at hadron colliders at N^3LO in QCD*, *JHEP* **05** (2018) 028 [[arXiv:1802.00833](#)] [[INSPIRE](#)].
- [44] X. Chen, T. Gehrmann, E.W.N. Glover and M. Jaquier, *Precise QCD predictions for the production of Higgs + jet final states*, *Phys. Lett. B* **740** (2015) 147 [[arXiv:1408.5325](#)] [[INSPIRE](#)].
- [45] R. Boughezal et al., *Higgs boson production in association with a jet at NNLO using jetiness subtraction*, *Phys. Lett. B* **748** (2015) 5 [[arXiv:1505.03893](#)] [[INSPIRE](#)].
- [46] R. Boughezal et al., *Higgs boson production in association with a jet at next-to-next-to-leading order*, *Phys. Rev. Lett.* **115** (2015) 082003 [[arXiv:1504.07922](#)] [[INSPIRE](#)].
- [47] X. Chen et al., *NNLO QCD corrections to Higgs boson production at large transverse momentum*, *JHEP* **10** (2016) 066 [[arXiv:1607.08817](#)] [[INSPIRE](#)].
- [48] F. Caola, K. Melnikov and M. Schulze, *Fiducial cross sections for Higgs boson production in association with a jet at next-to-next-to-leading order in QCD*, *Phys. Rev. D* **92** (2015) 074032 [[arXiv:1508.02684](#)] [[INSPIRE](#)].
- [49] L. Cieri et al., *Higgs boson production at the LHC using the q_T subtraction formalism at N^3LO QCD*, *JHEP* **02** (2019) 096 [[arXiv:1807.11501](#)] [[INSPIRE](#)].
- [50] G. Billis et al., *Higgs p_T Spectrum and Total Cross Section with Fiducial Cuts at Third Resummed and Fixed Order in QCD*, *Phys. Rev. Lett.* **127** (2021) 072001 [[arXiv:2102.08039](#)] [[INSPIRE](#)].
- [51] X. Chen et al., *Top-quark mass effects in H +jet and $H + 2$ jets production*, *JHEP* **03** (2022) 096 [[arXiv:2110.06953](#)] [[INSPIRE](#)].
- [52] X. Chen et al., *Fully Differential Higgs Boson Production to Third Order in QCD*, *Phys. Rev. Lett.* **127** (2021) 072002 [[arXiv:2102.07607](#)] [[INSPIRE](#)].
- [53] P. Cal, R. von Kuk, M.A. Lim and F.J. Tackmann, *The q_T spectrum for Higgs production via heavy quark annihilation at $N^3LL' + aN^3LO$* , [arXiv:2306.16458](#) [[INSPIRE](#)].
- [54] Y. Li and F. Petriello, *Combining QCD and electroweak corrections to dilepton production in FEWZ*, *Phys. Rev. D* **86** (2012) 094034 [[arXiv:1208.5967](#)] [[INSPIRE](#)].
- [55] S. Dittmaier, A. Huss and C. Schwinn, *Dominant mixed QCD-electroweak $O(\alpha_s\alpha)$ corrections to Drell-Yan processes in the resonance region*, *Nucl. Phys. B* **904** (2016) 216 [[arXiv:1511.08016](#)] [[INSPIRE](#)].
- [56] R. Bonciani et al., *NNLO QCD \times EW corrections to Z production in the $q\bar{q}$ channel*, *Phys. Rev. D* **101** (2020) 031301 [[arXiv:1911.06200](#)] [[INSPIRE](#)].
- [57] S. Dittmaier, T. Schmidt and J. Schwarz, *Mixed NNLO QCD \times electroweak corrections of $\mathcal{O}(N_f\alpha_s\alpha)$ to single- W/Z production at the LHC*, *JHEP* **12** (2020) 201 [[arXiv:2009.02229](#)] [[INSPIRE](#)].
- [58] R. Bonciani et al., *Mixed Strong-Electroweak Corrections to the Drell-Yan Process*, *Phys. Rev. Lett.* **128** (2022) 012002 [[arXiv:2106.11953](#)] [[INSPIRE](#)].
- [59] T. Armadillo et al., *Two-loop mixed QCD-EW corrections to neutral current Drell-Yan*, *JHEP* **05** (2022) 072 [[arXiv:2201.01754](#)] [[INSPIRE](#)].
- [60] F. Buccioni et al., *Mixed QCD-electroweak corrections to dilepton production at the LHC in the high invariant mass region*, *JHEP* **06** (2022) 022 [[arXiv:2203.11237](#)] [[INSPIRE](#)].
- [61] S. Actis, G. Passarino, C. Sturm and S. Uccirati, *NLO Electroweak Corrections to Higgs Boson Production at Hadron Colliders*, *Phys. Lett. B* **670** (2008) 12 [[arXiv:0809.1301](#)] [[INSPIRE](#)].

- [62] C. Anastasiou, R. Boughezal and F. Petriello, *Mixed QCD-electroweak corrections to Higgs boson production in gluon fusion*, *JHEP* **04** (2009) 003 [[arXiv:0811.3458](#)] [[INSPIRE](#)].
- [63] J.C. Collins and D.E. Soper, *Back-To-Back Jets in QCD*, *Nucl. Phys. B* **193** (1981) 381 [*Erratum ibid.* **213** (1983) 545] [[INSPIRE](#)].
- [64] J.C. Collins and D.E. Soper, *Back-To-Back Jets: Fourier Transform from B to K-Transverse*, *Nucl. Phys. B* **197** (1982) 446 [[INSPIRE](#)].
- [65] J.C. Collins, D.E. Soper and G.F. Sterman, *Transverse Momentum Distribution in Drell-Yan Pair and W and Z Boson Production*, *Nucl. Phys. B* **250** (1985) 199 [[INSPIRE](#)].
- [66] S. Catani, D. de Florian and M. Grazzini, *Universality of nonleading logarithmic contributions in transverse momentum distributions*, *Nucl. Phys. B* **596** (2001) 299 [[hep-ph/0008184](#)] [[INSPIRE](#)].
- [67] G. Bozzi, S. Catani, D. de Florian and M. Grazzini, *Transverse-momentum resummation and the spectrum of the Higgs boson at the LHC*, *Nucl. Phys. B* **737** (2006) 73 [[hep-ph/0508068](#)] [[INSPIRE](#)].
- [68] G. Bozzi, S. Catani, D. de Florian and M. Grazzini, *Higgs boson production at the LHC: Transverse-momentum resummation and rapidity dependence*, *Nucl. Phys. B* **791** (2008) 1 [[arXiv:0705.3887](#)] [[INSPIRE](#)].
- [69] M.A. Ebert and F.J. Tackmann, *Resummation of Transverse Momentum Distributions in Distribution Space*, *JHEP* **02** (2017) 110 [[arXiv:1611.08610](#)] [[INSPIRE](#)].
- [70] P.F. Monni, E. Re and P. Torrielli, *Higgs Transverse-Momentum Resummation in Direct Space*, *Phys. Rev. Lett.* **116** (2016) 242001 [[arXiv:1604.02191](#)] [[INSPIRE](#)].
- [71] W. Bizoń et al., *Momentum-space resummation for transverse observables and the Higgs p_{\perp} at $N^3LL+NNLO$* , *JHEP* **02** (2018) 108 [[arXiv:1705.09127](#)] [[INSPIRE](#)].
- [72] W. Bizoń et al., *The transverse momentum spectrum of weak gauge bosons at $N^3LL + NNLO$* , *Eur. Phys. J. C* **79** (2019) 868 [[arXiv:1905.05171](#)] [[INSPIRE](#)].
- [73] W. Bizoń et al., *Fiducial distributions in Higgs and Drell-Yan production at $N^3LL+NNLO$* , *JHEP* **12** (2018) 132 [[arXiv:1805.05916](#)] [[INSPIRE](#)].
- [74] T. Becher and M. Neubert, *Drell-Yan Production at Small q_T , Transverse Parton Distributions and the Collinear Anomaly*, *Eur. Phys. J. C* **71** (2011) 1665 [[arXiv:1007.4005](#)] [[INSPIRE](#)].
- [75] M.G. Echevarria, A. Idilbi and I. Scimemi, *Factorization Theorem For Drell-Yan At Low q_T And Transverse Momentum Distributions On-The-Light-Cone*, *JHEP* **07** (2012) 002 [[arXiv:1111.4996](#)] [[INSPIRE](#)].
- [76] T. Becher and G. Bell, *Analytic Regularization in Soft-Collinear Effective Theory*, *Phys. Lett. B* **713** (2012) 41 [[arXiv:1112.3907](#)] [[INSPIRE](#)].
- [77] J.-Y. Chiu, A. Jain, D. Neill and I.Z. Rothstein, *The Rapidity Renormalization Group*, *Phys. Rev. Lett.* **108** (2012) 151601 [[arXiv:1104.0881](#)] [[INSPIRE](#)].
- [78] J.-Y. Chiu, A. Jain, D. Neill and I.Z. Rothstein, *A Formalism for the Systematic Treatment of Rapidity Logarithms in Quantum Field Theory*, *JHEP* **05** (2012) 084 [[arXiv:1202.0814](#)] [[INSPIRE](#)].
- [79] Y. Li, D. Neill and H.X. Zhu, *An exponential regulator for rapidity divergences*, *Nucl. Phys. B* **960** (2020) 115193 [[arXiv:1604.00392](#)] [[INSPIRE](#)].
- [80] Y. Li and H.X. Zhu, *Bootstrapping Rapidity Anomalous Dimensions for Transverse-Momentum Resummation*, *Phys. Rev. Lett.* **118** (2017) 022004 [[arXiv:1604.01404](#)] [[INSPIRE](#)].

- [81] G. Bozzi et al., *Production of Drell-Yan lepton pairs in hadron collisions: Transverse-momentum resummation at next-to-next-to-leading logarithmic accuracy*, *Phys. Lett. B* **696** (2011) 207 [[arXiv:1007.2351](#)] [[INSPIRE](#)].
- [82] T. Becher, M. Neubert and D. Wilhelm, *Electroweak Gauge-Boson Production at Small q_T : Infrared Safety from the Collinear Anomaly*, *JHEP* **02** (2012) 124 [[arXiv:1109.6027](#)] [[INSPIRE](#)].
- [83] A. Banfi, M. Dasgupta and S. Marzani, *QCD predictions for new variables to study dilepton transverse momenta at hadron colliders*, *Phys. Lett. B* **701** (2011) 75 [[arXiv:1102.3594](#)] [[INSPIRE](#)].
- [84] A. Banfi, M. Dasgupta, S. Marzani and L. Tomlinson, *Probing the low transverse momentum domain of Z production with novel variables*, *JHEP* **01** (2012) 044 [[arXiv:1110.4009](#)] [[INSPIRE](#)].
- [85] A. Banfi, M. Dasgupta, S. Marzani and L. Tomlinson, *Predictions for Drell-Yan ϕ^* and Q_T observables at the LHC*, *Phys. Lett. B* **715** (2012) 152 [[arXiv:1205.4760](#)] [[INSPIRE](#)].
- [86] S. Catani, D. de Florian, G. Ferrera and M. Grazzini, *Vector boson production at hadron colliders: transverse-momentum resummation and leptonic decay*, *JHEP* **12** (2015) 047 [[arXiv:1507.06937](#)] [[INSPIRE](#)].
- [87] I. Scimemi and A. Vladimirov, *Analysis of vector boson production within TMD factorization*, *Eur. Phys. J. C* **78** (2018) 89 [[arXiv:1706.01473](#)] [[INSPIRE](#)].
- [88] A. Bacchetta et al., *Transverse-momentum-dependent parton distributions up to N^3LL from Drell-Yan data*, *JHEP* **07** (2020) 117 [[arXiv:1912.07550](#)] [[INSPIRE](#)].
- [89] T. Becher and T. Neumann, *Fiducial q_T resummation of color-singlet processes at $N^3LL+NNLO$* , *JHEP* **03** (2021) 199 [[arXiv:2009.11437](#)] [[INSPIRE](#)].
- [90] M.A. Ebert, J.K.L. Michel, I.W. Stewart and F.J. Tackmann, *Drell-Yan q_T resummation of fiducial power corrections at N^3LL* , *JHEP* **04** (2021) 102 [[arXiv:2006.11382](#)] [[INSPIRE](#)].
- [91] E. Re, L. Rottoli and P. Torrielli, *Fiducial Higgs and Drell-Yan distributions at $N^3LL'+NNLO$ with RadISH*, [arXiv:2104.07509](#) [[DOI:10.1007/JHEP09\(2021\)108](#)] [[INSPIRE](#)].
- [92] S. Camarda, L. Cieri and G. Ferrera, *Drell-Yan lepton-pair production: q_T resummation at N^3LL accuracy and fiducial cross sections at N^3LO* , *Phys. Rev. D* **104** (2021) L111503 [[arXiv:2103.04974](#)] [[INSPIRE](#)].
- [93] W.-L. Ju and M. Schönherr, *The q_T and $\Delta\phi$ spectra in W and Z production at the LHC at $N^3LL'+N^2LO$* , *JHEP* **10** (2021) 088 [[arXiv:2106.11260](#)] [[INSPIRE](#)].
- [94] S. Camarda, L. Cieri and G. Ferrera, *Drell-Yan lepton-pair production: q_T resummation at N^4LL accuracy*, *Phys. Lett. B* **845** (2023) 138125 [[arXiv:2303.12781](#)] [[INSPIRE](#)].
- [95] V. Moos, I. Scimemi, A. Vladimirov and P. Zurita, *Extraction of unpolarized transverse momentum distributions from fit of Drell-Yan data at N^4LL* , [arXiv:2305.07473](#) [[INSPIRE](#)].
- [96] A. Belyaev, P.M. Nadolsky and C.-P. Yuan, *Transverse momentum resummation for Higgs boson produced via $b\bar{b}$ fusion at hadron colliders*, *JHEP* **04** (2006) 004 [[hep-ph/0509100](#)] [[INSPIRE](#)].
- [97] T. Becher, M. Neubert and D. Wilhelm, *Higgs-Boson Production at Small Transverse Momentum*, *JHEP* **05** (2013) 110 [[arXiv:1212.2621](#)] [[INSPIRE](#)].
- [98] D. Neill, I.Z. Rothstein and V. Vaidya, *The Higgs Transverse Momentum Distribution at NNLL and its Theoretical Errors*, *JHEP* **12** (2015) 097 [[arXiv:1503.00005](#)] [[INSPIRE](#)].

- [99] X. Chen et al., *Precise QCD Description of the Higgs Boson Transverse Momentum Spectrum*, *Phys. Lett. B* **788** (2019) 425 [[arXiv:1805.00736](#)] [[INSPIRE](#)].
- [100] D. Gutierrez-Reyes, S. Leal-Gomez, I. Scimemi and A. Vladimirov, *Linearly polarized gluons at next-to-next-to leading order and the Higgs transverse momentum distribution*, *JHEP* **11** (2019) 121 [[arXiv:1907.03780](#)] [[INSPIRE](#)].
- [101] R.V. Harlander, A. Tripathi and M. Wiesemann, *Higgs production in bottom quark annihilation: Transverse momentum distribution at NNLO+NNLL*, *Phys. Rev. D* **90** (2014) 015017 [[arXiv:1403.7196](#)] [[INSPIRE](#)].
- [102] I. Balitsky and A. Tarasov, *Power corrections to TMD factorization for Z-boson production*, *JHEP* **05** (2018) 150 [[arXiv:1712.09389](#)] [[INSPIRE](#)].
- [103] I. Balitsky, *Gauge-invariant TMD factorization for Drell-Yan hadronic tensor at small x* , *JHEP* **05** (2021) 046 [[arXiv:2012.01588](#)] [[INSPIRE](#)].
- [104] I. Balitsky, *Drell-Yan angular lepton distributions at small x from TMD factorization*, *JHEP* **09** (2021) 022 [[arXiv:2105.13391](#)] [[INSPIRE](#)].
- [105] I. Balitsky and A. Tarasov, *Higher-twist corrections to gluon TMD factorization*, *JHEP* **07** (2017) 095 [[arXiv:1706.01415](#)] [[INSPIRE](#)].
- [106] A. Vladimirov, V. Moos and I. Scimemi, *Transverse momentum dependent operator expansion at next-to-leading power*, *JHEP* **01** (2022) 110 [[arXiv:2109.09771](#)] [[INSPIRE](#)].
- [107] M.A. Ebert, A. Gao and I.W. Stewart, *Factorization for azimuthal asymmetries in SIDIS at next-to-leading power*, *JHEP* **06** (2022) 007 [*Erratum ibid.* **07** (2023) 096] [[arXiv:2112.07680](#)] [[INSPIRE](#)].
- [108] L. Gamberg et al., *Transverse-momentum-dependent factorization at next-to-leading power*, [arXiv:2211.13209](#) [[INSPIRE](#)].
- [109] S. Rodini and A. Vladimirov, *Factorization for quasi-TMD distributions of sub-leading power*, *JHEP* **09** (2023) 117 [[arXiv:2211.04494](#)] [[INSPIRE](#)].
- [110] S. Rodini and A. Vladimirov, *Transverse momentum dependent factorization for SIDIS at next-to-leading power*, [arXiv:2306.09495](#) [[INSPIRE](#)].
- [111] A. Vladimirov, *Kinematic power corrections in TMD factorization theorem*, *JHEP* **12** (2023) 008 [[arXiv:2307.13054](#)] [[INSPIRE](#)].
- [112] S. Rodini, A.C. Alvaro and B. Pasquini, *Collinear matching for next-to-leading power transverse-momentum distributions*, *Phys. Lett. B* **845** (2023) 138163 [[arXiv:2306.15052](#)] [[INSPIRE](#)].
- [113] M.A. Ebert et al., *Subleading power rapidity divergences and power corrections for q_T* , *JHEP* **04** (2019) 123 [[arXiv:1812.08189](#)] [[INSPIRE](#)].
- [114] M. Inglis-Whalen, M. Luke, J. Roy and A. Spourdalakis, *Factorization of power corrections in the Drell-Yan process in EFT*, *Phys. Rev. D* **104** (2021) 076018 [[arXiv:2105.09277](#)] [[INSPIRE](#)].
- [115] M. Inglis-Whalen, *Power Corrections and Rapidity Logarithms in Soft-collinear Effective Theory*, Ph.D. thesis, Toronto University, Toronto, Ontario M5S 1A7, Canada (2022) [[INSPIRE](#)].
- [116] C. Oleari and M. Rocco, *Power corrections in a transverse-momentum cut for vector-boson production at NNLO: the qg -initiated real-virtual contribution*, *Eur. Phys. J. C* **81** (2021) 183 [[arXiv:2012.10538](#)] [[INSPIRE](#)].

- [117] L. Cieri, C. Oleari and M. Rocco, *Higher-order power corrections in a transverse-momentum cut for colour-singlet production at NLO*, *Eur. Phys. J. C* **79** (2019) 852 [[arXiv:1906.09044](#)] [[INSPIRE](#)].
- [118] S. Camarda, L. Cieri and G. Ferrera, *Fiducial perturbative power corrections within the q_T subtraction formalism*, *Eur. Phys. J. C* **82** (2022) 575 [[arXiv:2111.14509](#)] [[INSPIRE](#)].
- [119] M.A. Ebert and F.J. Tackmann, *Impact of isolation and fiducial cuts on q_T and N -jettiness subtractions*, *JHEP* **03** (2020) 158 [[arXiv:1911.08486](#)] [[INSPIRE](#)].
- [120] Z.L. Liu, M. Neubert, M. Schnubel and X. Wang, *Factorization at next-to-leading power and endpoint divergences in $gg \rightarrow h$ production*, *JHEP* **06** (2023) 183 [[arXiv:2212.10447](#)] [[INSPIRE](#)].
- [121] Z.L. Liu, B. Mecaj, M. Neubert and X. Wang, *Factorization at subleading power, Sudakov resummation, and endpoint divergences in soft-collinear effective theory*, *Phys. Rev. D* **104** (2021) 014004 [[arXiv:2009.04456](#)] [[INSPIRE](#)].
- [122] Z.L. Liu et al., *Renormalization and Scale Evolution of the Soft-Quark Soft Function*, *JHEP* **07** (2020) 104 [[arXiv:2005.03013](#)] [[INSPIRE](#)].
- [123] Z.L. Liu and M. Neubert, *Two-Loop Radiative Jet Function for Exclusive B -Meson and Higgs Decays*, *JHEP* **06** (2020) 060 [[arXiv:2003.03393](#)] [[INSPIRE](#)].
- [124] Z.L. Liu and M. Neubert, *Factorization at subleading power and endpoint-divergent convolutions in $h \rightarrow \gamma\gamma$ decay*, *JHEP* **04** (2020) 033 [[arXiv:1912.08818](#)] [[INSPIRE](#)].
- [125] T. Liu, S. Modi and A.A. Penin, *Higgs boson production and quark scattering amplitudes at high energy through the next-to-next-to-leading power in quark mass*, *JHEP* **02** (2022) 170 [[arXiv:2111.01820](#)] [[INSPIRE](#)].
- [126] T. Liu and A. Penin, *High-Energy Limit of Mass-Suppressed Amplitudes in Gauge Theories*, *JHEP* **11** (2018) 158 [[arXiv:1809.04950](#)] [[INSPIRE](#)].
- [127] T. Liu and A.A. Penin, *High-Energy Limit of QCD beyond the Sudakov Approximation*, *Phys. Rev. Lett.* **119** (2017) 262001 [[arXiv:1709.01092](#)] [[INSPIRE](#)].
- [128] L. Buonocore, M. Grazzini, F. Guadagni and L. Rottoli, *Subleading power corrections for event shape variables in e^+e^- annihilation*, [arXiv:2311.12768](#) [[INSPIRE](#)].
- [129] N. Agarwal et al., *Next-to-leading power corrections to the event shape variables*, [arXiv:2306.17601](#) [[INSPIRE](#)].
- [130] M. van Beekveld, W. Beenakker, E. Laenen and C.D. White, *Next-to-leading power threshold effects for inclusive and exclusive processes with final state jets*, *JHEP* **03** (2020) 106 [[arXiv:1905.08741](#)] [[INSPIRE](#)].
- [131] H. Chen, X. Zhou and H.X. Zhu, *Power corrections to energy flow correlations from large spin perturbation*, *JHEP* **10** (2023) 132 [[arXiv:2301.03616](#)] [[INSPIRE](#)].
- [132] M.A. Ebert et al., *Power Corrections for N -Jettiness Subtractions at $\mathcal{O}(\alpha_s)$* , *JHEP* **12** (2018) 084 [[arXiv:1807.10764](#)] [[INSPIRE](#)].
- [133] I. Moulton, I.W. Stewart, G. Vita and H.X. Zhu, *First Subleading Power Resummation for Event Shapes*, *JHEP* **08** (2018) 013 [[arXiv:1804.04665](#)] [[INSPIRE](#)].
- [134] I. Moulton et al., *N -jettiness subtractions for $gg \rightarrow H$ at subleading power*, *Phys. Rev. D* **97** (2018) 014013 [[arXiv:1710.03227](#)] [[INSPIRE](#)].
- [135] I. Moulton et al., *Subleading Power Corrections for N -Jettiness Subtractions*, *Phys. Rev. D* **95** (2017) 074023 [[arXiv:1612.00450](#)] [[INSPIRE](#)].

- [136] S. Pal and S. Seth, *On H -jet production at NLP accuracy*, [arXiv:2309.08343](#) [INSPIRE].
- [137] R. van Bijleveld, E. Laenen, L. Vernazza and G. Wang, *Next-to-leading power resummed rapidity distributions near threshold for Drell-Yan and diphoton production*, *JHEP* **10** (2023) 126 [[arXiv:2308.00230](#)] [INSPIRE].
- [138] M. van Beekveld, E. Laenen, J. Sinninghe Damsté and L. Vernazza, *Next-to-leading power threshold corrections for finite order and resummed colour-singlet cross sections*, *JHEP* **05** (2021) 114 [[arXiv:2101.07270](#)] [INSPIRE].
- [139] E. Laenen et al., *Towards all-order factorization of QED amplitudes at next-to-leading power*, *Phys. Rev. D* **103** (2021) 034022 [[arXiv:2008.01736](#)] [INSPIRE].
- [140] M. van Beekveld et al., *Next-to-leading power threshold effects for resummed prompt photon production*, *Phys. Rev. D* **100** (2019) 056009 [[arXiv:1905.11771](#)] [INSPIRE].
- [141] D. Bonocore et al., *Non-abelian factorisation for next-to-leading-power threshold logarithms*, *JHEP* **12** (2016) 121 [[arXiv:1610.06842](#)] [INSPIRE].
- [142] D. Bonocore et al., *A factorization approach to next-to-leading-power threshold logarithms*, *JHEP* **06** (2015) 008 [[arXiv:1503.05156](#)] [INSPIRE].
- [143] D. Bonocore et al., *The method of regions and next-to-soft corrections in Drell-Yan production*, *Phys. Lett. B* **742** (2015) 375 [[arXiv:1410.6406](#)] [INSPIRE].
- [144] E. Laenen, L. Magnea, G. Stavenga and C.D. White, *Next-to-Eikonal Corrections to Soft Gluon Radiation: A Diagrammatic Approach*, *JHEP* **01** (2011) 141 [[arXiv:1010.1860](#)] [INSPIRE].
- [145] E. Laenen, G. Stavenga and C.D. White, *Path integral approach to eikonal and next-to-eikonal exponentiation*, *JHEP* **03** (2009) 054 [[arXiv:0811.2067](#)] [INSPIRE].
- [146] E. Laenen, L. Magnea and G. Stavenga, *On next-to-eikonal corrections to threshold resummation for the Drell-Yan and DIS cross sections*, *Phys. Lett. B* **669** (2008) 173 [[arXiv:0807.4412](#)] [INSPIRE].
- [147] A. Broggio, S. Jaskiewicz and L. Vernazza, *Threshold factorization of the Drell-Yan quark-gluon channel and two-loop soft function at next-to-leading power*, *JHEP* **12** (2023) 028 [[arXiv:2306.06037](#)] [INSPIRE].
- [148] M. Beneke et al., *Leading-logarithmic threshold resummation of the Drell-Yan process at next-to-leading power*, *JHEP* **03** (2019) 043 [[arXiv:1809.10631](#)] [INSPIRE].
- [149] M. Beneke et al., *Next-to-leading power endpoint factorization and resummation for off-diagonal “gluon” thrust*, *JHEP* **07** (2022) 144 [[arXiv:2205.04479](#)] [INSPIRE].
- [150] M. Beneke, A. Broggio, S. Jaskiewicz and L. Vernazza, *Threshold factorization of the Drell-Yan process at next-to-leading power*, *JHEP* **07** (2020) 078 [[arXiv:1912.01585](#)] [INSPIRE].
- [151] M. Beneke et al., *Leading-logarithmic threshold resummation of Higgs production in gluon fusion at next-to-leading power*, *JHEP* **01** (2020) 094 [[arXiv:1910.12685](#)] [INSPIRE].
- [152] D. Bonocore and A. Kulesza, *Soft photon bremsstrahlung at next-to-leading power*, *Phys. Lett. B* **833** (2022) 137325 [[arXiv:2112.08329](#)] [INSPIRE].
- [153] A. Bhattacharya, M.C. Kumar, P. Mathews and V. Ravindran, *Next-to-soft-virtual resummed prediction for pseudoscalar Higgs boson production at NNLO+ $\overline{\text{NNLL}}$* , *Phys. Rev. D* **105** (2022) 116015 [[arXiv:2112.02341](#)] [INSPIRE].
- [154] A. A H et al., *Next-to-soft corrections for Drell-Yan and Higgs boson rapidity distributions beyond N^3 LO*, *Phys. Rev. D* **103** (2021) L111502 [[arXiv:2010.00079](#)] [INSPIRE].

- [155] N. Bahjat-Abbas et al., *Diagrammatic resummation of leading-logarithmic threshold effects at next-to-leading power*, *JHEP* **11** (2019) 002 [[arXiv:1905.13710](#)] [[INSPIRE](#)].
- [156] R. Balsach, D. Bonocore and A. Kulesza, *Soft-photon spectra and the LBK theorem*, [arXiv:2312.11386](#) [[INSPIRE](#)].
- [157] T. Engel, *Multiple soft-photon emission at next-to-leading power to all orders*, *JHEP* **03** (2024) 004 [[arXiv:2311.17612](#)] [[INSPIRE](#)].
- [158] T. Engel, *The LBK theorem to all orders*, *JHEP* **07** (2023) 177 [[arXiv:2304.11689](#)] [[INSPIRE](#)].
- [159] J.C. Collins, *Proof of factorization for diffractive hard scattering*, *Phys. Rev. D* **57** (1998) 3051 [*Erratum ibid.* **61** (2000) 019902] [[hep-ph/9709499](#)] [[INSPIRE](#)].
- [160] J.C. Collins and A. Metz, *Universality of soft and collinear factors in hard-scattering factorization*, *Phys. Rev. Lett.* **93** (2004) 252001 [[hep-ph/0408249](#)] [[INSPIRE](#)].
- [161] J.R. Gaunt, *Glauber Gluons and Multiple Parton Interactions*, *JHEP* **07** (2014) 110 [[arXiv:1405.2080](#)] [[INSPIRE](#)].
- [162] M.D. Schwartz, K. Yan and H.X. Zhu, *Factorization Violation and Scale Invariance*, *Phys. Rev. D* **97** (2018) 096017 [[arXiv:1801.01138](#)] [[INSPIRE](#)].
- [163] A.V. Manohar and I.W. Stewart, *The Zero-Bin and Mode Factorization in Quantum Field Theory*, *Phys. Rev. D* **76** (2007) 074002 [[hep-ph/0605001](#)] [[INSPIRE](#)].
- [164] A. Idilbi and T. Mehen, *Demonstration of the equivalence of soft and zero-bin subtractions*, *Phys. Rev. D* **76** (2007) 094015 [[arXiv:0707.1101](#)] [[INSPIRE](#)].
- [165] A. Idilbi and T. Mehen, *On the equivalence of soft and zero-bin subtractions*, *Phys. Rev. D* **75** (2007) 114017 [[hep-ph/0702022](#)] [[INSPIRE](#)].
- [166] J.-Y. Chiu et al., *Soft-Collinear Factorization and Zero-Bin Subtractions*, *Phys. Rev. D* **79** (2009) 053007 [[arXiv:0901.1332](#)] [[INSPIRE](#)].
- [167] X.-D. Ji, J.-P. Ma and F. Yuan, *QCD factorization for spin-dependent cross sections in DIS and Drell-Yan processes at low transverse momentum*, *Phys. Lett. B* **597** (2004) 299 [[hep-ph/0405085](#)] [[INSPIRE](#)].
- [168] X.-D. Ji, J.-P. Ma and F. Yuan, *QCD factorization for semi-inclusive deep-inelastic scattering at low transverse momentum*, *Phys. Rev. D* **71** (2005) 034005 [[hep-ph/0404183](#)] [[INSPIRE](#)].
- [169] R. Goerke and M. Luke, *Power Counting and Modes in SCET*, *JHEP* **02** (2018) 147 [[arXiv:1711.09136](#)] [[INSPIRE](#)].
- [170] M. Inglis-Whalen, M. Luke and A. Spourdalakis, *Rapidity logarithms in SCET without modes*, *Nucl. Phys. A* **1014** (2021) 122260 [[arXiv:2005.13063](#)] [[INSPIRE](#)].
- [171] M.G. Echevarria, I. Scimemi and A. Vladimirov, *Universal transverse momentum dependent soft function at NNLO*, *Phys. Rev. D* **93** (2016) 054004 [[arXiv:1511.05590](#)] [[INSPIRE](#)].
- [172] M.G. Echevarria, I. Scimemi and A. Vladimirov, *Transverse momentum dependent fragmentation function at next-to-next-to-leading order*, *Phys. Rev. D* **93** (2016) 011502 [*Erratum ibid.* **94** (2016) 099904] [[arXiv:1509.06392](#)] [[INSPIRE](#)].
- [173] M.-X. Luo et al., *Transverse Parton Distribution and Fragmentation Functions at NNLO: the Quark Case*, *JHEP* **10** (2019) 083 [[arXiv:1908.03831](#)] [[INSPIRE](#)].
- [174] M.-X. Luo, T.-Z. Yang, H.X. Zhu and Y.J. Zhu, *Transverse Parton Distribution and Fragmentation Functions at NNLO: the Gluon Case*, *JHEP* **01** (2020) 040 [[arXiv:1909.13820](#)] [[INSPIRE](#)].

- [175] M.-X. Luo, T.-Z. Yang, H.X. Zhu and Y.J. Zhu, *Quark Transverse Parton Distribution at the Next-to-Next-to-Next-to-Leading Order*, *Phys. Rev. Lett.* **124** (2020) 092001 [[arXiv:1912.05778](#)] [[INSPIRE](#)].
- [176] M.-X. Luo, T.-Z. Yang, H.X. Zhu and Y.J. Zhu, *Unpolarized quark and gluon TMD PDFs and FFs at N^3LO* , *JHEP* **06** (2021) 115 [[arXiv:2012.03256](#)] [[INSPIRE](#)].
- [177] B. Jantzen, *Foundation and generalization of the expansion by regions*, *JHEP* **12** (2011) 076 [[arXiv:1111.2589](#)] [[INSPIRE](#)].
- [178] I. Moulton, G. Vita and K. Yan, *Subleading power resummation of rapidity logarithms: the energy-energy correlator in $\mathcal{N} = 4$ SYM*, *JHEP* **07** (2020) 005 [[arXiv:1912.02188](#)] [[INSPIRE](#)].
- [179] M.G. Echevarria, I. Scimemi and A. Vladimirov, *Unpolarized Transverse Momentum Dependent Parton Distribution and Fragmentation Functions at next-to-next-to-leading order*, *JHEP* **09** (2016) 004 [[arXiv:1604.07869](#)] [[INSPIRE](#)].
- [180] J.C. Collins, D.E. Soper and G.F. Sterman, *Factorization of Hard Processes in QCD*, *Adv. Ser. Direct. High Energy Phys.* **5** (1989) 1 [[hep-ph/0409313](#)] [[INSPIRE](#)].
- [181] H. Kluberg-Stern and J.B. Zuber, *Ward Identities and Some Clues to the Renormalization of Gauge Invariant Operators*, *Phys. Rev. D* **12** (1975) 467 [[INSPIRE](#)].
- [182] N.K. Nielsen, *Gauge Invariance and Broken Conformal Symmetry*, *Nucl. Phys. B* **97** (1975) 527 [[INSPIRE](#)].
- [183] F. Wilczek, *Decays of Heavy Vector Mesons Into Higgs Particles*, *Phys. Rev. Lett.* **39** (1977) 1304 [[INSPIRE](#)].
- [184] N.K. Nielsen, *The Energy Momentum Tensor in a Nonabelian Quark Gluon Theory*, *Nucl. Phys. B* **120** (1977) 212 [[INSPIRE](#)].
- [185] T. Inami, T. Kubota and Y. Okada, *Effective Gauge Theory and the Effect of Heavy Quarks in Higgs Boson Decays*, *Z. Phys. C* **18** (1983) 69 [[INSPIRE](#)].
- [186] V.P. Spiridonov, *Anomalous Dimension of $G_{\mu\nu}^2$ and β Function*, [[INSPIRE](#)].
- [187] K.G. Chetyrkin, B.A. Kniehl and M. Steinhauser, *Decoupling relations to $O(\alpha_s^3)$ and their connection to low-energy theorems*, *Nucl. Phys. B* **510** (1998) 61 [[hep-ph/9708255](#)] [[INSPIRE](#)].
- [188] A. Djouadi, J. Kalinowski and P.M. Zerwas, *Higgs radiation off top quarks in high-energy e^+e^- colliders*, *Z. Phys. C* **54** (1992) 255 [[INSPIRE](#)].
- [189] K.G. Chetyrkin, B.A. Kniehl and M. Steinhauser, *Hadronic Higgs decay to order α_s^4* , *Phys. Rev. Lett.* **79** (1997) 353 [[hep-ph/9705240](#)] [[INSPIRE](#)].
- [190] K.G. Chetyrkin, J.H. Kühn and C. Sturm, *QCD decoupling at four loops*, *Nucl. Phys. B* **744** (2006) 121 [[hep-ph/0512060](#)] [[INSPIRE](#)].
- [191] Y. Schroder and M. Steinhauser, *Four-loop decoupling relations for the strong coupling*, *JHEP* **01** (2006) 051 [[hep-ph/0512058](#)] [[INSPIRE](#)].
- [192] P.A. Baikov, K.G. Chetyrkin and J.H. Kühn, *Five-Loop Running of the QCD coupling constant*, *Phys. Rev. Lett.* **118** (2017) 082002 [[arXiv:1606.08659](#)] [[INSPIRE](#)].
- [193] V. Ravindran, J. Smith and W.L. Van Neerven, *Next-to-leading order QCD corrections to differential distributions of Higgs boson production in hadron hadron collisions*, *Nucl. Phys. B* **634** (2002) 247 [[hep-ph/0201114](#)] [[INSPIRE](#)].
- [194] C.J. Glosser and C.R. Schmidt, *Next-to-leading corrections to the Higgs boson transverse momentum spectrum in gluon fusion*, *JHEP* **12** (2002) 016 [[hep-ph/0209248](#)] [[INSPIRE](#)].

- [195] S. Catani and M. Grazzini, *An NNLO subtraction formalism in hadron collisions and its application to Higgs boson production at the LHC*, *Phys. Rev. Lett.* **98** (2007) 222002 [[hep-ph/0703012](#)] [[INSPIRE](#)].
- [196] S. Catani et al., *Vector boson production at hadron colliders: hard-collinear coefficients at the NNLO*, *Eur. Phys. J. C* **72** (2012) 2195 [[arXiv:1209.0158](#)] [[INSPIRE](#)].
- [197] S. Catani and P.K. Dhani, *Collinear functions for QCD resummations*, *JHEP* **03** (2023) 200 [[arXiv:2208.05840](#)] [[INSPIRE](#)].
- [198] S. Catani and M. Grazzini, *Higgs Boson Production at Hadron Colliders: Hard-Collinear Coefficients at the NNLO*, *Eur. Phys. J. C* **72** (2012) 2013 [Erratum *ibid.* **72** (2012) 2132] [[arXiv:1106.4652](#)] [[INSPIRE](#)].
- [199] M.A. Ebert, B. Mistlberger and G. Vita, *Transverse momentum dependent PDFs at N^3 LO*, *JHEP* **09** (2020) 146 [[arXiv:2006.05329](#)] [[INSPIRE](#)].
- [200] T. Gehrmann, T. Lubbert and L.L. Yang, *Transverse parton distribution functions at next-to-next-to-leading order: the quark-to-quark case*, *Phys. Rev. Lett.* **109** (2012) 242003 [[arXiv:1209.0682](#)] [[INSPIRE](#)].
- [201] T. Gehrmann, T. Luebbert and L.L. Yang, *Calculation of the transverse parton distribution functions at next-to-next-to-leading order*, *JHEP* **06** (2014) 155 [[arXiv:1403.6451](#)] [[INSPIRE](#)].
- [202] T. Gehrmann and D. Kara, *The $Hb\bar{b}$ form factor to three loops in QCD*, *JHEP* **09** (2014) 174 [[arXiv:1407.8114](#)] [[INSPIRE](#)].
- [203] T. Gehrmann et al., *Calculation of the quark and gluon form factors to three loops in QCD*, *JHEP* **06** (2010) 094 [[arXiv:1004.3653](#)] [[INSPIRE](#)].
- [204] P.A. Baikov et al., *Quark and gluon form factors to three loops*, *Phys. Rev. Lett.* **102** (2009) 212002 [[arXiv:0902.3519](#)] [[INSPIRE](#)].
- [205] T. Gehrmann, T. Huber and D. Maitre, *Two-loop quark and gluon form-factors in dimensional regularisation*, *Phys. Lett. B* **622** (2005) 295 [[hep-ph/0507061](#)] [[INSPIRE](#)].
- [206] R.V. Harlander, *Virtual corrections to $gg \rightarrow H$ to two loops in the heavy top limit*, *Phys. Lett. B* **492** (2000) 74 [[hep-ph/0007289](#)] [[INSPIRE](#)].
- [207] C. Duhr, B. Mistlberger and G. Vita, *Four-Loop Rapidity Anomalous Dimension and Event Shapes to Fourth Logarithmic Order*, *Phys. Rev. Lett.* **129** (2022) 162001 [[arXiv:2205.02242](#)] [[INSPIRE](#)].
- [208] I. Moulton, H.X. Zhu and Y.J. Zhu, *The four loop QCD rapidity anomalous dimension*, *JHEP* **08** (2022) 280 [[arXiv:2205.02249](#)] [[INSPIRE](#)].
- [209] R.N. Lee et al., *Quark and Gluon Form Factors in Four-Loop QCD*, *Phys. Rev. Lett.* **128** (2022) 212002 [[arXiv:2202.04660](#)] [[INSPIRE](#)].
- [210] A. Chakraborty et al., *$Hb\bar{b}$ vertex at four loops and hard matching coefficients in SCET for various currents*, *Phys. Rev. D* **106** (2022) 074009 [[arXiv:2204.02422](#)] [[INSPIRE](#)].
- [211] M. Bonvini, *Resummation of soft and hard gluon radiation in perturbative QCD*, Ph.D. thesis, Genoa University, I-16146 Genoa, Genoa, Italy (2012) [[arXiv:1212.0480](#)] [[INSPIRE](#)].
- [212] M. Bonvini and S. Marzani, *Resummed Higgs cross section at N^3 LL*, *JHEP* **09** (2014) 007 [[arXiv:1405.3654](#)] [[INSPIRE](#)].
- [213] M. Diehl, R. Nagar and F.J. Tackmann, *ChiliPDF: Chebyshev interpolation for parton distributions*, *Eur. Phys. J. C* **82** (2022) 257 [[arXiv:2112.09703](#)] [[INSPIRE](#)].

- [214] M. Beneke and V.A. Smirnov, *Asymptotic expansion of Feynman integrals near threshold*, *Nucl. Phys. B* **522** (1998) 321 [[hep-ph/9711391](#)] [[INSPIRE](#)].
- [215] V.A. Smirnov and E.R. Rakhmetov, *The strategy of regions for asymptotic expansion of two loop vertex Feynman diagrams*, *Theor. Math. Phys.* **120** (1999) 870 [[hep-ph/9812529](#)] [[INSPIRE](#)].
- [216] V.A. Smirnov, *Problems of the strategy of regions*, *Phys. Lett. B* **465** (1999) 226 [[hep-ph/9907471](#)] [[INSPIRE](#)].
- [217] V.A. Smirnov, *Applied asymptotic expansions in momenta and masses*, *Springer Tracts Mod. Phys.* **177** (2002) 1 [[INSPIRE](#)].
- [218] I. Balitsky and G.A. Chirilli, *NLO evolution of color dipoles in $N = 4$ SYM*, *Nucl. Phys. B* **822** (2009) 45 [[arXiv:0903.5326](#)] [[INSPIRE](#)].
- [219] I. Balitsky and G.A. Chirilli, *Rapidity evolution of Wilson lines at the next-to-leading order*, *Phys. Rev. D* **88** (2013) 111501 [[arXiv:1309.7644](#)] [[INSPIRE](#)].
- [220] I. Balitsky and G.A. Chirilli, *Conformal invariance of transverse-momentum dependent parton distributions rapidity evolution*, *Phys. Rev. D* **100** (2019) 051504 [[arXiv:1905.09144](#)] [[INSPIRE](#)].
- [221] I. Balitsky and G.A. Chirilli, *Rapidity evolution of TMDs with running coupling*, *Phys. Rev. D* **106** (2022) 034007 [[arXiv:2205.03119](#)] [[INSPIRE](#)].
- [222] I. Balitsky, *Rapidity-only TMD factorization at one loop*, *JHEP* **03** (2023) 029 [[arXiv:2301.01717](#)] [[INSPIRE](#)].
- [223] F. De Fazio and M. Neubert, *$B \rightarrow X_u l \bar{\nu}_l$ lepton decay distributions to order $\alpha(s)$* , *JHEP* **06** (1999) 017 [[hep-ph/9905351](#)] [[INSPIRE](#)].
- [224] S.W. Bosch, B.O. Lange, M. Neubert and G. Paz, *Factorization and shape function effects in inclusive B meson decays*, *Nucl. Phys. B* **699** (2004) 335 [[hep-ph/0402094](#)] [[INSPIRE](#)].
- [225] C.W. Bauer, D. Pirjol and I.W. Stewart, *Soft collinear factorization in effective field theory*, *Phys. Rev. D* **65** (2002) 054022 [[hep-ph/0109045](#)] [[INSPIRE](#)].
- [226] C.W. Bauer and I.W. Stewart, *Invariant operators in collinear effective theory*, *Phys. Lett. B* **516** (2001) 134 [[hep-ph/0107001](#)] [[INSPIRE](#)].
- [227] C.W. Bauer, S. Fleming, D. Pirjol and I.W. Stewart, *An effective field theory for collinear and soft gluons: Heavy to light decays*, *Phys. Rev. D* **63** (2001) 114020 [[hep-ph/0011336](#)] [[INSPIRE](#)].
- [228] C.W. Bauer, S. Fleming and M.E. Luke, *Summing Sudakov logarithms in $B \rightarrow X_s \gamma$ in effective field theory*, *Phys. Rev. D* **63** (2000) 014006 [[hep-ph/0005275](#)] [[INSPIRE](#)].
- [229] C.W. Bauer et al., *Hard scattering factorization from effective field theory*, *Phys. Rev. D* **66** (2002) 014017 [[hep-ph/0202088](#)] [[INSPIRE](#)].
- [230] M. Beneke, A.P. Chapovsky, M. Diehl and T. Feldmann, *Soft collinear effective theory and heavy to light currents beyond leading power*, *Nucl. Phys. B* **643** (2002) 431 [[hep-ph/0206152](#)] [[INSPIRE](#)].
- [231] M. Beneke and T. Feldmann, *Multipole expanded soft collinear effective theory with nonAbelian gauge symmetry*, *Phys. Lett. B* **553** (2003) 267 [[hep-ph/0211358](#)] [[INSPIRE](#)].
- [232] C.W. Bauer, D. Pirjol and I.W. Stewart, *Factorization and endpoint singularities in heavy to light decays*, *Phys. Rev. D* **67** (2003) 071502 [[hep-ph/0211069](#)] [[INSPIRE](#)].
- [233] B.O. Lange and M. Neubert, *Factorization and the soft overlap contribution to heavy to light form-factors*, *Nucl. Phys. B* **690** (2004) 249 [[hep-ph/0311345](#)] [[INSPIRE](#)].

- [234] M. Beneke and T. Feldmann, *Factorization of heavy to light form-factors in soft collinear effective theory*, *Nucl. Phys. B* **685** (2004) 249 [[hep-ph/0311335](#)] [[INSPIRE](#)].
- [235] G. 't Hooft and M.J.G. Veltman, *Regularization and Renormalization of Gauge Fields*, *Nucl. Phys. B* **44** (1972) 189 [[INSPIRE](#)].
- [236] PARTICLE DATA GROUP collaboration, *Review of Particle Physics*, *PTEP* **2022** (2022) 083C01 [[INSPIRE](#)].
- [237] S. Bailey et al., *Parton distributions from LHC, HERA, Tevatron and fixed target data: MSHT20 PDFs*, *Eur. Phys. J. C* **81** (2021) 341 [[arXiv:2012.04684](#)] [[INSPIRE](#)].
- [238] A. Buckley et al., *LHAPDF6: parton density access in the LHC precision era*, *Eur. Phys. J. C* **75** (2015) 132 [[arXiv:1412.7420](#)] [[INSPIRE](#)].
- [239] E. Bothmann et al., *Accelerating LHC event generation with simplified pilot runs and fast PDFs*, *Eur. Phys. J. C* **82** (2022) 1128 [[arXiv:2209.00843](#)] [[INSPIRE](#)].
- [240] T. Gleisberg et al., *SHERPA 1. alpha: A proof of concept version*, *JHEP* **02** (2004) 056 [[hep-ph/0311263](#)] [[INSPIRE](#)].
- [241] T. Gleisberg et al., *Event generation with SHERPA 1.1*, *JHEP* **02** (2009) 007 [[arXiv:0811.4622](#)] [[INSPIRE](#)].
- [242] SHERPA collaboration, *Event Generation with Sherpa 2.2*, *SciPost Phys.* **7** (2019) 034 [[arXiv:1905.09127](#)] [[INSPIRE](#)].
- [243] A. Buckley et al., *Rivet user manual*, *Comput. Phys. Commun.* **184** (2013) 2803 [[arXiv:1003.0694](#)] [[INSPIRE](#)].
- [244] C. Bierlich et al., *Robust Independent Validation of Experiment and Theory: Rivet version 3*, *SciPost Phys.* **8** (2020) 026 [[arXiv:1912.05451](#)] [[INSPIRE](#)].